Imaging in Pediatric Dental Practice

A Guide to Equipment, Techniques and Clinical Considerations

Johan Aps

Springer

Imaging in Pediatric Dental Practice

Johan Aps

Imaging in Pediatric Dental Practice

A Guide to Equipment, Techniques and Clinical Considerations

Springer

Johan Aps
Dental School
University of Western Australia
Western Australia, WA
Australia

ISBN 978-3-030-12353-6 ISBN 978-3-030-12354-3 (eBook)
https://doi.org/10.1007/978-3-030-12354-3

Library of Congress Control Number: 2019934728

This Springer imprint is published by the registered company Springer Nature Switzerland AG
The registered company address is: Gewerbestrasse 11, 6330 Cham, Switzerland

Foreword

This textbook fills one of the most blatant gaps in the dental literature, imaging in pediatric dentistry! Although there are several guidelines for dental imaging in children, most clinicians, including experienced ones, are often caught in between enthusiasm for new methods and concerns about their safety and judicious use. This textbook is aimed at solving many of these riddles. The book is a comprehensive text on imaging in children, from an author who is both a pediatric dentist and also a specialist in dental radiology. The book covers all the principles of intra- and extraoral radiology, including the use of more advanced imaging techniques such as CBCT and MRI. With the increasing use of CBCT in dentistry, there are varied standards followed around the world on its use, from a more judicious use in Europe stemming from concerns over radiation protection for children to a more widespread and sometimes overuse in many other countries in the world. This book addresses these issues and also specifically issues around radiation protection. Finally excellent and varied clinical imaging examples are presented to enhance the readers' understanding of the techniques.

This text is of interest both to general dentists who treat children in their clinical practice, specialists in pediatric dentistry and also those who are following dental radiology as their profession. I highly recommend this book to the readers.

Monty Duggal
Faculty of Dentistry
National University of Singapore
Singapore, Singapore

Preface

Many colleagues are probably frowning their eyebrows when reading the title of this book. Why would there be a need for a textbook focusing specifically on pediatric patients and patients with special needs? Well, traditionally, textbooks on dental and maxillofacial radiology do not cover much on special patient populations, like children and patients with special needs. Unfortunately, one approach does not suit all. Being dual trained in pediatric dentistry and dental and maxillofacial radiology, I have always tried to implement these patient groups in my radiology teaching and presentations. After one of these presentations, at the California Society of Pediatric Dentistry (Las Vegas, 2016) to be precise, a representative from Springer contacted me with the idea to write this textbook.

The concept of this book is to provide the pediatric dental registrar, the pediatric dentist or anyone interested in dental and maxillofacial imaging in pediatric dentistry and patients with special needs with technical knowledge about X-ray equipment, techniques and radiation doses. It is important for clinicians to master different techniques, to be able to modify them, without deteriorating the quality of the image or the diagnostic yield, and to understand the technology behind them. Besides the technical aspects of diagnostic imaging, one should also be familiar with the magnitude and potential impact of radiation doses from different diagnostic imaging modalities. The last chapters of the book are merely a grasp out of the day-to-day practice and illustrate how the most common in practice diagnostic imaging technologies can be used.

I sincerely hope that you will enjoy this textbook and that you will be able to use the knowledge and the information in your practice or clinic.

Last but not least, I wish to thank all the colleagues who have contributed to this book, by sharing with me their images. Gratitude also goes to Springer publishers for giving me this unique opportunity.

Western Australia, WA, Australia — Johan Aps
December 2018

Preamble

November 8, 1895, is a historical day for humankind as this is the day when Wilhelm Conrad Roentgen discovered X-rays. The famous picture of the radiograph of his wife's hand initiated the first dental radiographs ever taken in the world by Doctor Otto Walkhoff on January 12, 1896, merely 2 weeks after Professor Roentgen published his discovery. The timeline below shows what the images looked like and how long the exposures had to be.

A new era was born, and ever since, dental radiographs have proven their significant value in dental and maxillofacial diagnosis. For many years, two-dimensional intraoral radiography and extraoral radiography were the only radiographic modality, but in recent years, three-dimensional imaging in dentistry (cone beam computed tomography, CBCT) has become common ground. Challenges regarding tomography of the skull were battled by the Finnish Professor Paatero, who developed the first panoramic machine. Many of us refer to the panoramic radiograph as "pan", "pano", "panorex" or "OPG". Other advanced imaging modalities such as multislice computed tomography (MSCT), magnetic resonance imaging (MRI) and ultrasound imaging are also available to the clinician. Both MSCT and MRI are too expensive to be used in a dental environment, but they have their applications in dentistry. Ultrasonography is in some countries around the world better accepted than in others for diagnostic purposes in the dental and maxillofacial region, but it has definitely a place in our armamentarium. In contrast to MSCT and CBCT and plain radiography, MRI and ultrasonography do not use ionizing radiation and can therefore be considered "safer" than the other imaging modalities.

The timeline below shows when different major imaging modalities were introduced to the medical and dental profession since 1895. We have been using digital imaging since 1970, and it is clear that the majority of diagnostic imaging is still performed with ionizing radiation. However, it is my opinion that in the next two decades, we will use less ionizing radiation for diagnostic purposes, especially in young patients. This book provides a general overview of the imaging techniques currently used in pediatric dental and maxillofacial radiology and will provide a clear overview of the image receptors, specialized techniques and indications and justifications for exposing pediatric patients to ionizing radiation or other imaging modalities. Examples from the clinic have been used to illustrate the techniques and the diagnostic value of the different techniques.

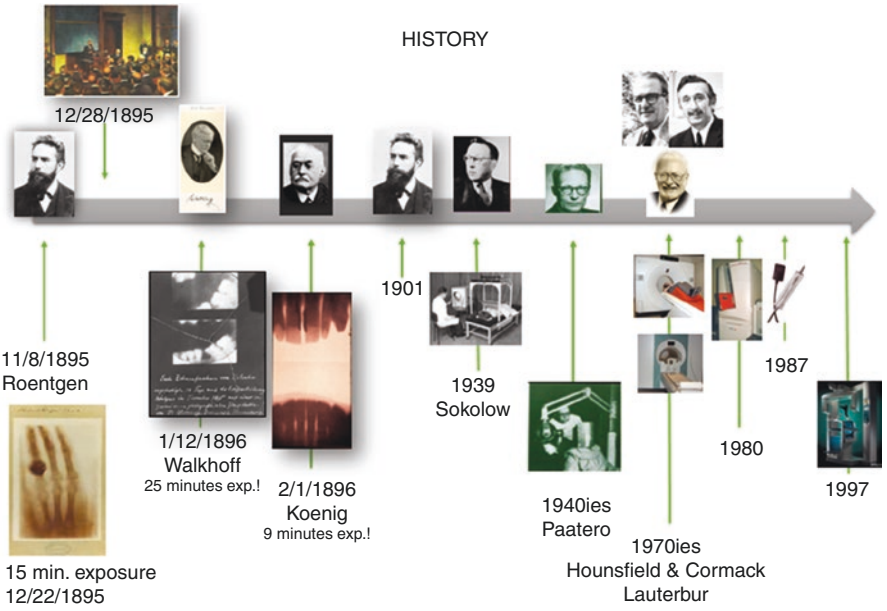
HISTORY
12/28/1895
11/8/1895
Roentgen
15 min. exposure
12/22/1895
1/12/1896
Walkhoff
25 minutes exp.!
2/1/1896
Koenig
9 minutes exp.!
1901
1939
Sokolow
1940ies
Paatero
1970ies
Hounsfield & Cormack
Lauterbur
1980
1987
1997

Contents

X-Ray Equipment in Dental Practice

1

1.1 The X-Ray Machine

All X-ray machines consist, generally speaking, of the same components. Figure 1.1 is a schematic illustration of an X-ray machine.

(a) *Vacuum glass tube*
Inside the vacuum glass tube, one can find the cathode, which looks like an incandescent light bulb's filament. This cathode is negatively charged. The number of electrons is determined by the amperage (usually milli-ampere or mA). The number of electrons is proportionate to the number of X-rays and hence to the X-ray dose as well. Opposite to the cathode is the positively

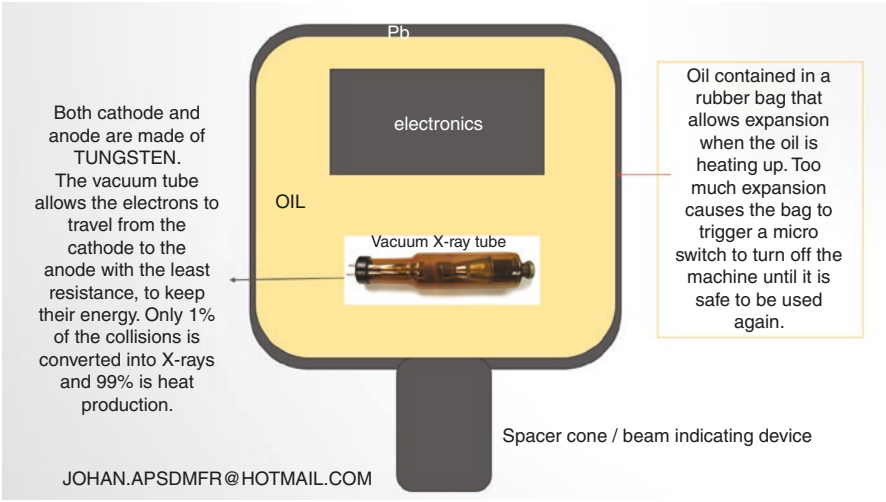

Fig. 1.1 Schematic drawing of an X-ray machine

J. Aps, *Imaging in Pediatric Dental Practice*,
https://doi.org/10.1007/978-3-030-12354-3_1

charged anode. Both anode and cathode are made of tungsten (W). The electrons are attracted to the anode due to a high voltage across both. Due to the vacuum glass tube, the electrons will not collide with air before hitting the anode (target). Due to the law of conservation of energy, the colliding electrons produce 99% heat and 1% X-rays. The penetration power of the X-rays is determined by the voltage across the tube (usually expressed as kilovoltage).

Medical X-ray machines have a rotating anode to dissipate the heat better, as they use longer exposure times, higher kV, and mA settings.

(b) *Step-up transformer*
The step-up transformer steps up the grid's power to the necessary kilovoltage (kV). Some dental X-ray machines allow for the kV to be changed; most intraoral machines have a fixed voltage. For intraoral X-ray machines the kV should be between 60 and 70 kV.

(c) *Cooling oil*
Since 99% of the collisions between the electrons and the target produce heat, the machine requires to be cooled. The oil is contained in a rubber bag, which, if expanded too much due to heat absorption, is able to push a microswitch to temporarily disable the machine so no subsequent exposure can be made. The machine will be ready for use when it has cooled down again.

(d) *Lead casing*
The lead casing prohibits X-rays from leaking from the machine while it is in use. Only X-rays going through the porthole are supposed to leave the machine.

(e) *Filter*
An aluminum filter is placed in front of the porthole to filter out all the lower energy X-rays, which otherwise would just be absorbed by the patient and which would not contribute to the diagnostic image. The manufacturer determines the thickness of that filter, based on the kV of the machine.

(f) *Electronic timer*
The timer determines the exposure time in milliseconds (ms). It is important that the timer works accurately, as a too long exposure time will result in overradiation of the patient. If one increases the exposure time, the penetration power of the X-rays is increased, but also the radiation dose to the patient, as more X-rays will be produced (mA x time, usually called the "mAs").

(g) *Collimators*
Manufacturers place a spacer cone or a beam-indicating device on intraoral X-ray machines, to make sure the correct distance from the anode to the patient's skin is respected. This distance is usually between 20 and 40 cm, but definitely not shorter than 20. The spacer cones usually look like cylinders and collimate the X-ray beam in a circle. However, since that is not the shape of our intraoral image detectors, this causes approximately 50% more tissue being irradiated than necessary. Therefore rectangular collimation is recommended as it reduces not only the radiation dose to the patient, but also the scattered radiation by the patient's tissues, and hence increases the image quality. Rectangular collimators can usually be retrofitted to the spacer cones (Fig. 1.2).

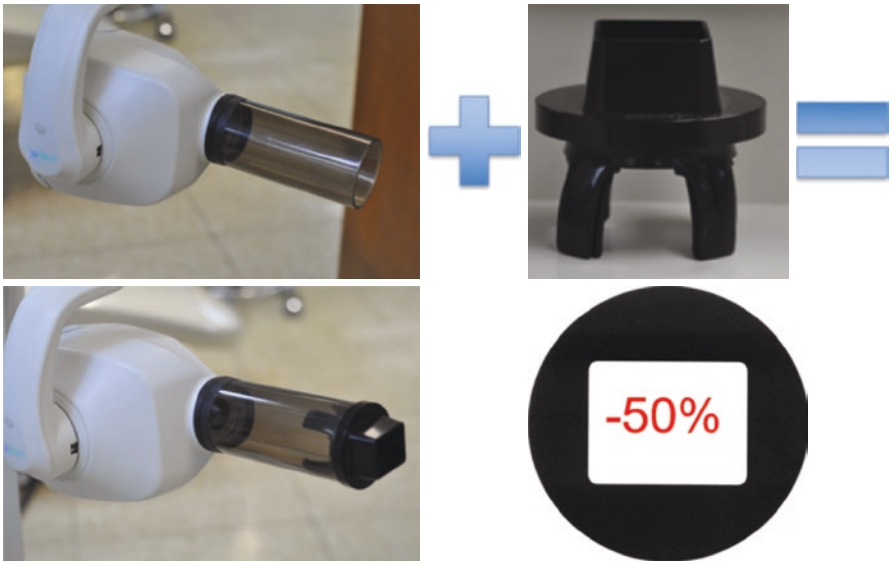

Fig. 1.2 Circular versus rectangular collimation: the retrofitted rectangular collimator enables a radiation dose reduction of approximately 50%

The collimation of the X-ray beam for extraoral X-ray machines is established immediately near the porthole. For panoramic machines the X-ray beam is collimated to a vertical narrow slit; for cone beam computed tomography, it is collimated to a pyramid; and for medical computed tomography, it is collimated into a fan beam.

Additionally it can be mentioned that only 1% of the electrons colliding with the anode will actually produce X-rays. That means that 99% of the collisions cause heating up of the machine. Over time, these electron collisions will cause the anode surface to become damaged, which is translated into a somewhat pebbled surface, which has two consequences. The first one is that there will be less X-rays leaving the X-ray tube through the window in the vacuum glass tube, as more X-rays will be scattered inside the glass tube than when the machine is new and the anode is as flat and smooth as a mirror. Secondly, because of the surface roughening, the focal spot (the spot where the electrons are supposed to collide the anode) will increase in size, which will cause penumbra in the image. Since this phenomenon of increase of the anode surface happens slowly over time and is related to the number of exposures taken with the machine and the kilovoltage applied across the tube, the changes are not easily visible. However, if one would compare an image taken when the machine was brand new and an image taken after 10 years of use, the image quality will be different.

*It is wise, when a new machine is taken into use, to expose a test object (*e.g., *a key) and repeat the same exposure every year with the same object under the same exposure conditions. This will allow one to monitor any changes to the anode of the machine.*

The phenomenon of penumbra is important when one converts from analogue to digital imaging. First of all, the tube current needs to be direct (DC machine) for digital image detectors and secondly the image quality will be better if the anode is new (thus a new X-ray machine).

Unfortunately there is no absolute maximum age or maximum amount of exposures when a machine needs to be replaced. Intraoral X-ray machines do not have a counter, which records the number of times the button is pressed. Extraoral X-ray machines have a counter and allow one to check how many exposures were taken with the machine. The latter can be important when one is considering purchasing a used X-ray machine.

One may also have asked oneself why some intraoral X-ray machines have a longer spacer cone than others. Essentially, the manufacturer has to ensure that the distance from focus to skin is not less than 20 cm. Therefore, if the vacuum glass tube is placed in the back of the housing, the spacer cone will be shorter than when the manufacturer placed the vacuum glass tube near the front of the housing of the machine.

1.2 Aiming Equipment for Intraoral Radiography

In order to be able to respect the correct geometry of the radiographic intraoral technique, one needs equipment to position the image detector parallel to the teeth to be imaged and subsequently to position the X-ray beam perpendicular to the image detector. Several manufacturers have such equipment available, but the most known is probably Rinn® (Fig. 1.3). The proper use of these image detector holder-aiming devices guarantees a correct geometry, with minimal distortion in the final image.

Different holders are available for different types of image detectors (e.g., photostimulable phosphor plates or solid-state sensors). Some are disposable, while others are reusable.

Fig. 1.3 Examples of Rinn® sets for different image detectors

For more details, the reader is deferred to the Rinn® website: www.RinnCorp.com.

It is important to use the proper image detector-holding devices, in order to assure a correct geometry between the X-rays and the image detector. Some manufacturers of solid-state sensors (see below) will have their own image detector-holding devices whereas others will not and one needs to explore manufacturers of image-holding devices' websites and catalogs to find the correct holder for one's solid-state sensor. Fortunately, there are different brands available.

1.3 Digital Image Detectors

This section does not handle about analog film. There are two types of digital image detectors. The first type is the photostimulable phosphor storage plate (Fig. 1.4), which physically resembles analog film, but which can be reused, opposed to analog film which is of single use only. Once the plate is exposed to X-rays it has to be scanned to acquire the final image. The second type is the solid-state sensor (Fig. 1.5), which is attached to a computer and which shows the image instantly on the computer screen after it has been exposed to X-rays. The solid-state sensors are easy to use, but a bit bulky in design sometimes. There are two types of the solid-state sensors: charge-coupled devices (CCD) and complementary metal oxide semiconductors (CMOS).

Fig. 1.4 Top row showing clean, undamaged photostimulable phosphor storage plates—bottom row showing damaged and dirty photostimulable phosphor storage plates

Fig. 1.5 Examples of solid-state sensors of different brands and sizes

1.3.1 Photostimulable Phosphor Plate (PSPP)

- Invented in 1980.
- These plates need to be wrapped to protect them from light (erases the image) and saliva (cross-contamination).
- They can be used several thousands of times.
- Are vulnerable to scratches or bite marks.
- Are available in all sizes.
- Can be double exposed without one's knowing, until scanned.
- Can be exposed back to front.
- Need to be scanned.
- Also referred to as direct digital imaging (image is captured on the phosphorous layer and is then scanned with a laser to release the stored energy as light, which is captured by a photomultiplier).
- Plate needs to be erased after it is scanned. (Automatically done in the scanner—but can be turned off! Careful!)

1.3.2 Solid-State Sensors (SSS)

- First developed in 1987 by Trophy®.
- Cable attaches computer to the sensor.
- Scintillation plate (cesium iodide) required inside the sensor to convert the photon energy into light (the photoelectric effect).
- Need to be wrapped to avoid cross-contamination.
- Cannot be accidentally exposed double (image is captured instantly and there is no latent image).
- Cannot be exposed back to front.
- Can be bulky for some patients.
- External dimensions do not match internal/real dimensions of the sensor.
- They have an actual resolution of 0.03 mm at pixel size 15 x 15 microns (=17 lp/mm, lp stands for line pairs, which is a pair of a white and a black line, often used in digital imaging to express the resolution).
- Do not come in all sizes as that would be too expensive.
- Two types:
  - Charge-coupled devices (CCD).
  - Complementary metal oxide semiconductors (CMOS).

Table 1.1 Comparing the characteristics of photostimulable phosphor storage plates and solid-state sensors

	PSPP	CCD/CMOS
Multiple use	Yes	Yes
Double images possible	Yes	No
Scanner required	Yes	No
Bending possible	Yes	No
Damage easy	Yes	No
Special detector holder required	Yes	Yes
Resolution	< / = 20 Ip/mm	>20 Ip/mm
Volume	Thin	Bulky
Sizes	0-1-2-4 – pano – ceph	(0)-1-2

Table 1.1 shows an overview of the characteristics of both photostimulable phosphor storage plates and solid-state sensors. From this table one can easily extract the advantages and disadvantages of either system. Ideally one should have both systems in place; however, that solution is pretty expensive. Therefore practitioners have to make a choice. In the case of pediatric dentistry phosphor storage plates are probably the best solution as they are not as bulky as solid-state sensors and come in different sizes, which makes it easier to obtain occlusal radiographs for instance (see Chap. 3). Solid-state sensors are not available in occlusal size.

The photostimulable storage phosphor plates consist of a europium-activated barium fluorohalide layer which is placed on a plastic carrier to make it rigid enough to be used. Exposure to X-rays causes a latent image to be formed, which then requires the plate to be scanned inside a special scanner that uses a red helium neon laser. This will cause the latent image to emit blue fluorescent light from the plate, which is subsequently captured by a photomultiplier. An analog digital converter will then facilitate displaying the image on the computer screen. The amount of fluorescent light is proportional to the energy captured by the plate during the X-ray exposure. When the plate is scanned, the latent image is still present. Therefore the next step consists of exposing the plate to a bright white LED light source. The latent image is now erased and the plate is ready to be reused. The latter explains why these plates should not be exposed to light when they are removed from their barrier envelope or pouch after X-ray exposure. Ideally the scanner should not be placed in a bright area in the office, as this will deteriorate the image quality, if the plates are exposed to light before scanning takes place.

The solid-state sensors use the same camera or sensor as a mobile phone. However, in order to convert the X-ray energy into light, which is what the camera can detect, a so-called scintillation plate (gadolinium oxysulfide or cesium iodide) is placed on top of the CCD or CMOS sensor. The amount of light being emitted is proportional to the amount of X-rays that hit the scintillation plate. This technology allows for faster image acquisition than the

phosphor storage plates, as the image can be displayed on a computer monitor immediately. Since there is no latent image, there is no risk of accidentally capturing double images either. The downside of the solid-state sensors is their size: limited in the surface (sizes 0, 1, and 2 only) and too bulky in some cases. Once the patient has been selected, the software allows for fast allocation and orientation of the images though, which is not the case when phosphor plates are used, as one will have to allocate and orientate the images one by one (images are scanned randomly which is not the case with solid-state sensors).

1.4 Computer Monitors

In the era of analog film, films were to be interpreted on a light box (negatoscope). Magnification was only possible using a magnifying glass and over- or underexposed films were either to be retaken or to be viewed under increased or decreased light, respectively, on the light box. The light box also had to produce homogenous light and collimation of the light would be ideal as to avoid light contamination around the films. Usually this was achieved with film mounts that could be placed on the light box.

Nowadays, with digital images, one is interpreting the images on a computer monitor (flat panel). The monitor has to be clean and has to be in a place where the light is dimmed and the light is not reflected in the monitor (e.g., never have a monitor facing a window or bright-light source). Most off-the-shelf monitors will satisfy for dental images, but one has to make sure that the monitor is calibrated. Usually the imaging software one uses in the office allows for monitor calibration. An example of a calibration screen is shown in Fig. 1.6. It is paramount that the monitor works perfect (e.g., no defective pixels showing red or blue hue). Current research is not conclusive about the fact if one should have high-performance monitors, like in medical imaging, for dental radiography interpretation. The higher the pixel density of the monitor, the higher the details that can be appreciated in the image.

The software one is using to view the images allows for “windowing” of the image (Fig. 1.7). That means that one always has to dynamically change contrast and brightness in order to view all the information that was captured on the image detector. Older generation dentists will fear changing contrast and brightness, because they were trained with analog film. They could change contrast and brightness only by changing the exposure parameters and changes could not be made after the exposure had taken place! Also image filters can be useful (e.g., edge enhancement). It should be emphasized that using a filter means omitting some of the information, so always go back and forth between the filtered and unfiltered image. Magnification of the image has its limitations as the image may become “pixelated”

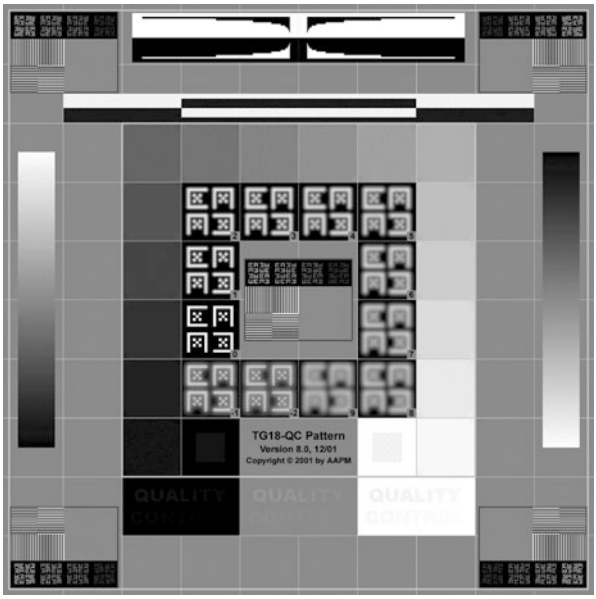

Fig. 1.6 Example of a monitor calibration screen (TG18-QC Pattern version 8.0 12/01, by AAPM)

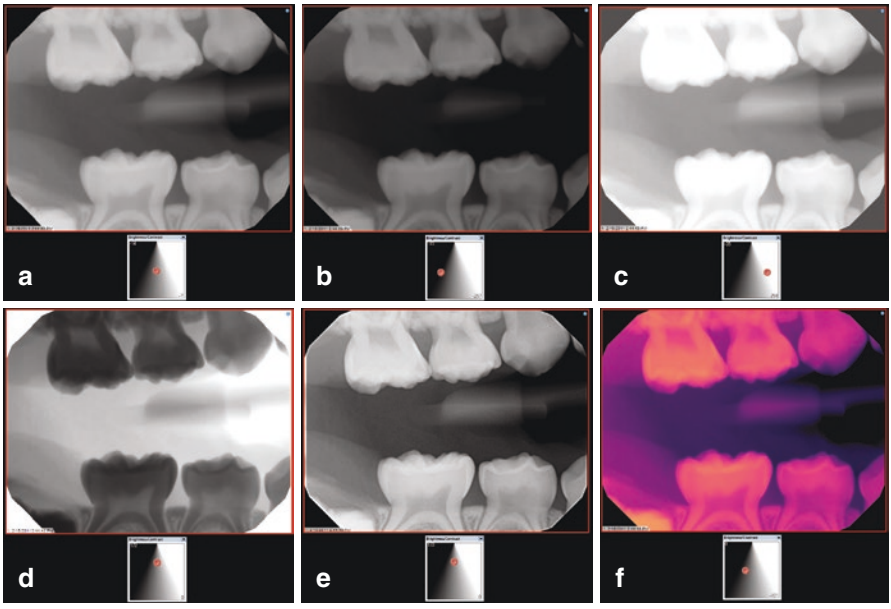

Fig. 1.7 Example of windowing of a bitewing radiograph: (**a**) through (**c**) show changes in contrast, and brightness, (**d**) shows inverting the image, (**e**) shows edge enhancement, and (**f**) illustrates colorization. These are a few examples to illustrate some of the features the viewing software may offer. The histogram below each image shows how contrast and brightness were changed

(little squares become visible in the image) and it is no longer diagnostic. Inverting the image can also be useful in some cases (changing it into a positive image: enamel becomes dark and pulp becomes light).

Always sit in front of a monitor and don't view from an angle, as the image may lose detail and brightness.

In medical imaging the monitors are high-end diagnostic monitors with 5 or 8 megapixel screens (up to $80 k or more). The latter is paramount for instance in mammography where radiologists have to be sure that pathology in soft tissue is found as accurately as possible. It can be a matter of life or death.

It is very important to remember to use the viewing software for digital images properly. The settings of the software are usually installed and checked by the installing technician. That does not mean that the image that is immediately displayed on the monitor is the most ideal or best image in terms of contrast and/or brightness. It is essential to dynamically use the tools in the software to visualize what you are after. For instance, one may want to assess the gingiva, instead of the enamel. In that case one has to increase the brightness as otherwise the gingiva will not be visible. However, this action changes the distinction between enamel and dentine to nondiagnostic. Dentists and radiographers trained in the analog film era will score the latter image as "underexposed" as it is too pale. As shown in Fig. 1.7*, dynamically changing the contrast and/or brightness parameters leads to the highest diagnostic yield. The use of color in the image may prove to be useful when one is assessing a radiopaque inclusion in a tooth or bone. Since materials of the same opacity will have the same color, one can derive what material the inclusion is made of. The latter, of course, assumes that there is similar material visible in that radiograph (*e.g., *amalgam and amalgam tattoo).*

The same software allows one to measure as well on radiographs. However, one has to be cautious with this feature as one needs to calibrate the measurement first and, if possible, take into account curvature in a tooth for instance when measuring the length of a tooth.

Further Reading

Arakai K, Fujikura M, Sano T. Effect of display monitors devices on intra-oral radiographic caries diagnosis. Clin Oral Invest. 2015;19:1875–9.

Butt A, Savage NW. Digital display monitor performance in general dental practice. Austr Dental J. 2015;60:240–6.

Cruz AD, MCN C, Aguiar MF, Guimaraes LS, Gomes CC. Impact of room lighting and image display device in the radiographic appearances of the endodontic treatments. Dentomaxil Radiol. 2018;47:20170372.

Iannucci JM, Howerton LJ. Dental radiography. In: Principles and techniques. 4th ed. Amsterdam: Elsevier; 2012.
Whaites E, Drage N. Essentials of dental radiography and radiology. 5th ed. Amsterdam: Churchill Livingstone, Elsevier; 2015.
White SC, Pharoah MJ. Oral radiology. In: Principles and interpretation. 7th ed. Amsterdam: Elsevier; 2014.

Radiation Protection in Dentistry

2

2.1 The Three Basic Principles of Radiation Protection

Justification is the first principle of radiation protection and states that one should only expose the patient after a thorough clinical examination and anamnesis. One should only expose the patient to ionizing radiation if the benefit outweighs the risk. That means that the information one gathers with taking a radiograph will have a substantial impact on the diagnosis, treatment, and outcome. If there is another method to gather that important piece of information, then the radiograph should not be taken. In pediatric dentistry, this also means that if the patient cannot cope with the procedure and the quality of the radiograph would not be diagnostic, the exposure should not take place.

Limitation is the second principle of radiation protection. This principle states that one should always try to keep the dose as low as possible, without compromising the image quality and the diagnostic yield. Under this principle one understands ALARA (as low as reasonably achievable), which has been twisted to ALADA (as low as diagnostically achievable) ALADAIP (ALADA indication oriented and patient specific) recently.

Optimization is the third principle, which states that one should always try to obtain the best image quality possible, however, with both previous principles in mind.

To illustrate these principles, Fig. 2.1 shows an example of non-justifiable exposure to ionizing radiation. The 3-year-old girl was submitted to a panoramic radiograph, while there were no clinical caries, swellings of any sort, or abnormalities. This is a useless exposure, which does not add important information, as what can be observed in the radiograph is normal dental development, as expected from the clinical examination and the dental and medical history. On the contrary there is the second panoramic radiograph in Fig. 2.1, which depicts the image of a 5-year-old boy with rampant caries, who had already his right-hand-side second deciduous molar extracted at an emergency visit prior to this exposure. This exposure can be justified, as the carious lesions have caused abscesses and infection, and the

J. Aps, *Imaging in Pediatric Dental Practice*,
https://doi.org/10.1007/978-3-030-12354-3_2

Fig. 2.1 The top panoramic radiograph is the radiograph of a perfectly healthy 3-year-old girl, whereas the bottom one is a 5-year-old boy with severe caries and a history of exodontia

information that can be obtained from this panoramic radiograph will have a significant impact on the diagnostic yield and ultimately also the treatment plan.

2.2 Radiation Doses of Different Medical and Dental Diagnostic Examinations

In order to understand what radiation dose means, one has to unravel the differences between absorbed, equivalent, and effective radiation dose (Fig. 2.2). The effective radiation dose (Table 2.1) will be used to compare different diagnostic exposures with each other and with the annual natural background radiation. The latter differs per continent and region, but varies between 1500 and 8000 μSv.

In Table 2.1 one can find effective radiation doses for several dental and medical diagnostic exposures. The figures in this table can be used to put diagnostic

ABSORBED RADIATION DOSE	EQUIVALENT RADIATION DOSE	EFFECTIVE RADIATION DOSE
"D"	"H"	"E"
Relates to the **amount of energy** per unit mass of tissue Unit = Gray (= J/Kg) 1 Gray (Gy) = 100 RAD (old unit)	Relates to the **type of radiation** that is involved Weighting factor for the type of radiation (W_R): ❖ W_R X-rays = 1 ❖ W_R alpha rays = 20 Unit = Sievert 1 Sievert (Sv) = 100 REM (old unit) Calculation of H: $H = W_R \times D$	Relates to the **parts of the body** being exposed to radiation Weighting factor for tissue or organ (W_T) The sum of all organs and tissue weighting factors = 1 Unit = Sievert (Sv) Calculation of E: $E = H \times W_T$

Fig. 2.2 Absorbed, equivalent, and effective radiation doses explained

Table 2.1 Effective doses in milli- and micro-sieverts for different dental and medical diagnostic exposures

X-ray examination	Effective dose (E) in mSv	Effective dose (E) in μSv
Typical effective doses for dental and medical diagnostic exposures/examinations		
Bitewing/periapical radiograph	0.0003–0.022	0.3–22
Panoramic radiograph	0.0027–0.038	2.7–38
Upper standard occlusal	0.008	8
Lateral cephalometric radiograph (dental)	0.0022–0.0056	2.2–5.6
Posterior-anterior skull radiograph	0.02	20
Lateral skull radiograph (medical)	0.016	16
Posterior-anterior chest radiograph	0.014	14
Lateral chest radiograph	0.038	38
CT skull	1.4	1400
CT chest	6.6	6600
CT abdomen	5.6	5600
CT maxilla and mandible	0.25–1.4	250–1400
Barium swallow	1.5	1500
Barium enema	2.2	2200
CBCT small/medium field of view	0.01–0.67	10–670
CBCT large field of view (craniofacial scan)	0.03–1.1	30–1100

exposures in perspective with daily background radiation which is, depending on the region where one lives, between approximately 4 and 22 μSv.

These are low doses compared to what is administered in therapeutic radiation. The diagnostic radiation dose range will never be able to cause any so-called deterministic effects, as they are far below the threshold dose of 100 mGy. However, the diagnostic radiation dose range may be putting the patient at risk to develop a fatal

cancer, but since there is no threshold dose, the risk is all about probability. These are the so-called stochastic effects. In Table 2.2 the potential risks are tabulated for different diagnostic exposures to ionizing radiation. These are the risk estimates for a male adult of 30 years old. Table 2.3 shows the multiplication factors one has to use when age is taken into account. From these numbers it becomes clear that the potential risk in children is higher than in adults, due to the fact that their mitotic cell activity is much higher and because they have much longer life expectancy, which enables enough time for a tumor to develop. One has to keep in mind that these numbers in Table 2.2 are estimates. This is the principle of the so-called "linear non-threshold model for radiation risk".

At the same time one also has to keep in mind that a life without natural ionizing background radiation is impossible. That means that one is always exposed to some

Table 2.2 Risk estimate for diagnostic radiation causing a fatal cancer

Exam type	Estimated risk
Broad estimate of the risk of a standard 30-year-old male patient developing a fatal radiation induced malignancy from a variety of dental and medical X-ray examinations	
Bitewing/periapical radiograph (70 Kv, round collimation and D-speed film)	1/1,000,000
Bitewing/periapical radiograph (70 Kv, rectangular collimation and F-speed film or digital image detector)	1/10,000,000
Panoramic radiograph	1/1,000,000
Upper standard occlusal	1/2,500,000
Lateral cephalometric radiograph (dental)	1/5,000,000
Posterior-anterior skull radiograph (medical)	1/1,000,000
Lateral skull radiograph (medical)	1/2,500,000
Posterior-anterior chest radiograph	1/1,430,000
Lateral chest radiograph	1/540,000
CT skull	1/14,300
CT chest	1/3,000
CT abdomen	1/3,500
CT mandible and maxilla	1/80,000–1/14,300
Barium swallow	1/13,000
Barium enema	1/9,100
CBCT maxilla and mandible (small and medium field of view)	1/2,000,000–1/30,000
CBCT craniofacial (large field of view-orthognathic)	1/670,000–1/18,200

Table 2.3 Age in risk assessment for ionizing radiation effects

Age category	Multiplication factor for the risk estimation to develop a fatal cancer
<10 years	× 3
10–20 years	× 2
20–30 years	× 1.5
30–50 years	× 0.5
50–80 years	× 0.3
>80 years	× 0 (Negligible)

ionizing radiation. This is exactly the basis for the opinion of the defenders of the so-called hormesis theory, who state that a little bit of radiation is actually training the cells in the body to respond better when exposed to higher radiation doses.

In the blue text below, additional information is provided on the interactions of ionizing radiation with biological tissues.

There Are Two Pathways in Which Ionizing Radiation Can Cause Damage to Biological Tissues

An incident photon can cause ionization and excitation of water molecules in the body, resulting in the formation of hydrogen peroxide and free radicals (H+ and OH-). This is indirect action of ionizing radiation on cells. The latter can cause cellular molecular damage. This takes place in picoseconds and results in either spontaneous repair (can be a different cell type though, like in fibrosis) or mutation (regeneration) of the DNA or RNA in the cell, which subsequently can lead to a biological response in the cell, which on its turn can lead to teratogenic effects or even cell death and hence patient death. These biological responses take minutes to decades to develop. These indirect effects are taking place in the majority of cases, as the human body consists of 70–85% water. The body's cells are most sensitive to ionizing radiation during the M phase (metaphase) of cell mitosis and during the G2 phase of RNA synthesis. The sensitivity appears to decrease during the G1 phase and further towards the S phase of DNA synthesis.

According to the law of Bergonie and Tribondeau, the cells with the greatest radiosensitivity are the cells that have a high mitotic activity, cells with a high mitotic future, and undifferentiated cells. In the slides one can find a table with classification of high-, medium-, and low-radiosensitive organs. Muscle and the central nervous system are so-called radioresistant tissues. The salivary glands belong to the low-sensitivity group, but are almost always in the primary radiation beam used in dental imaging. The thyroid gland is an intermediate sensitive organ, though it should at all times be protected from the primary radiation beam. In children the thyroid gland lies close to the mandible and hence can be irradiated more than one thinks during oral and maxillofacial imaging.

The second interaction is the direct action of ionizing radiation on cells. An incident photon can cause direct DNA, RNA, or protein changes in the cell. This interaction takes picoseconds to a few minutes to happen. Then, two possibilities are possible: spontaneous repair or development of a mutation. The latter subsequently can lead to a biological response in the cell, which on its turn can lead to teratogenic effects or even cell death and hence patient death. Again, these biological responses take minutes to decades to develop.

2.3 Guidelines for Radiographic Exposures in Children

Different local guidelines exist, but the European Academy for Pediatric Dentistry (EAPD) and the American Academy for Pediatric Dentistry (AAPD) have published guidelines and recommendations on this subject.

The EAPD published a table in their guidelines with selection criteria for taking dental radiographs. These include objective clinical findings (e.g., deep periodontal pocket, clinical caries, swelling) and information from the anamnesis (e.g., family history of dental anomalies or history of pain). It is obvious that the justification principle should always be borne in mind. Radiographic screening cannot be justified if there are no clinical signs or if there is no anamnestic information that requires so. The EAPD guidelines also emphasize on the fact that every decision is to be taken on an individual patient basis. The EAPD advises to take bitewings every 12 months in high-caries-risk patients, while, depending on patient's age, in low-caries-risk patients, one can wait for 24–36 months before taking new bitewings. They also advocate the use of sensitive image detectors and the use of rectangular collimation for intraoral radiographs as this will reduce the radiation burden to the children.

The AAPD has endorsed every year since 1981 the American Dental Association (ADA) recommendations in their booklet. The ADA's most recent revised publication was published in 2012. In summary, a radiographic examination is only supposed to be conducted after a thorough clinical examination and after assessment of the patient's dental and medical history. Based on these findings, and for every patient individually, one has to decide which, how many, and how frequently radiographs have to be taken. Radiographs are only to be taken if there is an expectation that the diagnostic yield will affect the patient and if the patient can cope with the procedure (the justification principle of radiation protection). In the AAPD guidelines on prescribing dental radiographs for infants, children, adolescents, and persons with special healthcare needs, recommendations for ALARA are also made: collimation of the X-ray beam, proper use of shielding, and use of the most sensitive image detectors. Their guidelines or recommendations for bitewing intervals for caries detection are slightly different from the EAPD's. It appears that the AAPD would accept more radiographs being taken than EAPD. But the bottom line is that it has to be decided on a patient individual basis.

On a broader platform, there is "The Image Gently Alliance" [https://www.imagegently.org/About-Us/Campaign-Overview], which was initiated by the medical radiology profession, to make radiologists and radiographers aware of the fact that dose reduction for children does not impact image quality. The Image Gently Alliance started in 2006 as a committee within the Society for Pediatric Radiology and has since then reached out to other professional associations and academies to raise the awareness and knowledge of radiation dose reduction opportunities in pediatric imaging.

Extract from the Image Gently Alliance website [https://www.imagegently.org/About-Us/The-Alliance]:

> *"The Image Gently in Dentistry Campaign is designed to improve safety and effectiveness of pediatric imaging of the maxillofacial complex by informing dental professionals and parents about radiation safety best practices. The campaign, supported by the American Dental Association, the American Academy of Oral and Maxillofacial Radiology and other dental specialty groups, in concert with the Alliance for Radiation Safety in Pediatric Imaging, aims to raise awareness of the special considerations required in pediatric dental radiology, outlined in a* ***'Six Step Plan.'*** *The plan is based on the concepts of justification on the use and reduction of radiographic exposure in accordance with the* As Low As Diagnostically Acceptable, (ALADA) *principle."*

Further Reading

American Dental Association Council on Scientific Affairs. Dental radiographic examinations: recommendations for patient selection and limiting radiation exposure; 2012.

Espelid I, Mejare I, Weerheijm K. EAPD guidelines for use of radiographs in children. Eur J Paediatr Dent. 2003:40–8.

Graham DT, Cloke P, Vosper M. Principles of radiological physics. 6th ed. London: Churchill Livingstone, Elsevier; 2016.

Hendee WR, Russell Ritenour E. Medical imaging physics. 3rd ed. Hoboken: Wiley-Liss; 2002.

Iannucci JM, Howerton LJ. Dental radiography. In: Principles and techniques. 4th ed. Amsterdam: Elsevier Saunders; 2012.

Mettler FA Jr, Upton AC. Medical effects of ionizing radiation. 3rd ed. Amsterdam: Saunders Elsevier; 2008.

Oenning AC, Jacobs R, Pauwels R, Stratis A, Hedesiu M, Salmon B, On behalf of DIMITRA Research Group. Cone beam CT in paediatric dentistry: DIMITRA project position statement. Pediatr Radiol. 2018;48:308–16.

Whaites E, Drage N. Essentials of dental radiography and radiology. 5th ed. Amsterdam: Churchill Livingstone, Elsevier; 2015.

White SC, Pharoah MJ. Oral radiology. In: Principles and interpretation. 7th ed. Amsterdam: Elsevier; 2014.

Intraoral Radiography in Pediatric Dental Practice

3

Intraoral radiography means that the image detector is placed inside the patient's mouth and the X-ray machine positioned extraorally, aiming at the image detector. Because the image detector is placed close to the teeth, the detail in the image should be optimal and the distortion minimal. There are three ways of obtaining intraoral radiographs: parallel technique, bisecting angle technique, and occlusal technique.

3.1 Parallel Technique

Ideally, the image detector should be as parallel and close as possible to the teeth, with the X-ray beam aligned perpendicular to the image detector. This is the so-called parallel technique. This creates geometrically accurate images of teeth and alveolar bone levels. To obtain proper alignment one should use image detector holders which also properly align the X-ray machine with the image detector. An example of such holders was shown in Chap. 1 (Fig. 1.3). The advantage of this technique is the fact that there is an extraoral guide for the X-ray machine. In Fig. 3.1 one can see a representation of the ideal parallel technique for both the maxilla and the mandible. It is clear that the image detector cannot always be placed in contact with the tooth, due to anatomical restrictions (e.g., shape of the palate, the level of the floor of the mouth, or a mandibular torus). The parallel technique is obviously also used for bitewing radiographs (Fig. 3.1), as the image detector needs to be placed parallel to the teeth and the X-rays need to be aimed perpendicular at the detector, allowing for interproximal caries detection and interdental bone level assessment.

J. Aps, *Imaging in Pediatric Dental Practice*,
https://doi.org/10.1007/978-3-030-12354-3_3

For each image detector, as mentioned in Chap. 1, the proper image detector holder needs to be used. Several brands are available worldwide. Rinn® and Hawe Neos® are among the best known brands but in each country or continent individual manufacturers may provide similar and equally performing equipment. The most important aspect is that the image detector must be able to be placed firmly into the holder without the image detector to be subject to damage. For instance photostimulable phosphor plates are too thin to fit in the Rinn® XCP kit for analog film. Therefore one needs to make sure that the correct equipment is used. If the image detector is not snuggly fitting into the holder, the image detector may become dislodged and the image quality may be affected and require a retake. Worst-case scenario, the child may swallow or even worse inhale the plate when it gets dislodged from the holder.

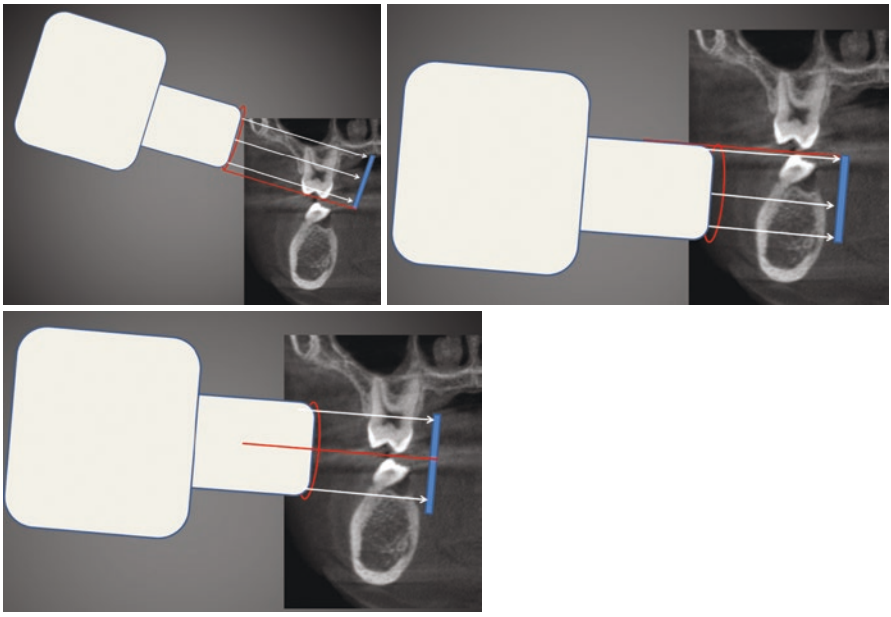

Fig. 3.1 The parallel technique illustrated schematically for a maxillary (left) and mandibular (right) right molar and for a bitewing radiograph (bottom image)

3.2 Bisecting Angle Technique

In some cases, the parallel technique cannot be performed as the patient does not tolerate the image detector placement parallel to the teeth. In that case, one can attempt the bisecting angle technique. This technique requires one to aim the X-ray beam perpendicular at an imaginary bisecting line between the long axis of the tooth

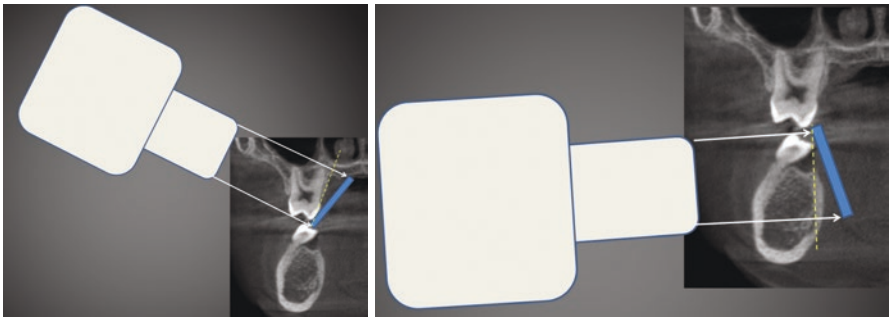

Fig. 3.2 Schematic illustration of the bisecting angle principle in the maxilla (right) and mandible (left). The yellow dotted line represents the imaginary bisecting angle between the tooth and the image detector

and the long axis of the image detector. The latter is placed against the teeth at an angle. This is a more difficult technique as there is usually no image detector holder involved with an extraoral guide to aid with the X-ray machine alignment. There is, however, an image detector holder on the market that allows for proper alignment using the bisecting angle technique: the Rinn® BAI (bisecting angle instrument). Unfortunately it is usually the image detector holder that causes issues for patients and as a consequence this holder is less frequently used. In Fig. 3.2 one can see a schematic illustration of the bisecting angle principle. The yellow dotted line is the imaginary bisecting angle between the long axis of the tooth and the long axis of the image detector.

3.3 Occlusal Technique

If neither the parallel nor the bisecting angle technique is possible, then one more alternative is still possible: the occlusal radiograph. For this technique, one uses best a photostimulable phosphor storage plate, as these come in different sizes and allow for proper placement in the patient's mouth. For primary teeth, a size 2 will suffice, while for permanent teeth a more useful size would be size 4. These images will not always produce the perfect geometrically aligned images as is the case with the parallel technique, but can still provide sufficient diagnostic yield.

The phosphor storage plate should be positioned on the occlusal plane as can be seen in Fig. 3.3.

3.3.1 Occlusal Radiograph in the Maxilla

The patient should be placed upright in the chair with the phosphor storage plate on the occlusal plane. The occlusal plane should be parallel to the floor, while the

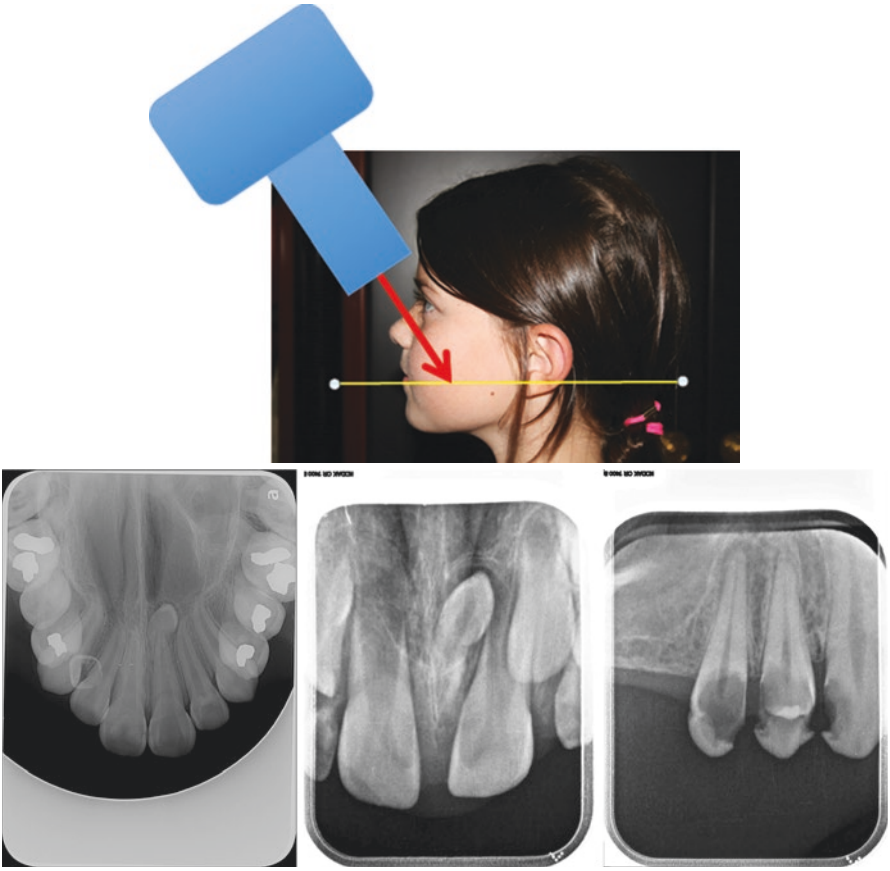

Fig. 3.3 The standard occlusal technique illustrated (yellow line represents the occlusal plane, the red arrow the X-ray beam aimed through the bridge of the nose at a 65° angle with the occlusal plane). At the bottom three examples of occlusal radiographic images of the maxilla are shown: left-hand-side image is a size 4 plate, middle and right-hand-side image is a size 2 plate

X-ray tube head is positioned at a 65° angle downward. For the anterior teeth, the X-ray tube spacer cone is placed at the bridge of the nose. This will produce an occlusal view of the entire maxilla and the anterior teeth in particular. For the posterior teeth, the angle of the X-ray machine remains unaltered, though the position of the X-ray tube head should be changed to the side one wishes to image. Figure 3.3 shows an example of that position and what an image could look like.

The anterior occlusal of the maxilla is especially indicated in case of dentoalveolar trauma, where placement of the image detector parallel to the incisors is difficult or impossible. Also for the detection of periapical pathology in early-childhood caries cases, this technique can prove to be very efficient.

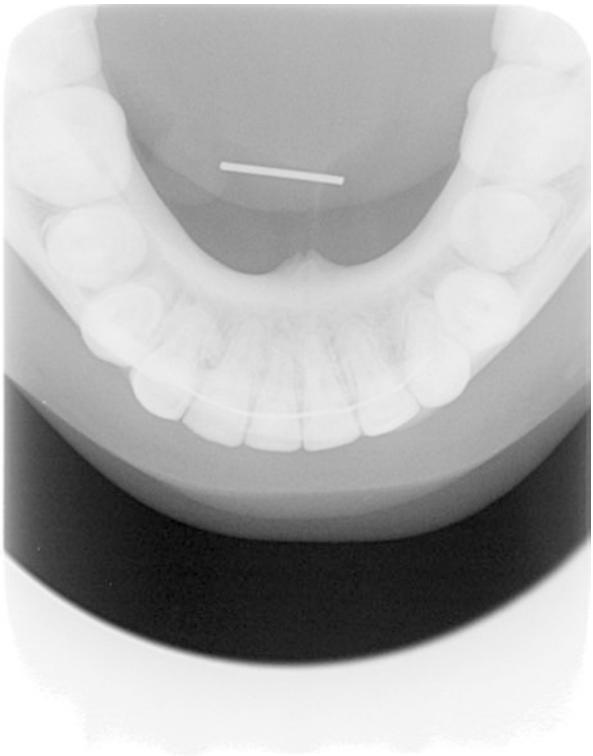

Fig. 3.4 Illustration of 90° angle occlusal images of the mandible (adolescent patient suffered a trauma, which resulted in a metal rod of about 15 mm being dislodged in the floor of the mouth)

3.3.2 90° Occlusal Radiograph in the Mandible

The 90° occlusal radiograph in the mandible provides a view of the floor of the mouth and the circumference of the mandible. This technique is ideal for imaging radiopaque sialoliths in the submandibular salivary gland, swellings on the buccal or lingual surfaces of the mandible, and foreign inclusions in the floor of the mouth.

The patient is placed upright in the chair and is asked to tilt the chin up, until the occlusal plane is perpendicular to the floor. The phosphor storage plate is placed on the occlusal plane and the X-ray tube head is then placed perpendicular at the plate. The phosphor plate can be placed with its long axis transverse or longitudinal. In Fig. 3.4 an example of such a view is shown. An alternative to patient placement is that the patient is placed supine in the dental chair and the occlusal plane is tilted until it is perpendicular to the floor. Obviously a similar image will result.

3.3.3 45° Occlusal Radiograph of the Mandible

The 45° occlusal radiograph provides a diagnostic image of the anterior mandibular teeth. Again the patient is placed upright in the dental chair, with the occlusal plane

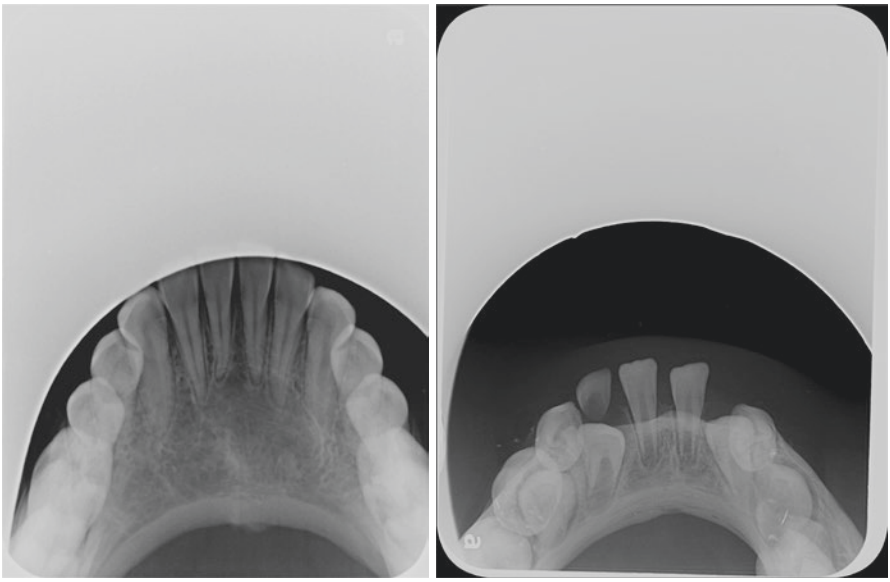

Fig. 3.5 Two examples of a 45° angle occlusal radiograph of the mandible

parallel to the floor. The phosphor storage plate is then placed on the occlusal plane and the X-ray tube is directed at a 45° upward angle through the chin. This provides a more comfortable situation for the patient than a periapical taken with the parallel or bisecting angle technique. In Fig. 3.5 one can appreciate an example of such a radiographic image.

3.3.4 25°–30° Occlusal Radiograph of the Mandible

This technique is a modification of the previous, as it is meant for the posterior mandibular teeth. The patient being upright in the chair, with the occlusal plane parallel to the floor, is asked to turn the head to the opposite side, in order for the X-ray tube to obtain enough place between the shoulder and the chest of the patient. The X-ray tube head is now tilted upward at a 25–30° angle. In Fig. 3.6 one can see an example of what the image might look like. It is obvious that there is a learning curve involved in this technique, as interproximal overlap and elongation or foreshortening can happen easily. Nevertheless this is a useful technique in young patients and patients who have difficulty with the image detector being placed parallel to the teeth.

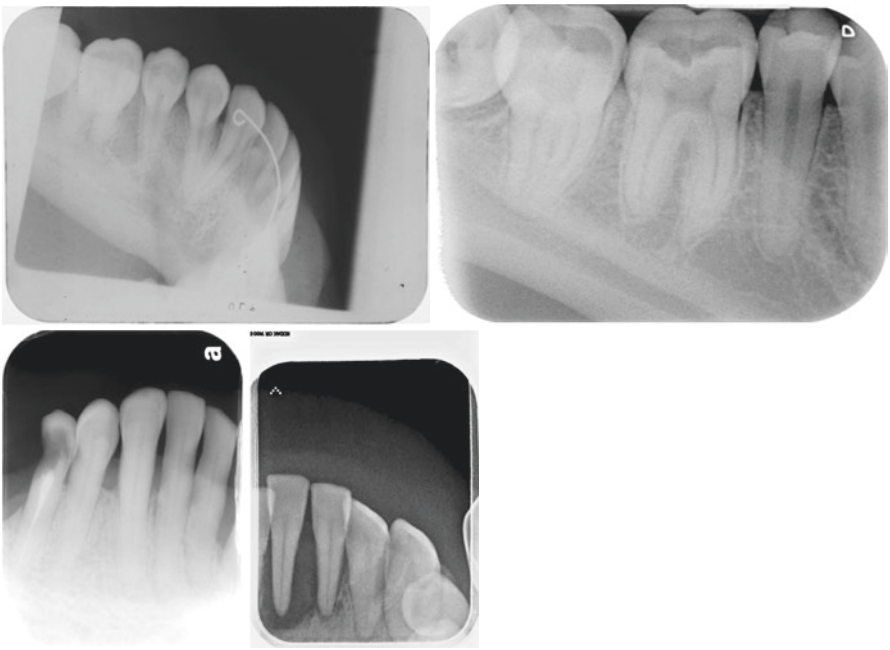

Fig. 3.6 Examples of oblique occlusal radiographs of the mandible. Top two images were taken in adolescent patients and bottom two images in an elderly patient with special needs

It is unfortunate that solid-state sensors are not available in larger sizes, like the phosphor storage plates. This implies that the techniques described for occlusal radiography can only be executed if one is using these plates. The largest size solid-state sensor allows one to capture an occlusal view of the deciduous incisors, but not of the molars. The most vulnerable part to the solid-state sensor is the cable and it is essential that the patient understands that biting it is not allowed. The same holds for the photostimulable phosphor plates which are vulnerable to bite marks. In the next section, some easy and cheap solutions are proposed to extend the lifetime of the plates.

3.3.5 Photostimulable Phosphor Storage Plate Protection

Since these techniques require the phosphor storage plate to be placed on the occlusal surface, one should try to protect them from bite marks and bending. Therefore the author has developed a simple and cheap technique to protect the plates, by simply taping two wooden tongue depressors around the plate (Fig. 3.7). The wood will not cause a shadow on the image and it will provide more than enough protection against biting by the patient.

Fig. 3.7 Protecting the phosphor storage plates from bite marks with wooden tongue depressors

An advantage of using the wooden tongue depressors is that one can see the tilting of the occlusal plane better. Also, if a younger child is sitting on a parent's lap during this procedure, the parent can help holding the plate in place while the spatulas provide information on the occlusal plane's tilt.

Historically intraoral radiographs have also been produced by placing the X-ray source inside the patient's mouth and a flexible cassette (pouch) with analog film outside of the patient's mouth and on the patient's face. This technique created beautiful radiographic images, of either the maxilla or the mandible, depending on where one placed the pen-like X-ray source inside the patient's mouth. Because of the high radiation to the thyroid gland when the mandible was imaged, or the lenses of the eyes, when the maxilla was imaged, the technique was deserted. In Fig. 3.8 an example is shown of such images. For the record, this technique cannot be executed anymore due to the high radiation dose!

Fig. 3.8 The machine used for intraoral radiography, with the X-ray source placed inside the patient's mouth. Illustrations of the images made with the X-ray source inside the mouth and the film in a flexible cassette held on the patient's face

Further Reading

Iannucci JM, Howerton LJ. Dental radiography. In: Principles and techniques. 4th ed. Amsterdam: Elsevier Saunders; 2012.

Whaites E, Drage N. Essentials of dental radiography and radiology. 5th ed. London: Churchill Livingstone, Elsevier; 2015.

White SC, Pharoah MJ. Oral radiology. In: Principles and interpretation. 7th ed. Amsterdam: Elsevier; 2014.

Extraoral Radiography in Pediatric Dental Practice

4

Extraoral radiography means that both the image detector and the X-ray machine are placed outside the patient's mouth. The X-ray source and the image detector have to be aligned in order to generate the desired image quality. There are two ways of obtaining extraoral radiographs: the first way is to work with a stationary X-ray source and image detector and the second is to have the X-ray source and image detector move in synchronicity in opposite directions. The first technique results in a plain radiographic image, while the other technique results in a tomographic image. The latter implies a focal trough, which ideally contains all the tissues one is interested in. More explanation is offered below.

4.1 Panoramic Imaging

The dental panoramic tomography is often called, depending on the region in the world, a panorex, a pan, an OPG, and a DPT, just to name some. They all refer to the same technique and the same image that is generated.

4.1.1 Technique Details

The technique implies that the X-ray source and the image detector move synchronously in opposite directions, with the image detector passing as close as possible to the patient's face. By doing so, one creates a focal trough, or a slice with a particular thickness. The thickness of the slice depends on the width of the X-ray beam. The narrower the beam, the thinner the slice. The latter means a more sharp image, but there is a limit of course.

Since the human head is not a sphere, a single pivoting point around which image detector and X-ray source revolve will not provide an optimal image result. Therefore the machines are constructed in such a way that multiple pivoting points are used, which follow the shape of the dental arches as close as possible. The focal

J. Aps, *Imaging in Pediatric Dental Practice*,
https://doi.org/10.1007/978-3-030-12354-3_4

trough of a panoramic image is therefore actually a three-dimensional horseshoe-shape slice through the patient's head, with the jaws in the focal trough (in focus).

Some machines allow for adjustments of that shape, while others don't. The latter are usually cheaper and assume that one size fits all. It is evident that this is incorrect and that if the shape of the jaw can be followed better, the image will be better as well.

The X-ray beam used in panoramic radiography is a vertical narrow slit beam, which can be adjusted (collimated) in height to accommodate for adult or pediatric settings. This collimation is essential when imaging children as it will reduce the radiation burden and avoid unnecessary parts of the head and neck to be exposed. The X-ray beam is also angled slightly upwards (8–12°), which explains why structures in the neck, like for instance a forgotten necklace, will be projected on the patient's chin in the final image (Fig. 4.1). The fact that the X-rays are angled upwards and are not passing through the patient from the front implies that the use of a protective apron to protect the lower positioned thyroid gland is not necessary. In fact, a protective apron, placed high in the patient's neck, will unfortunately result in an artifact in the image and might force one to retake the image without the apron. The latter would result in a higher radiation dose for the patient; hence it is better not to have the patient wear a radiation protection apron for panoramic radiographs. Local legislation should, however, always be respected.

It also deserves to be emphasized that the upward angulation of the X-ray beam causes distortion and magnification in a panoramic image, which is about 1.3 in magnitude. Therefore measuring tooth length or bone height for instance on a panoramic radiograph is not accurate at all, as differences in patient positioning may cause a different distortion in the final image.

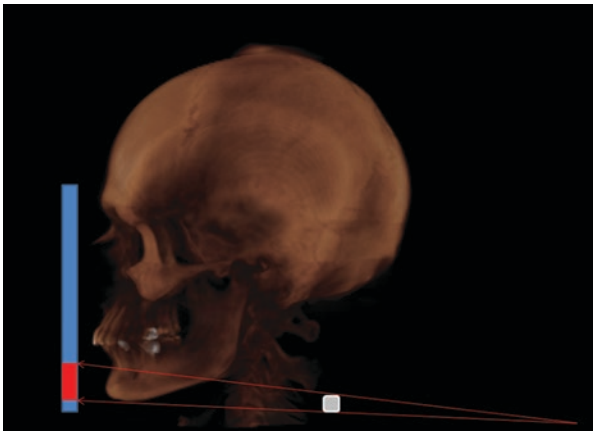

Fig. 4.1 Schematic illustration of the angled X-ray beam and the projection on the chin of structures in the neck: the gray square in the neck casts a shadow over the anterior part of the mandible, as the X-ray beam is angled upwards and aims from posterior to anterior. The blue rectangle represents the image detector and the red rectangle shows where the projection of the gray square will be superimposed over the real image of the mandibular symphysis

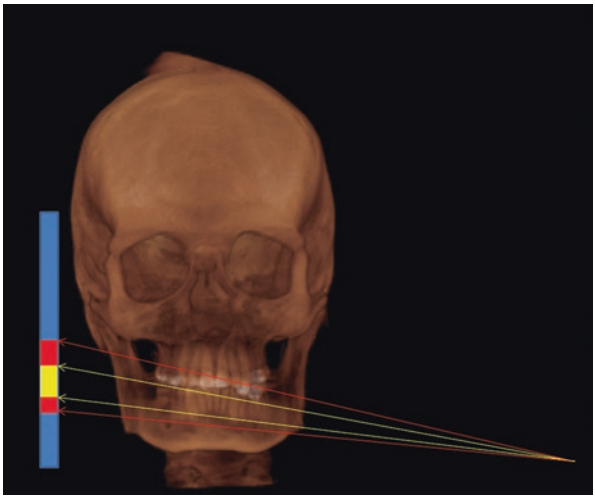

Fig. 4.2 Schematic illustration of the principle of ghost or phantom image in panoramic radiography: tooth 43 is in focus (yellow arrows from the radiation source), but tooth 33 is out of focus (red arrows from the radiation source). It is clear that the cast of tooth 43 (yellow rectangle) is smaller than the cast of tooth 33 (red rectangle). This principle of ghost imaging holds for all structures that lie between the radiation source and the focal trough (area in focus)

The most recent machines will produce an image with several focal trough layers, which ameliorates the image quality. However, this technology does not compensate for patient positioning errors, foreign object artifacts, or patient movement during the exposure. The radiation burden for the patient remains unaltered though with these multiple focal trough layers.

So-called ghost or phantom images are inherent to the panoramic tomography technique. Objects or structures lying between X-ray source and focal trough, and hence not in focus, will appear magnified, not sharp, higher (due to the angle of the X-ray beam), and on the opposite side in the image. Structures or objects that are positioned between the image detector and the focal trough will appear not sharp either, but will be projected narrower. The latter will, obviously, be projected on the same side as they are in reality. The principle of the formation of a ghost image is illustrated in Fig. 4.2. It should be emphasized that both anatomical (e.g., ramus of the mandible) and foreign objects (e.g., earrings) give rise to ghost images.

4.1.2 Patient Positioning

Patient positioning is paramount in order to obtain optimal image quality. Therefore it is necessary that one reads and respects the manufacturer's guidelines, as each brand is constructed differently. The angle of the X-ray beam differs per manufacturer which explains the differences in positioning instructions between them for

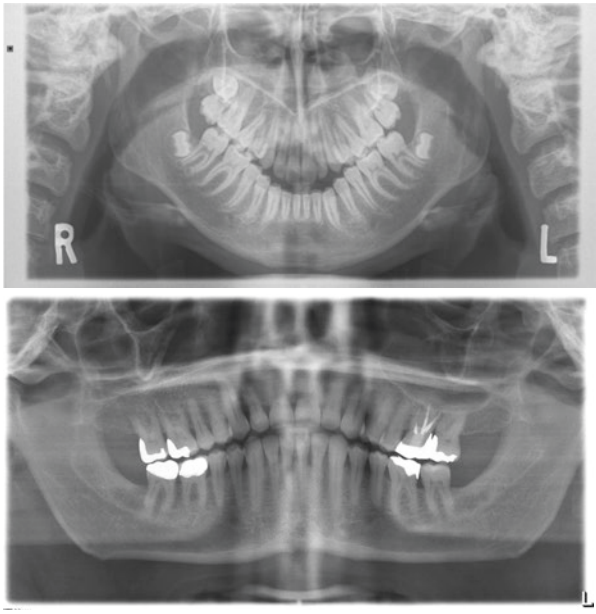

Fig. 4.3 The panoramic radiograph on the left-hand side shows a patient who was positioned with the chin too much down, resulting in a "smiling image" (Frankfort horizontal tilts down forward) and the panoramic radiograph on the right-hand side shows a patient who was positioned with the chin too much up, resulting in a "sad image" (Frankfort horizontal tilts down backwards)

the Frankfort horizontal. If the chin is too low (Frankfort plane tilts down to the front), the image will appear "smiling," whereas if the chin is positioned too high (Frankfort plane tilts down to the back), the image appears "sad." This is illustrated in Fig. 4.3.

The differences between the manufacturers in the size of the horseshoe-shaped focal trough explain the different instructions with regard to anterior-posterior positioning of the patient in the machine. The only plane that is always the same is the midsagittal plane of the patient's skull, which has to be in the middle of the machine and perpendicular to the floor. Lateral tilting of the head will result in increased distortion of the image. Use of the proper aids supplied with the machine (e.g., chin cup rest and temple supports) is required to make sure that the patient is positioned correctly in the machine. The patient's neck should be straight as well, which is usually accomplished by asking the patient to shuffle their feet forward, while supporting their back with your hand, until the tips of their shoes coincide with the same vertical line as their hands which hold on to the handle bars. The position should be as follows: if they would release the handle bars, the patient would tilt backwards. The examples shown in Fig. 4.4 are evidence of several different positioning errors.

In Fig. 4.5 one can see how to solve the positioning issue in a smaller child, if the machine cannot be lowered enough. If the machine cannot be lowered enough, then the patient would have to lift up the chin too much and the image would become nondiagnostic. In order to solve the problem, the patient can be placed on a step stool.

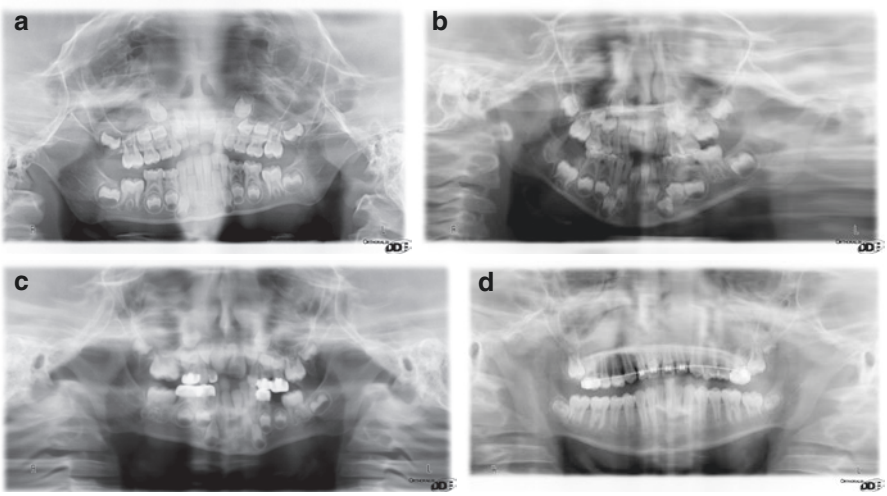

Fig. 4.4 Several positioning errors, different from the ones shown in Fig. 4.2, in panoramic radiography illustrated (**a**) chin up and head tilted down to the right, (**b**) midsagittal plane off to the right-hand side, (**c**) chin not on the chin rest and neck curved forward, (**d**) chin up, head tilted to the right-hand side and neck curved forward

Fig. 4.5 Four-year-old boy standing on a step stool while the dental radiographer is positioning the patient and giving instructions in order to obtain a diagnostic radiographic image

4.1.3 Patient Instructions

It is obvious that the patient must be able to cope with the technique of panoramic imaging. The revolving machine can be upsetting or worrying for some patients. Also, the patient needs to be able to understand the instructions. The patient is supposed to bite in end-to-end position with the maxillary and mandibular incisors positioned in a transverse slit on the bite block. This allows one to see the mandibular condyles better as they will be on their respective articular eminences instead of in their articular fossae. Then, once the positioning has been done according to the manufacturer's guidelines, the patient should be locked in that position, with the lips closed and the tongue against the hard palate. These two actions will allow one to see the apices of the maxillary teeth better in the final image, because both the lips and the tongue will have attenuated the incoming X-rays, which is not the case if the lips were open and the tongue was in the floor of the mouth. The latter results in a dark horizontal band in the image which obscures the view to the maxillary teeth's apices (Fig. 4.6).

It is also necessary for the patient to remove all metallic jewelry in the head and neck region, tongue piercings, lip or nose piercings, hair clips, etc. Also removable dentures or orthodontic appliances have to be removed, unless they don't contain metal. All of these will cause, besides a real image, also a ghost or phantom image, which can be projected over crucial anatomical landmarks. The latter will subsequently be obscured and the final diagnostic value of the panoramic radiograph will be degraded.

During the exposure the patient is supposed to be still at all times, and should not talk or swallow. The patient is not supposed to come out of the machine before told to do so. The latter is to avoid premature exiting the machine and damaging the

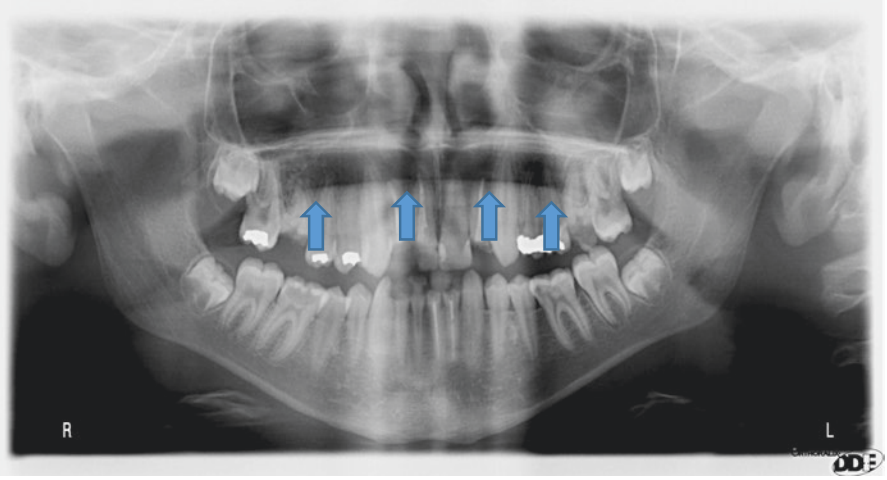

Fig. 4.6 A panoramic radiograph taken with the tongue not against the hard palate, showing a black band across the maxilla (arrows), obscuring the apices of the maxillary teeth

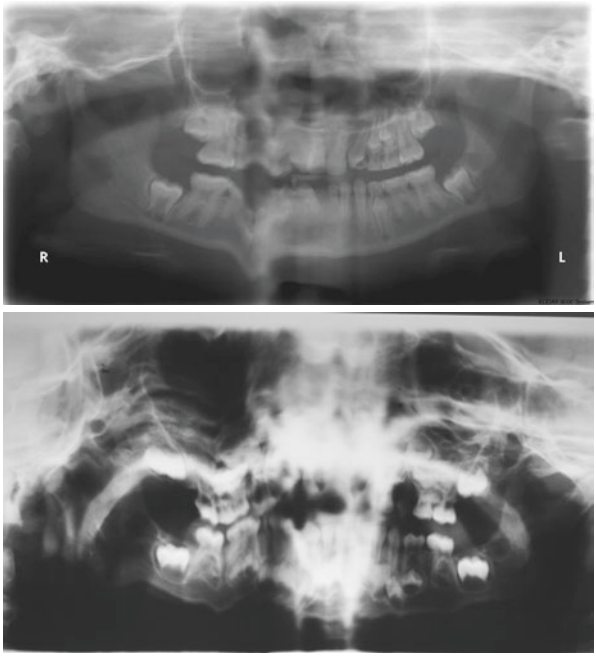

Fig. 4.7 Movement during the panoramic exposure results in severe image quality loss, as is illustrated in these panoramic radiographs of young children

machines' mechanical and rotating components and the patient from hurting themselves. Figure 4.7 is an example of an image during which the patient moved severely. One can appreciate the huge distortion in both maxilla and mandible.

4.1.4 Structures to be Identified on a Dental Panoramic Tomography

As is illustrated and documented in Fig. 4.8, both hard and soft tissues can be identified and will help one to extract diagnostic information from the radiographic image. Paramount is that one understands what normal anatomy can be identified on a panoramic radiograph, so that interpretation of pathology or aberrant anatomy will be easier.

4.1.5 Collimation of Panoramic Radiographs

An initial panoramic radiograph should include both mandibular condyles and rami in the image. However, if for follow-up a panoramic radiograph is required of a region that does not include the rami of the mandible, one can exclude that area from being exposed. The latter would reduce the radiation burden for the young patient. Some panoramic machines allow for segments in the image to be blocked out. This is useful in case one is only interested in the maxillary or mandibular teeth,

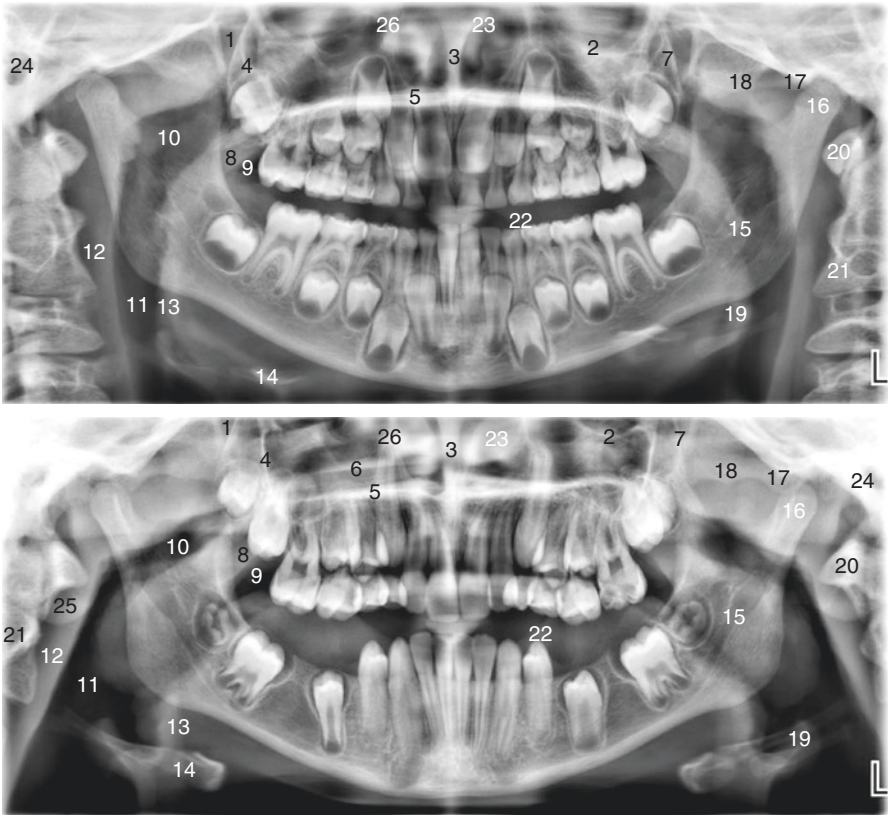

Fig. 4.8 Identification of anatomical landmarks on a panoramic radiograph: (*1*) pterygomaxillary fissure, (*2*) inferior border of the orbit, (*3*) nasal septum, (*4*) zygomatic buttress of the maxilla, (*5*) real image of the hard palate or the floor of the nose, (*6*) ghost image of the hard palate, (*7*) posterior wall of the maxillary sinus, (*8*) soft palate, (*9*) air space between tongue and soft palate, (*10*) air space of the nasopharynx, (*11*) air space of the pharynx, (*12*) posterior wall of the pharynx or anterior lining of the cervical spine, (*13*) tongue, (*14*) hyoid bone, (*15*) inferior alveolar canal, (*16*) mandibular condyle, (*17*) articular eminence, (*18*) zygomatic arch, (*19*) epiglottis, (*20*) anterior process of the atlas, (*21*) body of the axis, (*22*) open lips, (*23*) inferior nasal concha, (*24*) external acoustic meatus, (*25*) ear lobe, (*26*) lateral wall of the nasal cavity or medial wall of the maxillary sinus

or in the anterior region of both arches, for instance. The latter application is illustrated in Fig. 4.9.

4.1.6 Panoramic or Extraoral Bitewings

Some panoramic machines allow for so-called extraoral bitewing radiographs. From the literature there is evidence that this is a good alternative for intraoral bitewings, especially if patients cannot cope with intraoral bitewings. In fact, it is the author's

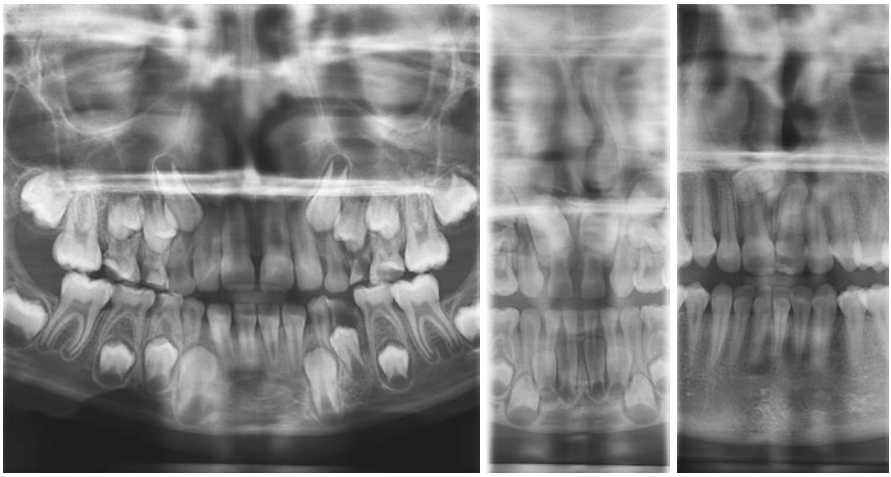

Fig. 4.9 Three examples of field reduced panoramic radiographs (courtesy of Dr. Marc Jeannin)

opinion that they should be called extraoral periapical radiographs. They show much more information than what is usually seen on a traditional bitewing radiograph (Fig. 4.10). Again paramount is the positioning of the patient, according to the manufacturer' guidelines, to obtain the best image quality possible, with the least of interproximal overlapping.

Panoramic images are associated with distortion and magnification and therefore are not reliable to be used to measure distances. Since there is a discrepancy between machine designs from different manufacturers, these distortions are different per machine brand. As mentioned above, positioning of the patient is paramount and obviously has an impact on the image quality and the just mentioned distortions and magnifications. Simultaneously, the shadows of the soft tissues and airway spaces may make diagnosis more challenging as they may mimic fracture lines.

If one has an analog film panoramic machine and wishes to convert to digital (and the machine is not too old and worth keeping it), one only needs to purchase a phosphor plate scanner that can handle panoramic phosphor storage plates. The cassette that one used for the films can be kept; however, the intensifying screen at the front latch of the cassette needs to be removed. Converting an analog film panoramic machine into a solid-state sensor operating machine is not possible and would be very expensive.

Anno 2019, there are probably very few manufacturers left worldwide that make panoramic machines for phosphor plate use.

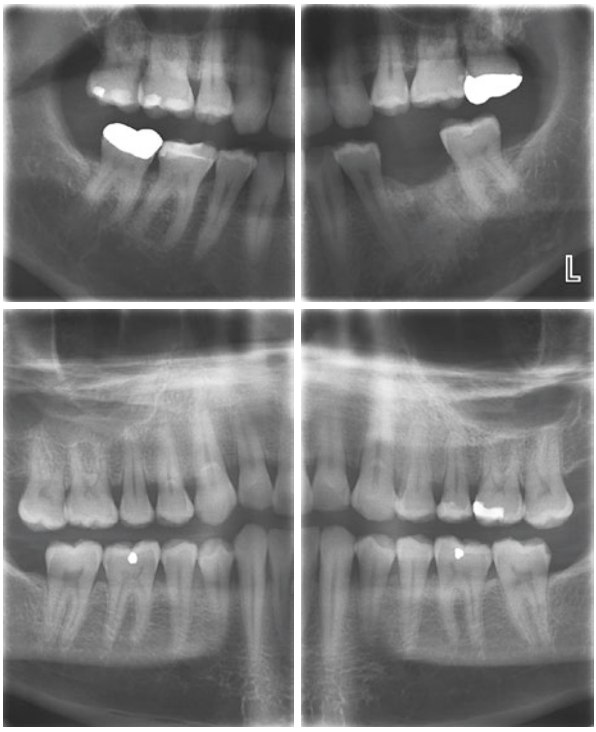

Fig. 4.10 Example of extraoral bitewing (courtesy of James Hughes, Planmeca® USA)

4.2 Cephalometric Imaging

The cephalometric radiograph is very often used in orthodontic and orthognathic surgery planning. The technique requires a specialized X-ray machine which provides a reproducible lateral skull view. That reproducibility is important as certain structures in the skull, and especially the sella turcica, have to be used as reference to verify the growth or impact of disease or surgery.

A dental cephalometric radiograph is therefore unique and that's exactly why the machine is equipped with a so-called cephalostat. This device helps positioning the patient with the midsagittal plane of the skull perpendicular to the floor, by putting an ear rod in each external acoustic meatus, while a support on the bridge of the nose reassures that the patient's head is in a natural position. The patient should have the teeth in occlusion during the exposure.

Some manufacturers use a one-shot approach, which implies a 1-s X-ray exposure and hence very little chance for motion artifacts. Other manufacturers use an anterior to posterior or vice versa scan of the skull, which takes several seconds, hence a higher chance for motion artifacts during the exposure. Some machines allow for collimation of the X-ray field, resulting in less radiation. The latter makes sense as for most orthodontic analyses one does not need the occipital bone nor the calvarium to be visualized.

Cephalometric images should always show the soft tissues overlying the face and neck, as these outlines are also used for planning purposes in several orthodontic and orthognathic analyses. By convention, the image is supposed to be viewed with the patient facing to the right-hand side.

The medical lateral skull radiograph differs significantly from a dental cephalometric image, as the first one does not use a cephalostat, and therefore reproducibility is impossible.

The cephalostat can also be rotated and allows one to take other skull radiographic projections: anterior-posterior skull, posterior-anterior-skull, submento-vertex skull, and any deviation or variation of the former positions. Since the use and availability of cone beam computed tomography (CBCT) have increased, most of these techniques have become obsolete, as these views of the skull can be easily regenerated from a CBCT scan.

The reader is referred to orthodontic and orthognathic textbooks for cephalometric reference points of interest. This lies out of the scope of this book. In Fig. 4.11 some important landmarks are marked on a cephalometric radiograph. These are not necessarily all used for orthodontic assessment, but are of importance when assessing the anatomy and possible pathology.

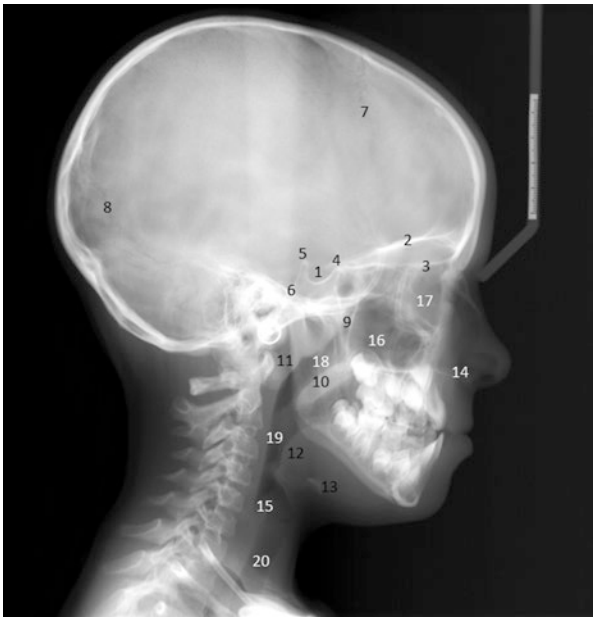

Fig. 4.11 Anatomical landmarks on a non-collimated cephalometric radiograph of an 11-year-old boy with a skeletal class III profile: (*1*) sella turcica, (*2*) roof of the orbits, (*3*) floor of the anterior cranial fossa, (*4*) anterior clinoid process, (*5*) posterior clinoid process, (*6*) clivus, (*7*) frontoparietal suture, (*8*) parieto-occipital suture, (*9*) pterygomaxillary fissures, (*10*) soft palate, (*11*) posterior wall of the nasopharynx, (*12*) tongue, (*13*) hyoid bone, (*14*) anterior nasal spine, (*15*) epiglottis, (*16*) maxillary sinuses, (*17*) orbitae and ethmoidal sinuses, (*18*) nasopharynx, (*19*) oropharynx, (*20*) larynx and trachea

Fig. 4.12 On the left one can see how the X-rays are pointed perpendicular at the cassette, which is held against the patient's nose and cheek. In the middle one can see the positioning of the cassette and the X-ray machine in a birds view perspective. On the right is an example of an oblique lateral radiograph taken in a child with autism spectrum disorder, who had eruption issues

4.3 Oblique Lateral Radiograph

This technique is overlooked by many, but definitely has a place in pediatric dentistry imaging. It can be a very good source of diagnostic information in the hands of an experienced user. This being said, it is needs to be emphasized that there is a learning curve to produce good oblique lateral radiographs.

For this technique one needs a stiff cassette with a phosphor storage plate inside and an X-ray machine that is used for intraoral radiography. The exposure time is 0.16 s at 65 or 70 kV. The image detector should not bend as that would cause significant distortion in the image, rendering the image nondiagnostic.

The cassette should be held against the side one wishes to image, and should be in contact with the tip of the nose and the cheek (see Fig. 4.12). Part of the cassette should be inferior to the inferior border of the mandible. Subsequently the patient has to turn the head towards the side the cassette is leaning against. This creates a radiographic keyhole on the opposite side between the cervical spine and the posterior border of the ramus of the mandible. The X-ray machine, with circular collimator, is now aimed perpendicular at the cassette, with the central X-ray beam following the occlusal plane. For the latter one can use the lips as a guide. If the geometry was correct, the image should be a perfect circle. If one sees an oval, it means that the X-rays were not aimed perpendicular at the cassette. It is obvious that this technique is only to be considered an alternative for a panoramic radiograph or a periapical or bitewing radiograph in cases where patients are not able to cope with the procedure.

The oblique lateral technique is an underestimated tool in pediatric dentistry and in dentistry for patients with special needs. Obviously the learning curve is steep if one doesn't use it often. The most important thing to remember when executing this technique is to make sure that the cassette is leaning against the patient's cheek and nose and that one aims the X-rays

perpendicular at the cassette. This technique can also be used under general anesthesia. The cassette can then be taped around the patient's head instead of someone holding it in place (radiation protection rule saying one should not be in the primary radiation beam if one is not the patient). Distortion in the image is a major factor, especially if one was not able to aim the X-rays perpendicular at the cassette.

4.4 Cone Beam Computed Tomography (CBCT)

4.4.1 Technique Details

As the name of the technique implies, the shape of the X-ray beam is conical. The X-ray beam revolves only once around the patient's head (single rotation) while the image detector moves in synchronicity on the opposite side of the skull. The image that is obtained is therefore a cylinder and is captured as a whole and not in segments as is the case in multislice computed tomography (MSCT). The latter technique, also called medical CT, uses a fan-shaped beam which revolves multiple times around the patient (see Chap. 5).

For CBCT, one has to decide where the pivoting point or rotation axis is positioned, in order to get the region of interest in the center of the scan volume. The latter is impossible with MSCT.

Some manufacturers allow for the field of view, or the size of the volume that is scanned, to be changed. For the clinician it is important that the field of view covers the area of interest. That means that if the area of interest is small, the field of view, ideally, should be small and vice versa. The latter implies that some machines, due to their design, do not allow the field of view to be altered, and therefore might be covering much more volume than they should.

The design of the machines also differs between manufacturers. There are machines that have a chair fixed to the machine (e.g., Morita® Accuitomo 170) and there are machines that have no chair (e.g., Planmeca® 3D Max). The latter usually allows for patients to either stand, or sit on a stool, or sit in a wheelchair for the exposure. It is obvious that the wheelchair should not interfere with the machine. In machines with a chair, the patient will be moved to the correct position for the axis of rotation to fall through the center of the region of interest. In machines that have no chair attached to its frame, the C-arm will maneuver around the patient's head to ensure the correct position of the rotation axis. The resulting images from both machines are similar.

The positioning of the patient's Frankfort horizontal is somewhat less crucial than for panoramic radiography, as the obtained image volume can always be reoriented for assessment. That does not mean, however, that the patient can be placed in the machine in any position. The field of view should coincide as much as possible with the area of interest (ALARA, see Chap. 2) and as such correct and accurate positioning is still required.

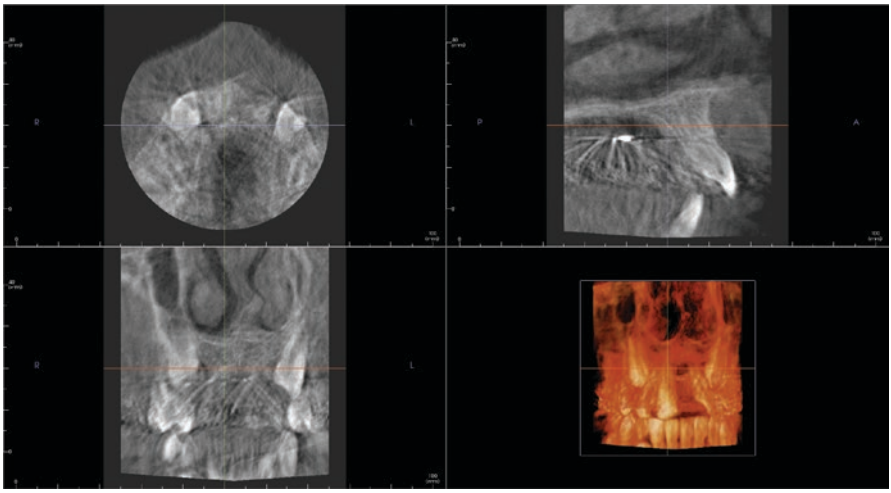

Fig. 4.13 Example of the poor quality of a CBCT taken in a 10-year-old boy, who wiggled his feet during the CBCT exposure

A so-called scout view is used to check the positioning. It exists of a low-radiation-dose lateral and anterior-posterior radiograph which shows in two dimensions how large the field of view is and if the region of interest is entirely included in the field of view.

Then there is the resolution of the image. The resolution has to be decided before the patient is exposed. It deserves to be emphasized that the higher the resolution, the higher the radiation dose will be, as the exposure time will increase. This has to be balanced with the goal of the study. A high resolution (e.g., 76 μm) is indicated for endodontic purposes, while a lower resolution (e.g., 200 μm) would suffice for root resorptions or eruption issue cases.

Some manufacturers allow to alter the rotation arc of the machine, for instance from 360° to 180° rotation. This reduces the radiation dose with approximately 50%, without affecting the image quality significantly. The latter should be considered when imaging children (cfr. Chap. 2).

Paramount is that the patient must be still during the exposure, as motion artifacts are detrimental to the image quality and hence the diagnostic yield (Fig. 4.13).

4.4.2 Image Details

Since this is a three-dimensional image, the image is built out of voxels (volumetric picture elements or pixels). The voxel size determines the resolution capacity of the image. The smaller the voxels the higher the accuracy or detail of the image.

The viewer will show the image in three orthogonal planes: axial, coronal, and sagittal (Fig. 4.14). One can navigate through the three planes to analyze the image in all three planes. Most software will also provide a three-dimensional

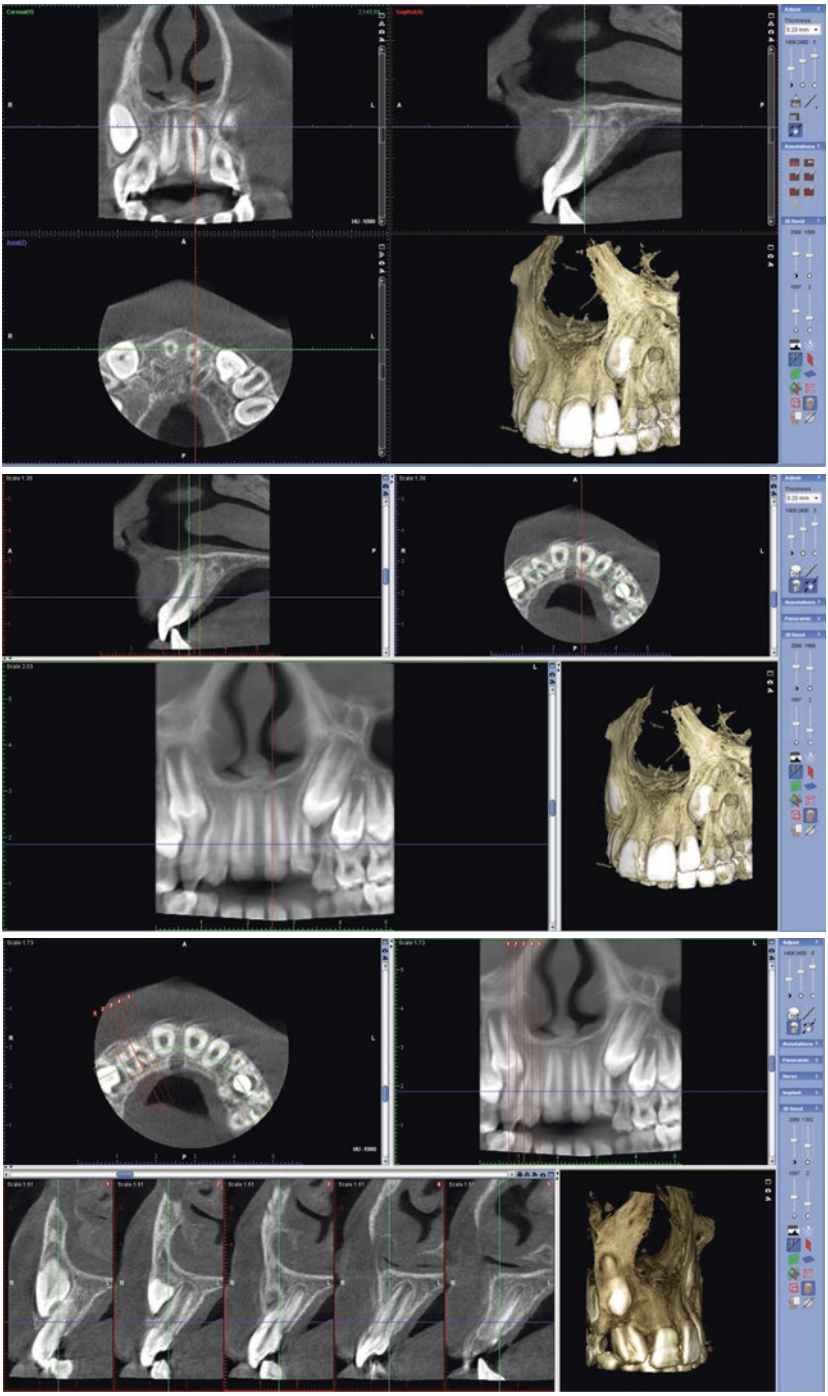

Fig. 4.14 An example of a typical screen in CBCT with three orthogonal planes and a 3D reconstructed image of the scan (top). The panoramic reconstruction of the same volume (middle) and some of the transverse slices (bottom)

reconstructed example of the scan. This is rarely used for diagnostic purposes, but can visualize the anatomy or pathology better in some cases.

Once the image has been acquired, one should reorient the volume so it can be viewed in all three planes under the best circumstances (e.g., anterior nasal spine and posterior nasal spine parallel to the floor). Once that is done, adjusting of contrast and brightness (so-called windowing) has to be performed to ensure that all details can be seen well. However, the latter does not mean it cannot or should not be changed afterwards, nor does it mean that it will be ideal for everyone who is assessing the images. Everyone may have their preference windowing. Subsequently the three orthogonal slices should be scrolled dynamically, in order to check for pathology and/or aberrant anatomy. This is also called paging or going through the image stack in cine mode. Since there are hairs visible in all three planes, one can always check which structures are viewed and at which level they are sliced. It needs to be emphasized that if the orientation is changed, the slices change as well (non-orthogonal slices) and being able to check the other two orthogonal planes is extremely useful.

Typical for CBCT and dentistry is the panoramic reconstruction option, for which a line with a focal trough can be drawn on the axial slice of the image volume. The software then makes perpendicular cuts through that panoramic line, to create transverse or cross-sectional slices (Fig. 4.14). The width of the slices as well as the distance between the slices can be changed. One should be cautious with these panoramic reconstructions, as what is outside of the focal trough will not be visible in the image at all, as is the case in real panoramic radiographs, albeit blurry. That being said, it can be useful to increase the slice thickness (ray sum) to inspect thicker slices of bone for pathology (Fig. 4.15). Full-thickness ray sum images can be used to reconstruct a cephalometric image for instance. One should keep in mind that

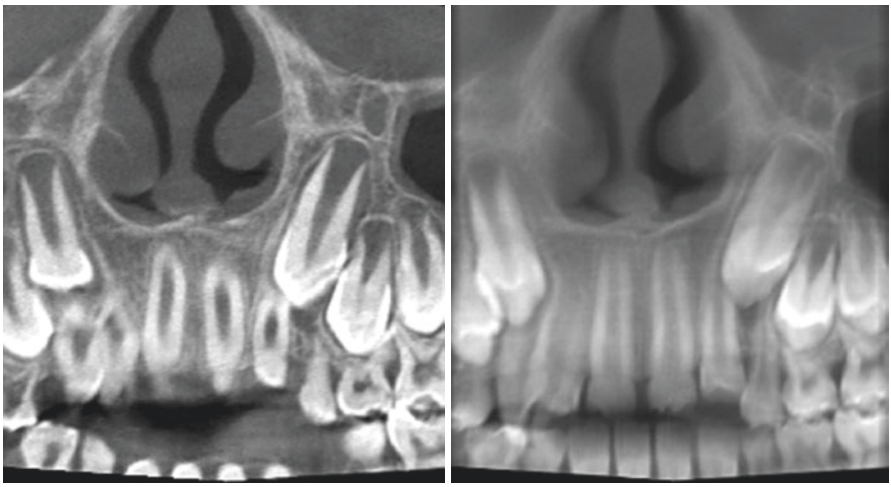

Fig. 4.15 Example of a 1 mm thin image slice (left) versus a 10 mm thick image slice (right) of the same patient as in Fig. 4.13

these full ray sum images are negatively affected by anatomical noise, due to superimposition of multiple structures in the skull.

Measurements on CBCT are accurate, as the image in CBCT has isotropic voxels. This means that the width, depth, and height of the voxel are identical, which allows one to measure as accurate as the resolution is (e.g., if a CBCT image is made at 200 μm and a tooth is measured to be 20 mm long, then that measurement is 20 mm ± 0.200 mm).

There are a few very important aspects of CBCT one has to remember:

- There is no differentiation possible between the different soft tissues. Due to poor soft-tissue contrast, all soft tissue looks homogenously gray. That means one cannot distinguish between lymph nodes and salivary glands and muscle for instance. This makes CBCT useless for soft-tissue pathology, but very useful for assessing bone and teeth. However the gingiva can be better visualized when cotton rolls are positioned in the buccal folds or if the patient is asked to blow up the cheeks during the scan. Both the latter cause the cheeks to be pushed away from the gingiva, which allows one to measure gingiva thickness in CBCT.
- Radiopaque materials, like gutta-percha or metals, will cause streaking artifacts in the axial plane. The latter is important to know when assessing possible root fractures in endodontically obturated teeth. The black streaks in the axial view can mimic a fracture line.
- Also radiopaque objects outside the field of view (e.g., earrings, stainless steel crown), but in the radiation beam, can cause axial streaking artifacts. This means that patients should remove all metallic jewelry in the head and neck region, including tongue piercings, lip and nose piercings, and hair clips. Also removable dentures or orthodontic appliances have to be removed, except if they don't contain metal.
- It is almost impossible to compare radiation doses from different CBCT machines, as there is no standardization regarding field of view and exposure parameters. Publications about radiation dose and CBCT should always be interpreted carefully as the type of machines used in different studies influences greatly the outcome of the study.

Cone beam computed tomography (CBCT) is currently overused by several clinicians as many forget about the radiation dose aspect and potential impact and only see the aesthetic aspects of the images, which are a great selling point towards patients and their parents. The attractiveness of the image should not be the reason why one submits a young child to CBCT. As always the three basic principles of radiation protection (Chap. 2) hold: justification—limitation—optimization. Only if the three-dimensional information would affect the diagnosis and/or the treatment plan, CBCT is justifiable. Confirmation of what is known from clinical examination and two-dimensional imaging information is not a legitimate reason for CBCT.

Another fact that one should know is that there is currently absolutely no intention among manufacturers and/or regulatory agencies to standardize the exposure parameters and the field of view of CBCT units. The latter makes it very difficult to identify the CBCT machine that is best suited for pediatric dentistry. The size of the field of view is probably the most important aspect when attempting to keep the radiation dose as low as possible. In the second place, there is the option to reduce the rotation arc, which then reduces the radiation dose. At the same time, one needs to keep the optimization principle in mind as well, because if high-detailed images are required, the radiation dose will be higher as well due to the higher mA and longer exposure time settings. In other words, the justification principle will determine if there is a need for a CBCT and then the individual case will determine what resolution is required. Essentially there is no difference with any other exposure to ionizing radiation: justification—limitation—optimization (Chap. 2).

4.4.3 Radiation Dose Considerations

Despite the fact that more dental offices have CBCT at their availability and that CBCT is abundantly used in dentistry these days, one should not forget that its radiation dose is higher than that of conventional two-dimensional dental radiographs (see Table 2.1). However, that does not mean that there is no place for CBCT in pediatric dentistry. Complicated dentoalveolar trauma, eruption issues, and endodontic complications are a few examples of when CBCT can be used if two-dimensional images do not provide sufficient diagnostic information.

There are some golden rules to remember when considering radiation dose and CBCT:

- There is a proportional linear relationship between radiation dose and mA setting of the machine. The absorbed radiation dose at 5 mA is half of the dose absorbed at 10 mA.
- There is a proportional linear relationship between the radiation dose and exposure time. If the exposure time is doubled, then so does the radiation dose.
- There is a proportional linear relationship between the radiation dose and the resolution of the image. The latter goes hand in hand with exposure time and therefore an image taken at 400 μm will result in half the radiation dose as the image taken at 200 μm.
- The effect of kV on the radiation dose is exponential, which means that changing the kV does not necessarily result in a huge change in radiation dose.

One should, however, keep in mind the ALADA (as low as diagnostically acceptable) principle and therefore reducing the radiation dose beyond the diagnostic acceptable level is not desirable.

As mentioned before in this chapter, interpretation of published data on radiation doses from different CBCT machines is difficult as all manufacturers use different exposure parameter settings: mA, kV, exposure time, resolution, and field of view. Therefore it is difficult to answer questions about which machine is better or worse in terms of radiation burden for the patient. The latter implies that one has to know and understand the principles of radiation physics and the characteristics of the machine one is using. Adjusting of exposure parameters is possible, but should be done with caution. Most manufacturers' standard settings are selected because they produce good crisp images, which does not mean that they should not be altered to reduce the radiation dose in children, under the condition that the diagnostic yield isn't altered.

Further Reading

Goulston R, Davies J, Horner K, Murphy F. Dose optimization by altering the operating potential and tube current exposure time product in dental cone beam CT: a systematic review. Dentomaxillofacial radiology. 2016;45:20150254.

Graham DT, Cloke P, Vosper M. Principles of radiological physics. 6th ed. Amsterdam: Churchill Livingstone, Elsevier; 2016.

Hendee WR, Russell Ritenour E. Medical imaging physics. 3rd ed. Hoboken: Wiley-Liss; 2002.

Iannucci JM, Howerton LJ. Dental radiography. In: Principles and techniques. 4th ed. Amsterdam: Elsevier Saunders; 2012.

Mettler FA Jr, Upton AC. Medical effects of ionizing radiation. 3rd ed. Amsterdam: Saunders Elsevier; 2008.

Oenning AC, Jacobs R, Pauwels R, Stratis A, Hedesiu M, Salmon B, on behalf of DIMITRA Research Group (http://www.dimitra.be). Cone-beam CT in pediatric dentistry: DIMITRA project position statement. Pediatr Radiol. 2018;48:308–16.

Pauwels R, Seynaeve L, Henriques JCG, de Oliveira-Santos C, Souza PC, Westphalen FH, Rubira-Bullen IRF, Ribeiro-Rotta RF, Rockenbach MIB, Haiter-Neto F, Pittayapat P, Bosmans H, Bogaerts R, Jacobs R. Optimization of dental CBCT exposures through mA reduction. Dentomaxillofacial Radiology. 2015;44:20150108.

Ribeiro Nascimento HA, Almeida Andrade ME, Gomes Frazao MA, Nascimento EHL, Ramos-Perez FMM, Queiroz Freitas D. Dosimetry in CBCT with different protocols: emphasis on small FOVs including exams for TMJ. Braz Dent J. 2017;28(4):511–6.

Rottke D, Patzelt S, Poxleitner P, Schulze D. Effective dose span of ten different cone beam CT devices. Dentomaxillofacial Radiology. 2013;42:20120417.

Theodorakou C, Walker A, Horner K, Pauwels R, Bogaerts R, Jacobs R, The Sedentexct Project Consortium. Estimation of pediatric organ and effective doses from dental cone beam CT using anthropomorphic phantoms. Br J Radiol. 2012;85:153–60.

Whaites E, Drage N. Essentials of dental radiography and radiology. 5th ed. Amsterdam: Churchill Livingstone, Elsevier; 2015.

White SC, Pharoah MJ. Oral radiology. In: Principles and interpretation. 7th ed. Amsterdam: Elsevier; 2014.

Additional Imaging Techniques in Pediatric Dental Practice

5

This chapter contains information on machines and techniques not covered in the previous chapters. However, that doesn't mean these are not used in pediatric dentistry; it is just that most of them are not available in a private dental setting, as either they are very specialized and require specially trained radiographers and technicians to operate the machines or the technology is very expensive and will only be found in hospitals. Nevertheless, pediatric dentists should be aware of these techniques and imaging modalities as they might be faced with medically compromised patients requiring this type of imaging. Just as with the techniques described and discussed in the previous chapters, every technique has its applications and indications, as well as contraindications.

5.1 Multislice Computed Tomography (MSCT)

Sir Godfrey Hounsfield invented computed tomography in 1973. Since then many improvements have been realized to increase image quality and patient comfort. Professor Willi Kalender is credited for his significant contributions to develop helical computed tomography. Commonly this technique is called "a CT." It is however very different from the cone beam computed tomography (CBCT) that was discussed in Chap. 4. Multislice CT uses a narrow fan-shaped beam, which revolves around the patient, while on the opposite side of the patient image detectors capture the image. The patient is simultaneously moved slow or fast through that X-ray field. If it is done fast, the resolution will be low, as the slices will be thicker (large pitch), whereas if the patient is moved slowly through the X-ray field, the slice thickness is thinner (smaller pitch) and hence the resolution is higher (maximum 350 μm, compared to CBCT where the highest resolution today is 70 μm). However, one has to keep in mind that the higher the resolution, the higher the radiation dose will be. These machines require the patient to lie absolutely still on a table, while the table is moved into the machine's gantry.

J. Aps, *Imaging in Pediatric Dental Practice*,
https://doi.org/10.1007/978-3-030-12354-3_5

At the writing of this chapter, the fourth-generation CT scanners have been developed and are referred to as stationary-rotate geometry scanners as the X-ray tube rotates within a stationary circle of detectors. Technology allows the detectors to be arranged in a continuous circular array containing as many as 40,000 individual detectors. Whereas in the past scanning time could be substantially long (minutes), today that scanning time is merely a few seconds anymore. The latter causes less movement artifacts to be present in the image, which is a great advantage. However, the resolution of the image can be affected negatively by this fast scanning, as the patient is moved faster through the gantry. Reducing the speed would increase the resolution, but also the radiation dose. It is obvious that this is a trade-off that needs to be made for the pathology one is investigating. That decision lies with the radiologist/radiographer team. An example of a CT machine is shown in Fig. 5.1.

MSCT is ideal for hard- and soft-tissue imaging and as its exposure settings and algorithms are standardized one can obtain information about the type of tissue one is assessing. The soft-tissue resolution is much better than that of CBCT and one can distinguish several tissues from one another. The technique also allows for the use of so-called Hounsfield units. These units allow for finer diagnosis in assessing the nature of a lesion or a tissue. In Table 5.1 the Hounsfield units are shown.

Fig. 5.1 An example of a CT machine (General Electric®, courtesy of GE® website)

Table 5.1 Hounsfield units for several organs and tissues

Tissue	CT number
Cortical bone	+1000
Fresh blood (trauma and hemorrhage)	+200
Muscle	+50
Brain: white matter	+45
Brain: gray matter	+40
Cerebrospinal fluid	+15
Water	0
Fat	−100
Lung	−200
Air	−1000

It is obvious that MSCT, because of its high radiation dose associated, is not an imaging modality one would order for common dental pathology, such as dentigerous cyst or radicular cyst. However, patients who suffered a severe trauma with risk of intracranial hemorrhage would benefit from being submitted for MSCT immediately after the accident, as it could save their lives, because the CT images would be able to show the bleeding.

MSCT has its place in pathology diagnosis and as such children suffering from systemic disease or pathology, involving both hard and soft tissues, would benefit from this technology (e.g., abdominal and brain tumors).

Typical effective doses from MSCT vary between 2000 and 16,000 μSv, whereas for panoramic radiography it is around 24 μSv and for CBCT it varies between 5 and 500 μSv. From these figures, it is clear that MSCT is not indicated in routine pediatric dental care. The main reason for the higher radiation doses in MSCT is the fact that MSCT uses significantly higher mA values than CBCT or two-dimensional imaging modalities.

Hybrid imaging systems combine MSCT with additional imaging modalities, such as positron-emission tomography (PET-CT) and single-photon emission computed tomography (SPECT-CT), and are used in cancer diagnosis and follow-up. The patient is therefore injected with a radiopharmaceutical (e.g., ^{18}F-2-fluoro-2-deoxy-D-glucose or Technetium 99m), which emits radiation that is picked up by a special scanner. In fact, the patient is emitting the radiation and is actually radioactive for a given time. As exponential breakdown of the radiopharmaceutical occurs, the time between injection of the radioisotope and the scan is to be accurately timed. Proper caution, in terms of contact with other people and discarding human waste, is required when patients are being injected with these products. The images acquired from the PET or SPECT are merged with the MSCT image to enable the diagnostician to accurately identify the affected organ(s) and/or the extent of the pathology (also called functional imaging). CT perfusion is another illustration of CT that is used to visualize the functional blood flow. It is obvious that all these are beyond the scope of this book.

Medical CT is obviously not available in dental offices; however, a pediatric dentist should have enough knowledge about this technology to know when to refer a patient. In most cases, this will be coordinated with other care givers in the medical field (e.g., *pediatrician, oncologist, ENT specialist). For common dental pathology in children medical CT will never be used. Pediatric dentists working in a hospital environment will probably be more exposed to patients who need a medical CT examination or a combination of CT and MRI (see below).*

5.2 Magnetic Resonance Imaging (MRI)

In the beginning this technique was called nuclear magnetic resonance (NMR), but the public's erroneous perception that there was a connotation with nuclear energy made the medical profession change the name to magnetic resonance imaging (MRI). This technique does not use ionizing radiation, but magnetism and the fact that hydrogen atoms, hence the original name nuclear imaging, can be influenced in their precession when a high magnetic field is applied.

The principle is to place the patient in a very strong magnetic field (1.5 or 3.0 T), several times higher than the earth's magnetic field (approximately 0.5 μT). This will have an effect on the hydrogen atoms (protons) in the human body, which can be considered as positively charged randomly spinning tops. These hydrogen atoms will respond to the high magnetic field and will start spinning in a particular direction and at a specific speed and with a particular magnitude. Since the hydrogen content is different per type of tissue in the body, every type of tissue will result in a different signal. When the magnetic field is turned off, the hydrogen atoms return to their resting state. The speed of this depends on the tissue. The software translates these returns into an image of gray values, which allows for differentiation between soft tissues very well. Therefore MRI is the preferred technology to image soft tissue and soft tissue pathology. Tissues with a lot of hydrogen atoms will give a strong signal (e.g., salivary glands are bright white) and tissues with a low amount of hydrogen will result in a low signal (e.g., cortical bone is black).

Several so-called sequences can be used, which result in images with differences in appearance of the tissues. In a T1 sequence, fat will give a high signal (white), while water will give a low signal (dark), whereas in a T2 sequence, water will give a high signal (white) as will fat. Some other examples of particular sequences that are used are spin echo, fluid-attenuated inversion recovery or FLAIR, short time inversion recovery or STIR, and turbo spin echo or TSE.

In Fig. 5.2 one can appreciate the design of the MRI machine. There is some resemblance with the MSCT machine, but as explained the technology is completely different. Caution is required when entering the MRI area in the hospital. All ferromagnetic materials need to be banned from the room and its immediate surroundings as it would cause harm to the patients and damage the machine. Since the magnetic field in the MRI is several hundred times stronger than the earth's magnetic field (30 μT near the equator and 70 μT at the poles), objects like scissors, oxygen tanks, and metal carts would be attracted into the magnet with great force. Accidents have happened and as such precaution is key when entering the zone around an MRI machine. Audible and visual signaling is always in place to announce visitors of potential risks entering the zone.

MRI in pediatric dentistry is indicated if the patient has soft tissue pathology that requires imaging (e.g., ranula) or a temporomandibular joint disorder that affects the muscles and/or condylar disc. In the latter case MRI will enable one to visualize the disc clearly (low signal as the disc does not contain as much hydrogen atoms as muscle for instance) in the joint space.

Fig. 5.2 An example of a Siemens® MRI machine (courtesy Siemens® website)

One has to keep in mind that MRI machines produce a banging sound (sometimes more than 95 decibels, which requires earplugs or headphones to be worn by the patient), which might be frightening and which may require the child to be sedated. Claustrophobia is another issue as often a mask (magnetic coils) is placed over the patient's face, which again may be a reason for the child to be sedated.

5.3 Ultrasonography

Ultrasonography or echography is another imaging modality that does not use ionizing radiation. However, compared to MRI, this machine is very cheap (millions of dollars versus thousands). This technique is probably best known for its application in OBGYN medicine to visualize the unborn child in the womb. The technique uses ultrasonic waves which are generated in a piezoelectric crystal inside the so-called transducer, which not only emits but also receives the ultrasonic waves. An example of a linear and hockey stick-type transducer is shown in Fig. 5.3.

The speed of sound is affected by the compressibility of the medium (acoustic impedance); therefore it travels faster in rigid materials which are more resistant to compression and it travels slower in fluids and gases as these are more susceptible to compression. Reflection of the sound is paramount in this technique as the sound will be reflected at boundaries of tissues. Tissues or pathology that reflect little to no sound waves will produce no "echo," hence the jargon hypoechoic or anechoic, respectively, whereas tissues or pathology that do reflect the sound waves will return an echo and will be identified as echoic or hyperechoic (high signal or white shadow).

The particular characteristics of each of the soft tissues will enable one to distinguish between them (e.g., healthy salivary gland tissue shows a homogenously gray echo, whereas muscular tissue is hypoechoic). When the ultrasound beam hits a boundary between two materials with different acoustic impedance, some of the beam will be reflected and the remainder will be transmitted.

Fig. 5.3 Example of a linear Philips® transducers (left-hand side is a traditional linear transducer and right-hand side is a hockey stick-type transducer, which can be used intraorally on the cheek or tongue for instance)

For diagnostic imaging an ultrasound frequency between 2.5 and 40 MHz (megahertz) is required. This is initiated inside the transducer, which is held in contact with the soft tissues. However, since air is a bad medium for sound, a so-called coupling agent (a gel or a gel pad) is required to ensure a good contact. If ultrasound is used intraorally, saliva or a gel pad will be the coupling agent.

The frequency affects the travel depth or penetration of the ultrasound waves. The lower the frequency, the deeper the ultrasound will travel, while the higher the frequency, the more superficial the penetration will be. The images from the latter will, however, have a higher resolution than the former.

Color Doppler is a feature in ultrasound that allows for visualization of vascularization. That is a feature that will be useful in identifying pathology (e.g., hypervascularization in a tumor) or assessing healing tissue (e.g., check blood flow after a flap or major orthognathic surgery).

The technique is very much operator dependent, which means that different pressures applied to the transducer generate different images. Variation in operators, in terms of application of amount of pressure on the patient's tissues with the transducer, will result in different images. But then again, ultrasonography does not pose any danger for the patients and can be repeated as often as needed, if one requires to check the patient again.

In the field of pediatric dentistry, ultrasonography is useful in patients with salivary gland problems (e.g., sialolith, mumps), muscular issues, and hypertrophy of lymph nodes (lymphadenopathy). Since it requires special training and is not often

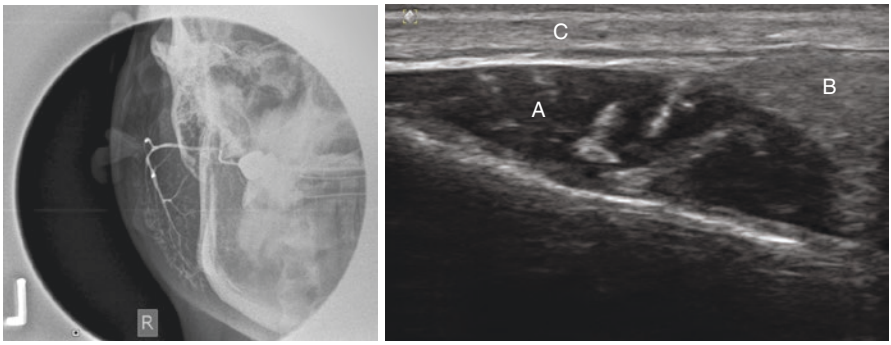

Fig. 5.4 A sialogram of the right-hand side parotid gland (anterior view) performed with Omnipaque® 350 is shown on the left-hand side of a patient with a unilateral facial swelling which was not related to teeth. The swelling of the face and the expansion of the parotid gland can be seen clearly in this image. On the right-hand side the ultrasonography of the right-hand-side masseteric muscle (A) is shown, in the same patient with a unilateral swelling of the face, later diagnosed as mumps. The parotid gland (B) looks normal in the ultrasound image, as does the skin (C)

used in the dental setting, this imaging modality will usually be available in specific hospital settings or private specialty clinics.

Figure 5.4 illustrates the use of ultrasound imaging in a case of a swollen parotid gland in a teenage patient. Dental examination did not indicate a dental cause for the swelling. A sialogram with contrast medium (Omnipaque® 350) was performed to assess the parotid salivary gland. Since the patient also complained of pain in the masseteric muscle, an ultrasonography was made of the masseteric muscle, to rule out a muscular issue or any other pathology that could cause the same symptoms. The swelling was diagnosed as mumps and confirmed with a blood test.

Further Reading

Armstrong P, Wastie M, Rockall A. Diagnostic imaging. 6th ed. Oxford: Wiley-Blackwell; 2009.
Graham DT, Cloke P, Vosper M. Principle and applications of radiological physics. 6th ed. Edinburgh: Churchill Livingstone; 2011.
Hendee WR, Russell Ritenour E. Medical imaging physics. 3rd ed. Hoboken: Wiley-Liss; 2002.
Mettler FA Jr, Upton AC. Medical effects of ionizing radiation. 3rd ed. Amsterdam: Saunders Elsevier; 2008.
Multislice CT, Baert AL, Knauth M, Sartor K. Diagnostic imaging. In: Medical radiology. 3rd ed. Berlin: Springer; 2009.
Whaites E, Drage N. Essentials of dental radiography and radiology. 5th ed. Amsterdam: Churchill Livingstone, Elsevier; 2015.
White SC, Pharoah MJ. Oral radiology. In: Principles and interpretation. 7th ed. Amsterdam: Elsevier; 2014.
Wolters Kluwer MM. MDCT physics. In: The basics. Philadelphia: Lippincott Williams & Wilkins; 2009.

Incidental Radiographic Findings in Pediatric Dental Practice

6

This chapter contains a myriad of examples of incidental radiographic findings, and it also illustrates that good diagnostic skills are essential and paramount in distinguishing normal from abnormal or aberrant anatomy and the latter from pathology. Foreign objects can be another challenge, especially if they are not radiopaque. Often endoscopic nasal investigations by ear, nose, and throat specialists result in incidental findings of pieces of toys or a coin or an earring being stuck in the nasal cavity. Sometimes they have been there for months or years. As pediatric dentist, one should keep an open mind as to what children can push into their ears, noses, and mouth. Our greatest fear is when objects are being aspirated and cause stridor or even worse asphyxiation. A good clinical examination and a justified radiographic examination can answer most clinical complaints or issues.

Names of distinguished colleagues who supplied the images for this chapter are mentioned with the radiographs. If there is no name mentioned with the radiographs, the radiographs were taken by the author of this book or collected from the different university clinics he has worked in (Ghent University in Belgium, University of Washington in Seattle, USA, and University of Western Australia in Perth, Australia). Figures 6.1 through 6.16 are illustrations of incidental findings with or without a significant impact on the treatment plan or therapy.

J. Aps, *Imaging in Pediatric Dental Practice*,
https://doi.org/10.1007/978-3-030-12354-3_6

Fig. 6.1 Inverted right-hand-side second maxillary premolar. Notice the chin-down positioning error, rendering a "smiling" panoramic radiographic image (courtesy of Dr. Hilde Beyls, Belgium)

Fig. 6.2 Supernumerary mandibular premolar on the right-hand side and a mesiodens (Fig. 6.3)

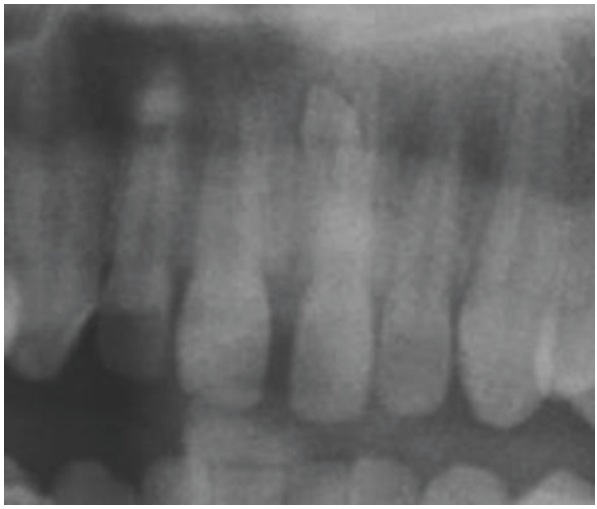

Fig. 6.3 Cropped image from the panoramic radiograph (courtesy of Dr. Hilde Beyls, Belgium)

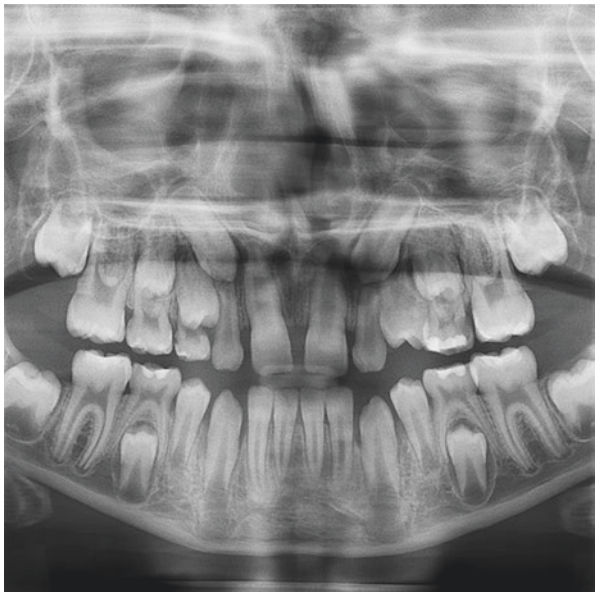

Fig. 6.4 Congenitally missing maxillary lateral incisors and generalized occlusal wear (courtesy of Dr. Marc Jeannin, Belgium)

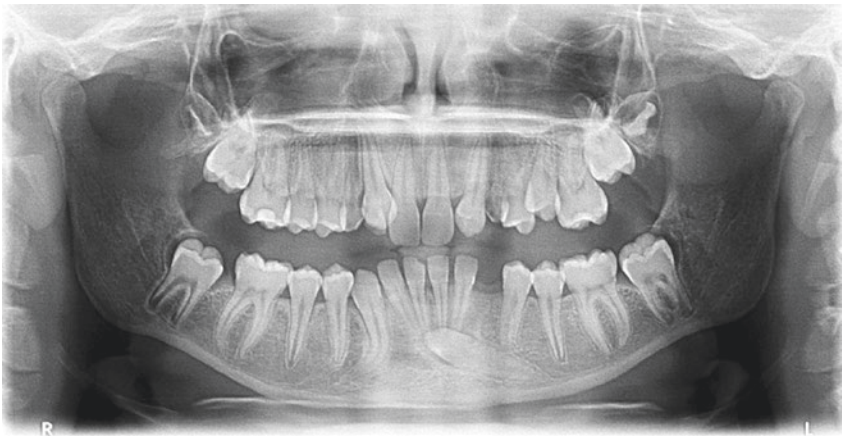

Fig. 6.5 Impaction of left-hand-side mandibular canine and congenitally missing maxillary lateral incisors and mandibular third molars. Notice the root dilacerations on the right-hand-side mandibular canine and the unusual spacing between the right-hand-side mandibular molars, which may indicate a small dentigerous cyst. Also notice the ghostlike appearance of the deciduous maxillary canines. Since the impacted mandibular canine is not magnified, it is likely to be positioned in the same plane or slightly anterior to the erupted incisors and premolar (courtesy of Dr. Veronique Noens, Belgium)

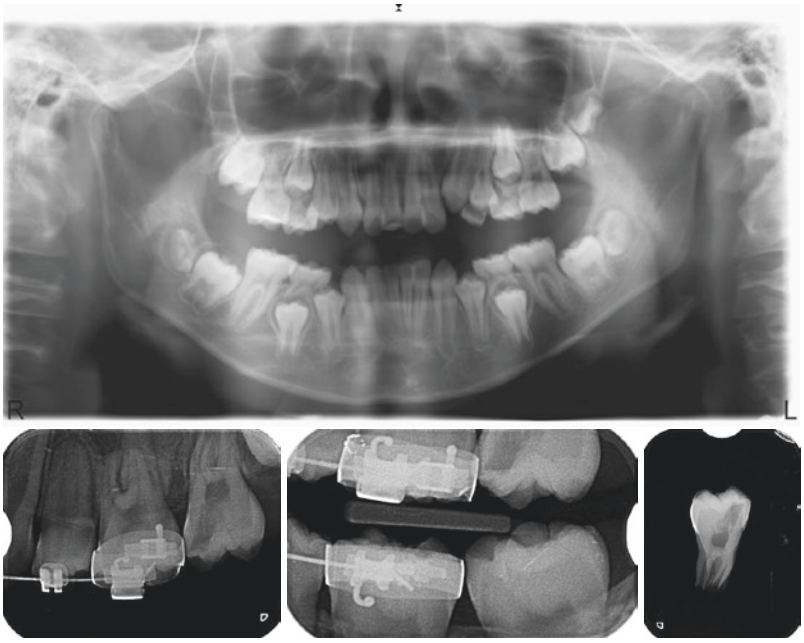

Fig. 6.6 Preeruptive intracoronal resorption in the left-hand-side second permanent maxillary molar was noticed on the panoramic and subsequently followed up upon eruption and when the patient required orthodontic treatment. In the periapical and bitewing radiographs one can appreciate the intracoronal resorption better. The image on the right-hand side shows the radiographic appearance when the tooth was extracted. No coronal breach was observed (courtesy of Dr. Wouter Van den Steen, Belgium)

Fig. 6.7 This periapical radiograph, taken with the standard occlusal technique at 65° downward angle of the X-ray beam to the occlusal plane, which is parallel to the floor, was taken prior to extraction of the root remnants of the deciduous central maxillary incisors. The child apparently had stuffed beads into the pulp canals of both teeth (courtesy of Dr. Elise Sarvas, USA)

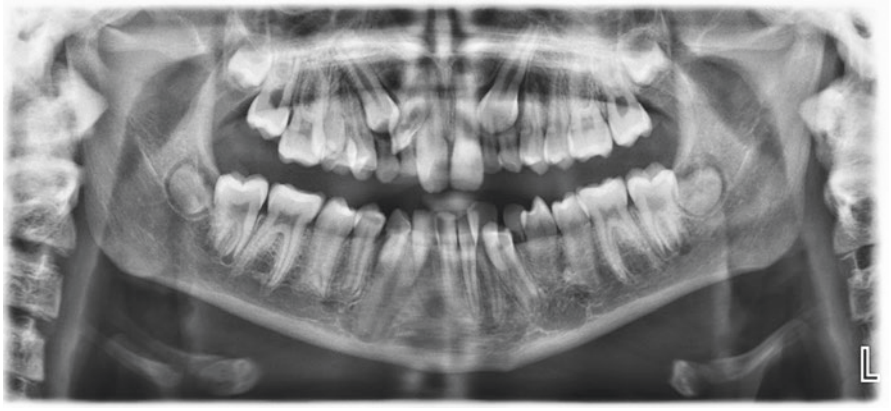

Fig. 6.8 This panoramic radiograph was taken because of eruption issues in both jaws. One can appreciate a congenitally missing left-hand-side maxillary lateral incisor, dens invaginatus of the right-hand side's, a lingually erupting right-hand-side mandibular canine (hence the magnification in the panoramic radiograph), and a buccal erupting left-hand-side mandibular canine. The image of the left-hand-side maxillary canine is magnified compared to the right-hand side's, which means that the left-hand-side one is positioned more palatally

Fig. 6.9 This panoramic radiograph of a 6-year-old boy was taken because of eruption issues in the maxilla. It was observed that the right-hand-side maxillary permanent central incisor was positioned horizontally. The maxillary lateral on that same side appeared to be 90° mesio-rotated (courtesy of Dr. Tracey Takenaka, USA)

Fig. 6.10 This panoramic radiograph of a 6-year-old girl was taken because of what was observed in the patient in Fig. 6.9, as these were twin siblings. Both permanent maxillary central incisors appeared to be positioned horizontally and mesio-rotated (courtesy of Dr. Tracey Takenaka, USA). Unfortunately there was no follow-up available to assess the eruption of these teeth

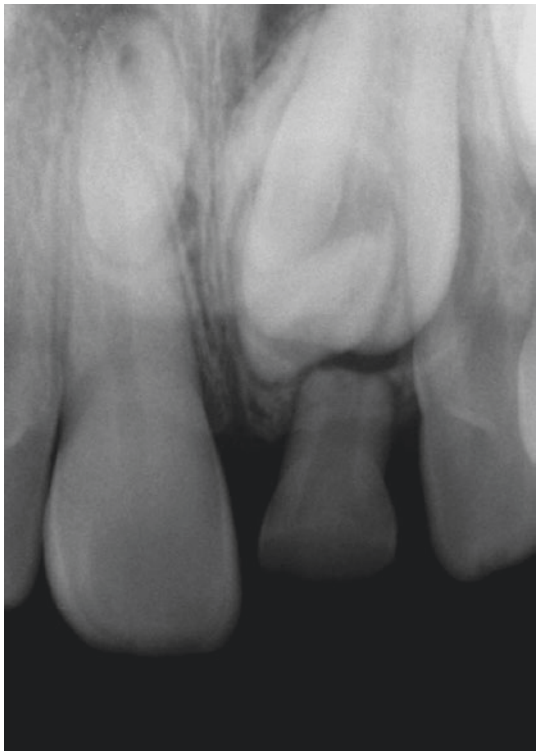

Fig. 6.11 This periapical radiograph was taken because of severe delayed eruption problems with the left-hand-side permanent maxillary central incisor (11-year-old boy). Besides the impacted central incisor and the retained predecessor, three supernumerary teeth can be appreciated: one on the right-hand side and two on the left side of the midline. Spontaneous eruption of the permanent incisor was observed, once the supernumerary teeth were surgically removed

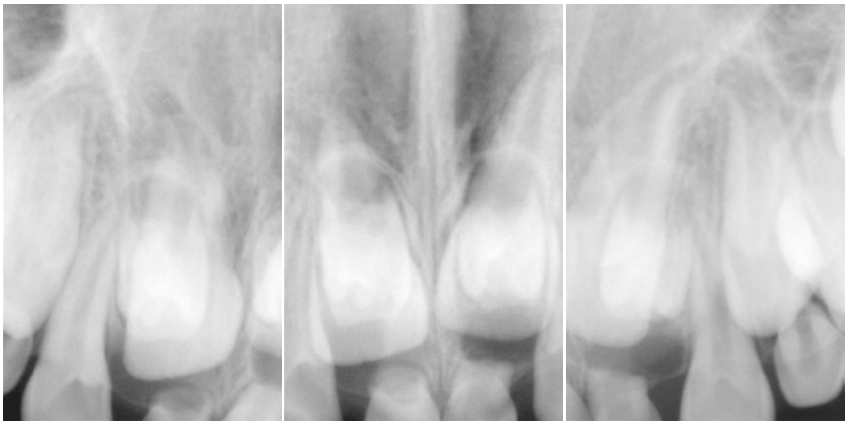

Fig. 6.12 The middle of these three periapical radiographs in an 8-year-old girl was taken to investigate the unusual eruption pattern of the permanent central maxillary incisors. It was discovered that two supernumerary teeth were obstructing the already reasonably developed permanent central incisors. Subsequently two additional radiographs were made from a different horizontal angle (tube shift technique or parallax technique or SLOB rule technique, standing for "s"ame "l"ingual "o"pposite "b"uccal) to determine whether these supernumerary were positioned buccally or palatally, relative to the central incisors. Since both supernumerary teeth are projected towards the side the X-ray machine was moved, they were positioned more palatally. Anecdotal to this case is that the patient also appeared to have a supernumerary in the mandibular incisor area, which was observed on a cone beam CT of the patient, taken prior to the surgery to remove the maxillary supernumerary teeth (courtesy of Dr. Filip Van der Borgh, Belgium)

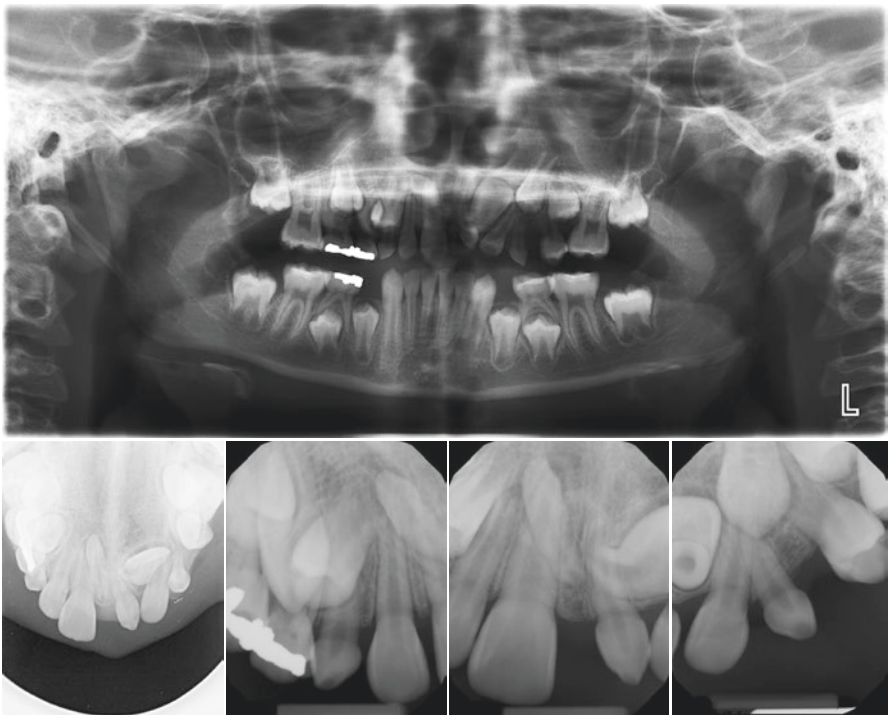

Fig. 6.13 A panoramic radiograph of this 9-year-old boy was taken because a microdont had erupted in the position of the left-hand-side permanent maxillary central incisor. The panoramic radiograph shows the permanent incisor inverted and erupting towards the floor of the nasal cavity. Closer inspection shows an additional supernumerary tooth projected over the right-hand-side permanent central incisor's root. Additional periapical radiographs and a standard maxillary occlusal are subsequently taken. From these it appears that the supernumerary on the right-hand side is positioned more palatally, relative to the central permanent incisor, and that the unerupted left permanent central incisor has a dilacerated root. There was also transposition of the right-hand-side permanent maxillary canine and the first premolar. This case required good orchestrated pediatric and orthodontic care and communication with patient and parents, to ensure that unrealistic expectations from the parent's side could be answered adequately

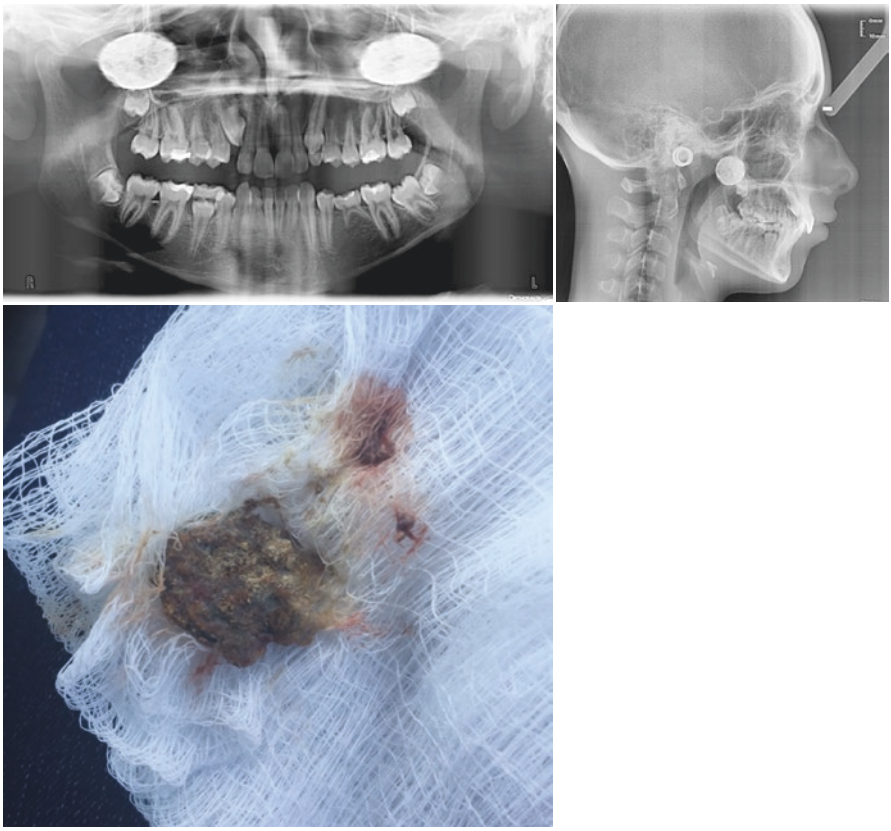

Fig. 6.14 A panoramic radiograph was taken to evaluate tooth eruption and development. Two radiopaque entities were observed that were projected over the maxillary sinuses and the pterygomaxillary fissures. A closer inspection of the radiograph shows also that the nasal septum is more radiopaque than normal. The oval shape of the radiopaque entities appeared to come from a coin in the patient's left-hand-side nasal cavity. The cephalometric radiograph shows the coin to be stuck on the floor of the nose near the choanae. Only a short ear, nose, and throat specialist intervention was necessary to retrieve the coin. The clinical picture of the coin shows corrosion and bacterial buildup on the coin, as it must have been in the patient's nose for a significant amount of time (courtesy of Dr. Bernard Friedlander, USA)

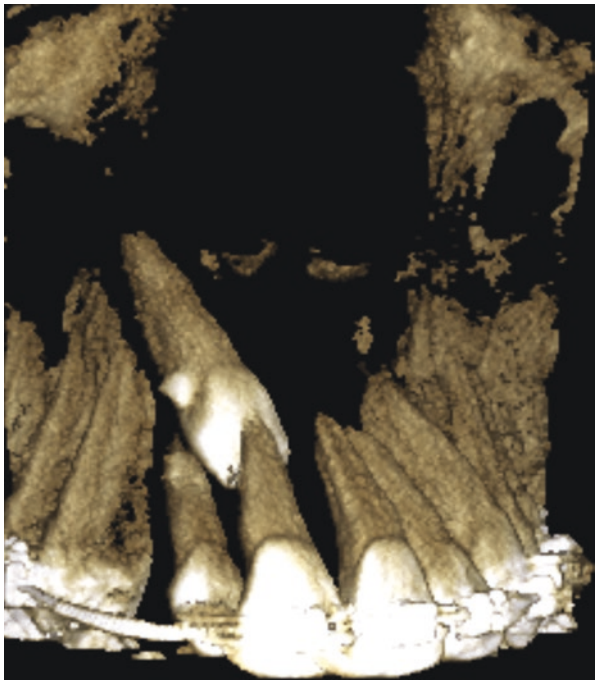

Fig. 6.15 This three-dimensional reconstruction image of a small-field-of-view cone beam computed tomography scan shows an enamel pearl on the distal aspect of the permanent right-hand-side maxillary canine. The canine not erupting spontaneously and the two-dimensional radiographs not showing any explanation were the reasons why the scan was taken

Fig. 6.16 This panoramic radiograph was taken to check the eruption pattern prior to the start of an orthodontic treatment. The left-hand-side second maxillary permanent molar appears to have preeruptive intracoronal resorption. The follow-up clinical examination and the periapical radiograph confirm the noncarious lesion in this tooth. This is typically an asymptomatic process driven by activated osteoclasts. The exact mechanism is unknown, but the prevalence is reported to be 8–15% in Jordanian and Turkish population, respectively. However, when one takes into account the number of teeth examined in the studies, the prevalence is 0.62–3.5%, respectively. Usually it is a single tooth that is affected and the second and third permanent molars seem to be affected most. In some publications the condition is named preeruptive caries; however, that is incorrect as caries assumes bacterial involvement, which is not the case in these teeth (courtesy of Dr. Wouter Van den Steen, Belgium)

From these examples one can appreciate the importance of assessing the radiographic material accurately. One should also keep in mind that endoscopy of the nasal cavity is a good alternative to referring the patient for MRI if one suspects a nonradiopaque foreign body in the nasal cavity. Sometimes collaboration between ENT specialist and pediatric dentist is required. In the latter case, remember that our medical colleagues are not always familiar with dental radiographs and that appropriate explanation might be required. This chapter also showed that it is important to plan treatment in a multidisciplinary approach, especially when impacted supernumerary teeth are diagnosed and a complex surgical-orthodontic treatment might be required. In that case, the pediatric dentist could be the coordinator of the multidisciplinary team, as he/she is the perfect person to keep an overview of the different steps required in the treatment plan while keeping an eye on the patient's oral hygiene and dietary habits, for instance. The use of sophisticated advanced imaging, such as medical CT, is not mentioned, but would require the pediatric dentist to adequately refer the patient to a medical radiologist and provide them with sufficient and relevant imaging material, so the latter can decide which technique would be best for this particular case.

Further Reading

Al-batayneh OB, GA AJ, EK AT. Pre-eruptive intracoronal dentine radiolucencies in the permanent dentition of Jordanian children. Eur Arch Paediatr Dent. 2014;15:229–36.

Avsever H, Gunduz K, Karakoc O, Akyol M, Orhan K. Incidental findings on cone-bean computed tomographic images: paranasal sinus findings and nasal septum variations. Oral Radiol. 2018;34:40–8.

Edwards R, Altalibi M, Flores-Mir C. The frequency and nature of incidental findings in cone-beam computed tomographic scans of the head and neck region: A systematic Review. JADA. 2013;144(2):161–70.

Lenzi R, Marceliano-Alves MF, FRF A, Pires FR, Fidel S. Pre-eruptive intracoronal resorption in a third upper molar: clinical, tomographic and histological analysis. Austr Dental J. 2017;62:223–7.

Lopes IA, RMA T, Handem RH, ALA C. Study of the frequency and location of incidental findings of the maxillofacial region in different fields of view in CBCT scans. Dentomaxillofacial Radiology. 2017;46:20160215.

MAR K, Pazera A, Admiraal RJ, Berge SJ, Vissink A, Pazera P. Incidental findings on cone beam computed tomography scans in cleft lip and palate patients. Clin Oral Invest. 2014;18:1237–44.

O'Sullivan JW, Muntinga T, Grigg S, JPA I. Prevalence and outcomes of incidental imaging findings: umbrella review. BMJ. 2018;361:k2387.

Oser DG, Henson BR, Shiang EY, Finkelman MD, Amato RB. Incidental findings in small field of view cone-beam computed tomography scans. JOE. 2017;43:901–4.

Timucin A. Management of hidden caries: a case of severe pre-eruptive intracoronal resorption. J Can Dent Assoc. 2014;80:e59.

Warhekar S, Nagarajappa S, Dasar PL, Warhekar AM, Parihar A, Phulambrikar T, Airen B, Jain D. Incidental findings on cone beam computed tomography and reasons for referral by dental practitioners in Indore City (M.P). J Clin Diagn Res. 2015;9(2):ZC21–4.

Common Dental Anomalies in Pediatric Dental Practice

7

This chapter contains examples of common dental anomalies, as encountered in pediatric dental practice, which were not treated in Chap. 6. The radiographic images taken with different radiographic techniques and their radiographic differential diagnoses are presented. The aim of this chapter is to familiarize the reader with the different results of the techniques explained in the previous chapters. Obviously not all types of anomalies were captured in this textbook chapter, but at least the reader will get a better feel about how the images turn out and what information can be retrieved from them.

Names of distinguished colleagues who supplied the images for this chapter are mentioned with the radiographs. If there is no name mentioned with the radiographs, the radiographs were taken by the author of this book or collected from the different university clinics he has worked in (Ghent University in Belgium, University of Washington in Seattle, USA, and University of Western Australia in Perth, Australia).

7.1 Amelogenesis Imperfecta

There are three types of amelogenesis imperfecta (AI): hypoplastic type (type 1 in which the enamel matrix is inadequately formed, causing pitted, grooved, and thin enamel); hypomaturation type (type 2, in which the form appears normal, but the enamel is soft and vulnerable, and brownish-yellow in color); and hypocalcified type (type 3, in which the enamel is normal in quantity but poorly calcified, which gives it an opaque appearance and makes it weak). Figure 7.1 is an illustration of a case of amelogenesis imperfecta of the hypomaturation type.

J. Aps, *Imaging in Pediatric Dental Practice*,
https://doi.org/10.1007/978-3-030-12354-3_7

Fig. 7.1 This panoramic radiograph was taken in a 9-year-old patient with amelogenesis imperfecta type 2 (hypomaturation type). Notice the missing, chipped off, enamel on occlusal surfaces of the molars (courtesy of Dr. Bieke kreps, Belgium)

Non-syndromic amelogenesis imperfecta (AI) belongs to a group of rare disorders that affect tooth enamel formation in either a qualitative or a quantitative fashion. Recent studies on genome sequencing have revealed more information about its mechanism of inheritance and phenotype appearance. In hypoplastic AI, the enamel is thin and the interproximal contacts are often missing (spacing between teeth) and the patients also have a tendency to develop an anterior open bite. In hypocalcification AI, the enamel is extremely soft, but has the normal thickness, as opposed to the hypoplastic form. However, due to its hypocalcified nature, the enamel is quickly worn and lost after eruption, leaving the remaining enamel to be rough and discolored. In hypomaturation AI, the enamel appears brown or yellowish due to a defective mechanism during maturation of the enamel matrix, though the enamel has the normal thickness. This type also leads to quick wear and chipping off of the enamel. Because of the phenotypical similarities between these three types, a more simple and broader classification system was developed by Prasad et al. *in 2016. They suggested only hypoplastic AI and hypomineralized AI to be used. The hypomineralized AI holds both the hypomaturation and hypocalcification AI types. Based on the recent literature, there are more than 17 genes involved in non-syndromic AI. Both autosomal dominant and recessive mutations in these genes (mutations in enamel matrix proteins or protease-encoding genes) can result in any of the abovementioned phenotypes. For further detailed information, the interested reader is referred to the literature.*

7.2 Dentinogenesis Imperfecta

Dentinogenesis imperfecta (DI) is a hereditary developmental anomaly of dentin, in the absence of any systemic disease. Osteogenesis imperfecta may be associated with similar dentinal aberrant anatomy and appearance. It is then called osteogenesis imperfecta with opalescent teeth (DI type 1). Three classification systems (Shields versus Witkop versus Levin) are used, but discussing this is beyond the scope of this chapter and book. Dentinogenesis imperfecta can be divided into three types: type 1 is associated with osteogenesis imperfecta and teeth appear opalescent, type 2 is isolated opalescent teeth, and type 3 is isolated opalescent teeth with wide pulp chambers and canals. What is specific to dentinogenesis imperfecta is that all teeth in both dentitions are affected. That is the greatest differential with the dentinal dysplasia types that will be discussed and illustrated in Sect. 7.3. Since the dentin is affected, the adherence between enamel and dentin is compromised and patients will suffer from chipping enamel and hence sensitive teeth, which subsequently wear down quickly too. The teeth have a blue to brown color when they erupt. Pulp chambers may get obliterated, but sometimes they don't and seem to be expanded, which renders the radiographic appearance typical and is called "shell teeth." Usually the shape of the crowns of the teeth is bulbous and sometimes called tulip shaped. Figure 7.2 is an illustration of an adult patient with dentinogenesis imperfecta and figure 7.3 is a child with dentinogenesis imperfecta.

Fig. 7.2 This panoramic radiograph of a 20-year-old woman with dentinogenesis imperfecta type 2 shows generalized pulpal obliterations and bulbous crowns of the premolars in particular. Unfortunately she has a serious caries problem, with periapical inflammations, which makes treatment more complicated

Fig. 7.3 The panoramic in the upper left-hand-side corner is taken 5 years before the panoramic radiograph at the bottom. One can appreciate the clinical opalescent appearance of the teeth in the upper right-hand-side corner image. Besides the bulbous crowns of the teeth, it can be observed that the pulp systems in nearly all teeth have obliterated. This is a case of dentinogenesis imperfecta type 2 (courtesy of Dr. Marc Jeannin, Belgium)

Dentinogenesis imperfecta (DI) is a rare hereditary disorder, primarily characterized by defective dentine formation, which subsequently results in early enamel loss. The latter is usually normal in its histological appearance though and is not affected by the DI mutations. However, one study reported the enamel to be hypoplastic (Bloch-Zupan et al. *2016). The estimated incidence is 1:8000 and 1:45,455 live births. The non-syndromic types of DI are associated with mutations in the dentine sialophosphoprotein gene DSPP (chromosome 4, 4q22.1). The latter plays a paramount role in the mineralization and maturation of dentine and especially in the non-collagenous component of the dentine. DI type II affects both the primary and the permanent dentition, but the former is usually more severely affected. The teeth usually have an opalescent hue, ranging from amber brown to grayish-blue. The teeth show typical bulbous crowns with a cervical constriction, leading to a narrow root,*

which contains an obliterated pulp canal. Histologically the dentine appears as dysplastic with reduced mineralization, irregular dentine tubules, and in some cases interglobular dentine. The obliterated pulp system does not mean that there is no access for bacteria, as the dentine tubules will allow for bacterial spreading and eventually for periapical inflammation. It is possible that DI type 1 is often not diagnosed accurately as it has a great variety in appearance and expression and therefore osteogenesis imperfecta might be underdiagnosed as well, as this condition also shows a myriad of expressions (bruising, prolonged bleeding, spraining, fractures, hearing impairment, joint hypermobility, and blue sclerae).

7.3 Dentinal Dysplasia and Regional Odontodysplasia

Dentinal dysplasia (DD) should not be confused with dentinogenesis (or sometimes called odontogenesis) imperfecta (see Sect. 7.2). The first differential diagnosis is that DD does not affect the entire dentition. In DD the roots are short and conical, hence the name rootless teeth, and the pulp chambers are obliterated by multiple nodules of poorly organized dentine. Usually patients loose these teeth early after eruption. There are two types of DD: type 1 involves radicular dentin (rootless teeth) and type 2 involves coronal dentin and is easily mistaken for dentinogenesis imperfecta. DD type 2 teeth are similar to dentinogenesis imperfecta teeth, but the coronal pulp chambers contain denticles accompanied by thistle tube appearance of the pulps in the permanent teeth. However the pulps will be totally obliterated in deciduous teeth, which clinically resemble dentinogenesis imperfecta (amber colored and translucent).

Regional odontodysplasia is a localized condition affecting only a few teeth in a quadrant. These teeth have aberrant enamel, dentine, and pulp and therefore are called ghost teeth, because of their radiolucent appearance on radiographs. They usually fail to erupt, but if they do they appear yellowish and rough. Regional odontodysplasia can occur both in the deciduous and permanent dentition and maxillary teeth are supposedly more often involved.

Segmental odontomaxillary dysplasia (formerly known as hemimaxillofacial dysplasia) is another type of condition, which can be mistaken for fibrous dysplasia (see Chap. 8) or regional odontodysplasia. It is a rare disorder (only 62 well-documented cases have been published) of unknown etiology, and it causes hemimaxillofacial dysplasia with expansion of the maxilla in the primary or mixed dentition. The enlargement is caused by fibrous tissue of the gingiva and expansion of the alveolar crest. Teeth in this area are usually delayed in eruption and appear hypoplastic with varying degrees of aberrant pulp and dentin. Therefore there is an easy confusion with regional odontodysplasia. The latter, however, is not associated with expansion of the maxilla. Figures 7.4 through 7.8 are all illustrations of patients with either dentinal dysplasia or regional odontodysplasia.

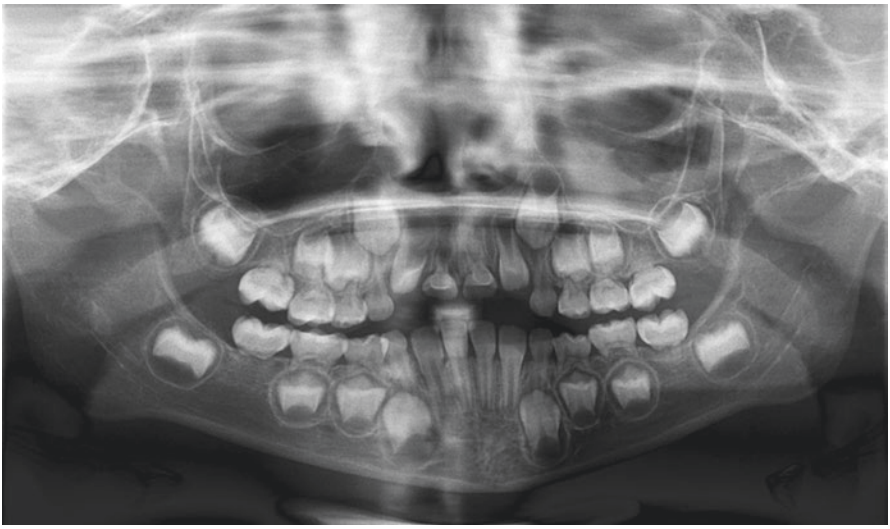

Fig. 7.4 This panoramic radiograph of a 7-year-old boy shows lack of root formation on both deciduous and permanent molars. Also his maxillary permanent central incisors appear to have aberrant anatomy and radiographic appearance. This is a case of dentinal dysplasia

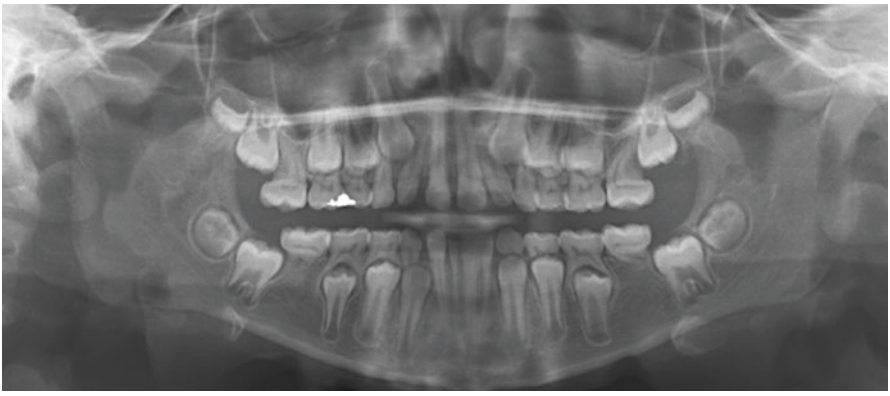

Fig. 7.5 This panoramic radiograph of a 10-year-old with dentinal dysplasia shows the lack of roots on the first permanent mandibular molars and the partially missing roots on the first permanent maxillary molars (courtesy of Dr. James Howard, USA)

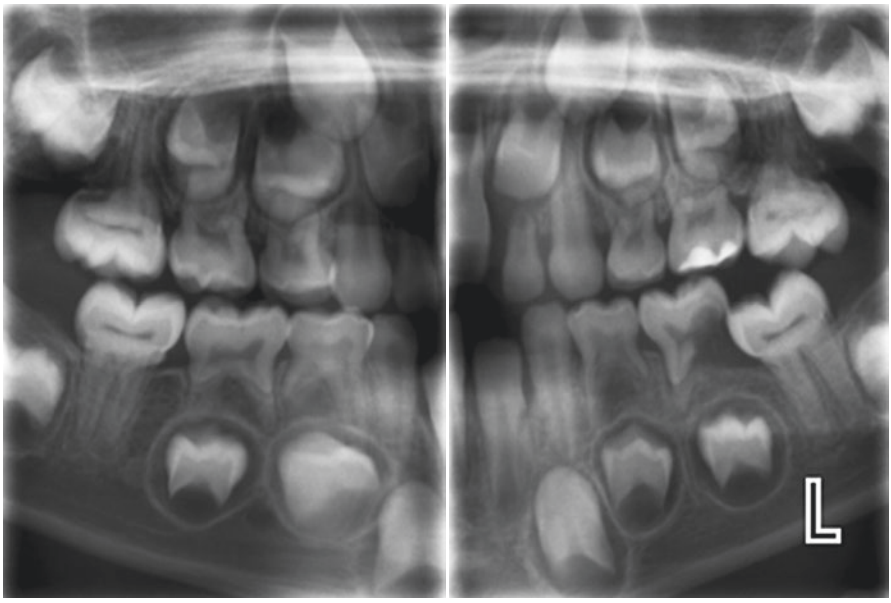

Fig. 7.6 These extraoral bitewing radiographs taken on a 7-year-old boy with dentinal dysplasia show clearly the thistle-shaped pulp chambers in the first permanent molars, which also appear to have poorly developed roots (courtesy of Dr. Elise Sarvas, USA)

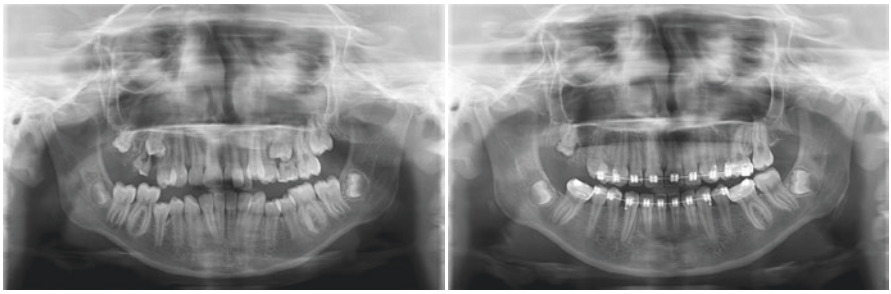

Fig. 7.7 The panoramic radiograph on the left-hand side was taken to evaluate the clinical appearance of the first permanent maxillary right-hand-side molar. Dental development and radiographic appearance of the second permanent right-hand-side molar appeared to be similar with aberrant enamel and dentin, which confirmed the diagnosis of regional odontodysplasia. It was decided to extract the first permanent right-hand-side maxillary molar and to wait for spontaneous eruption of the second premolar. Follow-up panoramic radiograph during the orthodontic treatment shows the delayed development and lack of spontaneous eruption of the second maxillary molar (courtesy of Dr. Anouk Eloot, Belgium)

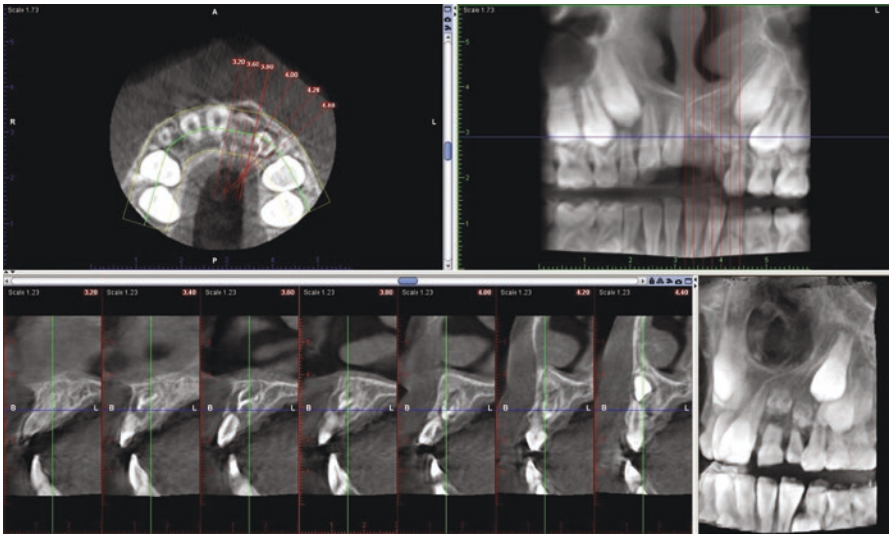

Fig. 7.8 This is a small-field-of-view cone beam computed tomography of a 9-year-old girl with regional odontodysplasia of the permanent left-hand-side maxillary incisors. Notice the ghostlike appearance of both teeth due to poor and aberrant development of enamel and dentine, as well as the fact that the teeth are not erupted and never will

- *Dentine dysplasia (DD) type 1 has been linked to three pathogenicity genes (VPS4B, SSUH2, SMOC2) and it is believed that it is a genetically heterogeneous disease, which needs to be distinguished from other dentine disorders. DD type 1 teeth appear clinically as normal teeth, but show hypermobility due to the short conical roots. Radiographically the latter is confirmed as well as the pulpal obliteration changes. Even in noncarious DD type 1 teeth, periapical inflammation is noticed. In contrast DD type 2 and dentinogenesis imperfecta appear as amber translucent teeth, short and thin roots with obliterated pulps. DD type 2, coronal DD, is more rare than DD type 1 and its prevalence is not really known. DD type 2 is inherited autosomal dominantly. Histologically the dentine shows entrapped cells within lacunae, suggestive of osteodentine, and also a breakup between dentine and predentine can be found, as well as irregular arrangement of the dentine tubules.*
- *Regional odontodysplasia, unlike general odontodysplasia, is thought to be linked to viral infection, use of certain inappropriate medication during pregnancy, trauma, nutritional deficiency, infection, and metabolic abnormalities.*

- *The etiology of segmental odontomaxillary dysplasia is unknown, but according to some researchers it should be linked to a nonhereditary localized developmental anomaly of the first branchial arch that occurs* in utero. *Other reports link it to endocrine abnormalities, and even bacterial or viral infections. Some patients have been reported with local facial or cutaneous abnormalities on the same side as the segmental odontomaxillary dysplasia: hypertrichosis, hyperpigmentation, hypopigmentation, erythema, rough erythema, ectopic eyelashes, increased number of melanocytic nevi, Becker nevus, facial depression, commissural lip pits, and unilateral lip clefting. With regard to the affected teeth, reports have described the following: smaller or larger teeth than normal, over-retained primary teeth, congenitally missing teeth, delayed eruption of especially premolars, increased spacing between teeth, and primary molars in particular can show abnormal coronal and/or root morphology, and atrophic pulp chambers. Also multiple white papules have been described overlying the alveolar crest, mimicking the dental lamina cysts of the newborn. Erythema with blanchable patch on the gingiva has also been described. The alveolar bone shows aberrant patterns as well: ill-defined sclerosis or coarse bone trabeculation, which may affect the maxillary sinus. The latter changes often cause confusion with fibrous dysplasia (Chap. 8); however fibrous dysplasia is not accompanied by the typical dental abnormalities described above.*

7.4 Fusion, Gemination, and Concrescence

Fusion implies two tooth germs fused into one tooth, whereas *gemination* assumes a single tooth bud that has separated into two teeth. In the first case one will have one tooth too few albeit it is a wider tooth, whereas in the second there will be a supernumerary tooth in the arch. The latter is usually fused at the root though, making it a challenge to treat if indicated. The prevalence of fusion in the primary dentition is reported to be about 0.4–0.9%, whereas in the permanent dentition it is around 0.2%. Bilateral fusion of permanent teeth is even more rare and is estimated at 0.05%. *Concrescence* is another phenomenon where teeth are fused at root level, but by formation of root cementum and not dentin. Examples of fusion and gemination are shown in figures 7.9 through 7.12.

Fig. 7.9 This panoramic radiograph shows a fusion of left-hand-side mandibular canine and lateral incisor. Counting the number of teeth in the third quadrant shows only seven teeth, including the third molar. Also notice the impacted mandibular canines as well as the right-hand-side mandibular canine

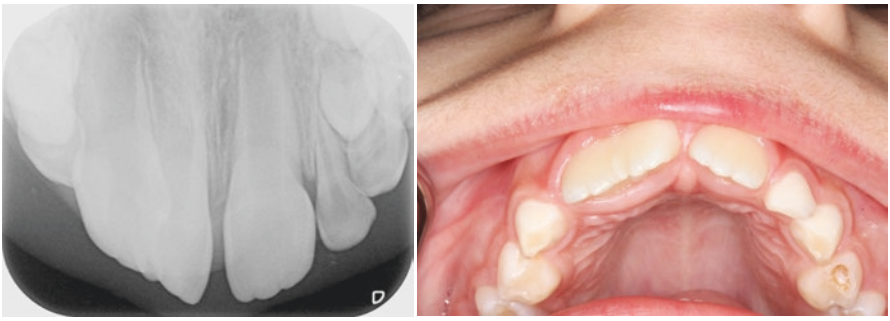

Fig. 7.10 This periapical radiograph was taken to verify the true nature of the clinical finding of an unusual wide permanent maxillary right-hand-side central incisor. The crowns of the lateral and central incisors have fused, while the roots and pulp canals appear to be separate. Therefore the final tooth count is one too few (courtesy of Dr. Wouter Van den Steen, Belgium)

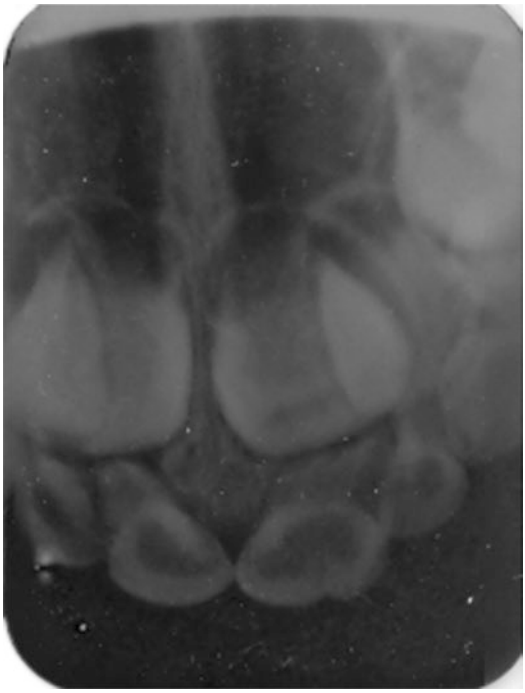

Fig. 7.11 This periapical radiograph was taken because of the unusual large deciduous left-hand-side maxillary central incisor. The presence of the lateral deciduous incisor implies that the central incisor is the result of a gemination; hence the count of teeth in the second quadrant equals five, which is normal in this 3-year-old child

Fig. 7.12 This periapical radiographs was taken to verify if this was a fusion or gemination or even a supernumerary tooth, as clinically there were two crowns visible. The radiograph shows the single root and the bifid pulp chamber. This was a gemination (courtesy of Dr. Amelie Julie Lambregts, Belgium)

7.5 Odontomas

Odontomas are the most common types of odontogenic tumors and are considered hamartomas (developmental anomalies), consisting of enamel, dentin, and pulpal tissue. A compound odontoma is composed of toothlike particles, whereas a complex odontoma is a conglomerate mass of enamel and dentin. We will leave it open for discussion if a supernumerary tooth (e.g., mesiodens or fourth molar) is a compound odontoma or not. The etiology of odontomas is unknown. Some have reported links with trauma, infection, genetic mutations, odontoblastic hyperactivity, and even alterations of dental development control gene.

In general they are asymptomatic, but in some cases they can lead to swelling, pain, suppuration, or bony expansion. Eruption of inverted odontomas into the nasal cavity has been described. Radiographically they are typically surrounded by a radiolucent rim, which again is surrounded by a radiopaque rim. The treatment is enucleation as they do not recur. Figures 7.13 through 7.17 show examples of odontomas.

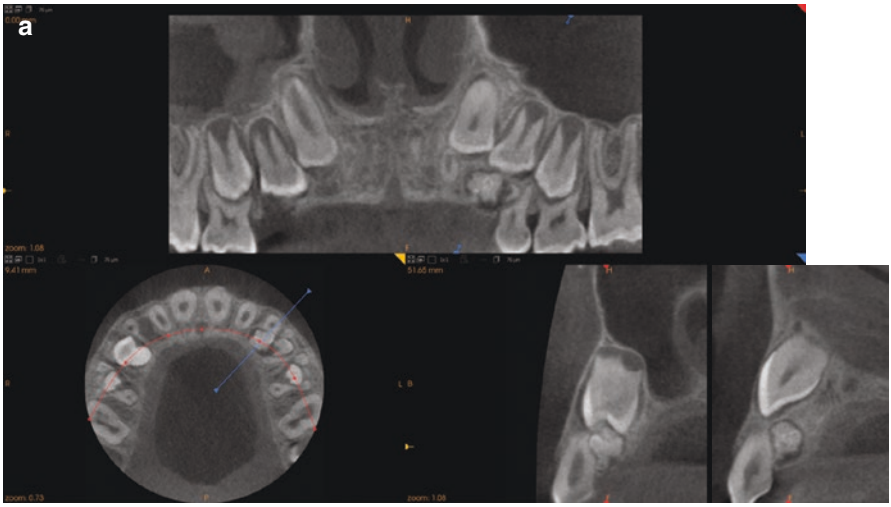

Fig. 7.13 This small-field-of-view cone beam computed tomography was taken to verify what was obstructing the maxillary left-hand-side premolars. From the images one can appreciate a complex odontoma at the occlusal surface of the left-hand-side first premolar and palatal of the deciduous canine

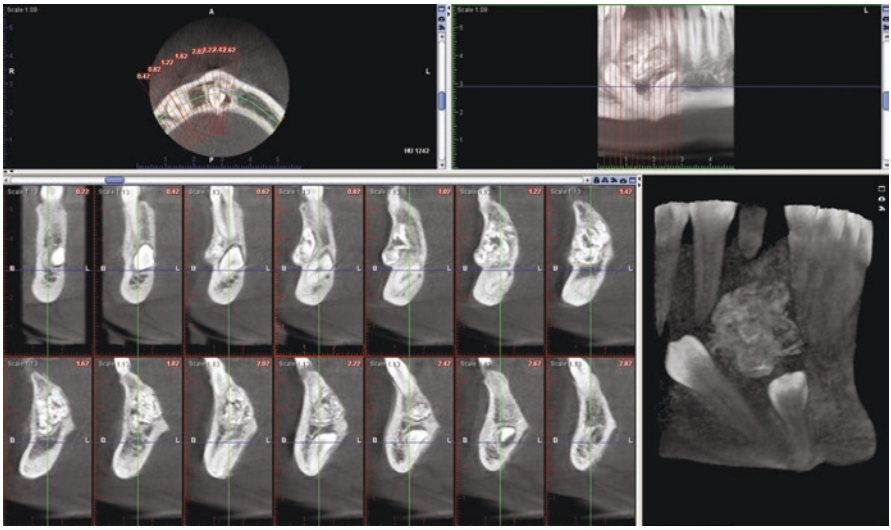

Fig. 7.14 This is a small-field-of-view cone beam computed tomography of a 17-year-old male, who was missing his right-hand-side mandibular lateral incisor and canine, while his deciduous mandibular canine was still present. The scan shows a large irregular mixed radiopaque-radiolucent mass and two impacted permanent teeth. The mass is a complex odontoma, which has also caused expansion of the buccal mandibular cortical plate

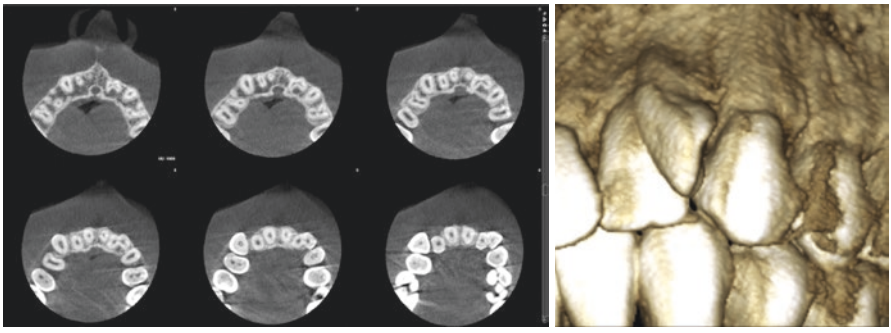

Fig. 7.15 This small-field-of-view cone beam computed tomography of the left-hand-side permanent maxillary lateral incisor, which clinically appeared to have a double crown or to be a dens evaginatus (see Sect. 7.6), shows that the tooth is actually a gemination with fused pulp systems

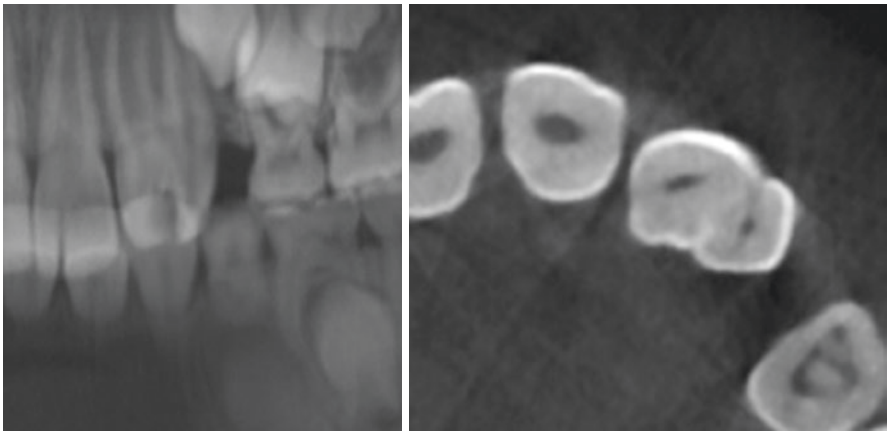

Fig. 7.16 These cropped cone beam computed tomography images illustrate a fusion of the left-hand-side maxillary permanent lateral incisor with a supernumerary tooth or a compound odontoma. The splitting of the pulp and root is clearly visible (courtesy Dr. Annelore De Grauwe, Belgium)

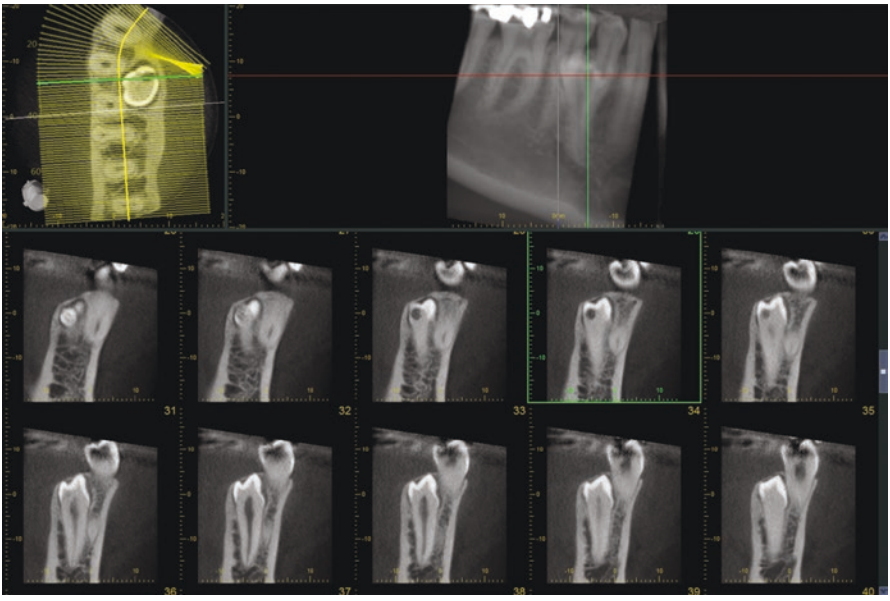

Fig. 7.17 This is a small-field-of-view cone beam computed tomography of a 17-year-old patient soon to undergo orthodontic treatment. From the CBCT one can observe that the supernumerary mandibular premolar is positioned lingually and that it shows preeruptive intracoronal resorption (also see Chap. 6)

7.6 Dens Invaginatus and Dens Evaginatus

A *dens evaginatus* (Figs. 7.18–7.20) is a cusp-like elevation of enamel located in the central groove or lingual ridge of the buccal cusp of a premolar or permanent molar. It occurs mostly in mandibular premolars and consists of enamel, dentin, and pulp. The latter means that attrition may cause pulpal exposure and hence periapical infection can develop. One can also find it in shovel-shaped incisors.

Dens invaginatus (dens in dente) (Figs. 7.21 and 7.22) is a deep enamel-lined invagination in the crown and/or root of a tooth. Maxillary permanent lateral incisors are the most common teeth involved, followed by central incisors, premolars, canines, and molars. The extent of the invagination will determine the caries risk and the treatment options.

Fig. 7.18 The periapical radiograph was taken to evaluate the extent of pulpal tissue into the extra palatal cusp of this maxillary left-hand-side permanent lateral incisor. It can be appreciated that there is no pulpal extension into the extra cusp

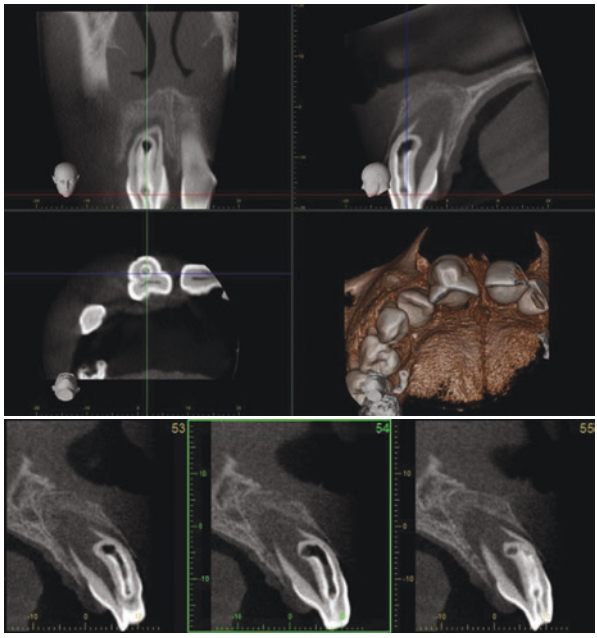

Fig. 7.19 This small-field cone beam computed tomography was taken to evaluate the unusual dens evaginatus on the right-hand-side maxillary permanent central incisor in this 9-year-old boy. The scan shows the complexity of the pulpal anatomy and a periapical infection that has developed since the eruption of the tooth probably

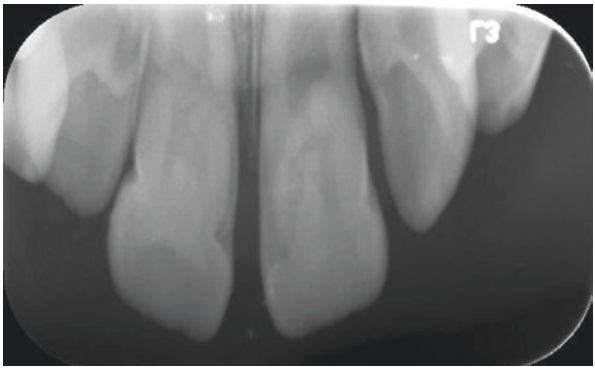

Fig. 7.20 This occlusal radiograph, taken with the wrong-size photostimulable phosphor plate (size 1 should have been size 2), shows two maxillary central incisors with both a dens in dente. The complex nature of the pulp system does not really require cone beam computed tomography, but a proper occlusal or periapical radiograph in this 7-year-old would be better, as one would want to assess the periapical tissues better

Fig. 7.21 This panoramic radiograph shows besides two supernumerary premolars in the mandible a dens in dente on the mandibular left-hand-side second premolar. Also notice the small radiolucent areas mesial of the tooth buds of the mandibular third molars, which could indicate two more supernumerary tooth buds. Follow-up is required

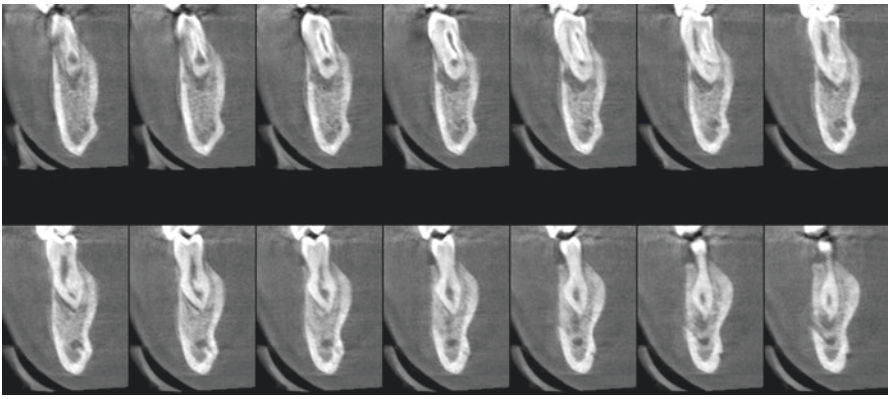

Fig. 7.22 This is a small-field-of-view cone beam computed tomography scan of the first left-hand-side mandibular premolar which shows a dens invaginatus. It can be appreciated that there is already a periapical infection present and that the endodontic treatment will be complicated due to the complexity of the pulp system

An attempt to classify dens invaginatus was first proposed by Hallett (1953). The first three types in Hallett's classification refer to crown invaginations. However, all crown invaginations were designated as type 1 in a classification system put forward by Oehlers (1957). Other classifications have also been described by Ulmansky and Hermel (1964), Schulze and Brand (1972), Vincent-Townend (1974), Parnell and Wilcox (1978), and Hicks and Flaitz (1985). The broad classification put forward by Schulze and Brand (1972) includes 12 variations, starting at the incisal edge of teeth, and therefore classifies malformations with respect to morphology of the invagination as well as the anatomic crown form and dysmorphic root configurations. However, the system described by Oehlers (1957) appears to be the most widely used, possibly because of its simple nomenclature and ease of application. The invagination varies in size and shape from a small dip in the enamel to a severe form, which looks like tooth within a tooth. The invagination frequently communicates with the oral cavity, allowing the entry of irritants and microorganisms either directly into pulpal tissues or into an area that is separated from pulpal tissues by only a thin layer of enamel and dentin. This continuous ingress of irritants and the subsequent inflammation usually lead to necrosis of the adjacent pulp tissue and then to periapical or periodontal abscesses. In many cases dens invaginatus and also dens evaginatus pose serious clinical and therapeutic problems. Endodontic treatment seems extremely difficult in a lot of cases and therefore a good long-term vision and plan are essential, which necessitates well-orchestrated collaboration between several dental specialties: pediatric dentist—orthodontist—periodontist—endodontist and perhaps even oral surgeon in some cases. Cone beam CT is the ideal imaging modality as it will clearly show the complexity of the pulpal system and its relationship with the periodontal surroundings of the tooth.

7.7 Taurodontism

Taurodontism Fig. 7.23 is an enlargement of a multiradicular tooth's body and pulp chamber with consequent apical displacement of the pulpal floor and bifurcation of the roots of the tooth. Taurodontism can be associated with amelogenesis imperfecta, ectodermal dysplasia, and Down syndrome, to name a few.

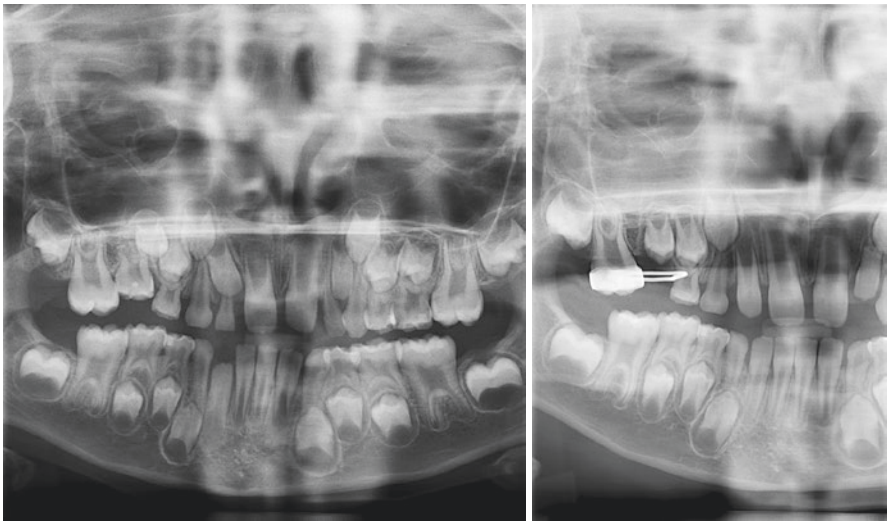

Fig. 7.23 The collimated panoramic radiograph on the left-hand side shows infraocclusion of the right-hand-side maxillary second deciduous molar, which was the reason for this radiograph to be taken. One can also appreciate the presence of taurodont-type permanent first molars in the four quadrants. The partial panoramic radiograph (not cropped) on the right-hand side is taken a year later (courtesy of Dr. Marc Jeannin, Belgium)

Taurodontism was first introduced in 1913 by Sir Arthur Keith, but it had been described in 1908 by Gorjanovic-Kramberger. The word originates from the Latin word Taurus, which means bul, and the Greek word odos, which means tooth. Shaw in 1928 tried to make classifications in taurodontism, by describing the level of apical displacement of the pulp chamber (hypo-, meso-, and hyper-taurodontism). The prevalence of taurodontism lies between 0.1 and 48%, depending on the population studied and the criteria used to determine the anatomical aberration. There does not seem to be a gender difference. The most commonly affected teeth are the mandibular first molars, but it has also been described in primary molars. It can appear unilateral or bilateral and it can be present in more than two quadrants as well. The etiology is unknown, but it has been proposed that failure of the Hertwig's epithelial root sheath to invaginate at the proper height is responsible. Other causes that have been put forward are interference in the epithelia-mesenchymatose induction, genetic transmission, increased number of X chromosomes, polygenetics, heavy masticatory habits, infection, disrupted developmental homeostasis, high-dose chemotherapy, and bone marrow transplantation. One should keep in mind that the association with other dental anomalies and/or syndromes may indicate a same genetic origin.

7.8 Cementoblastoma, Hypercementosis

A *cementoblastoma* (Fig. 7.24) is also called a *true cementoma* and is an odontogenic neoplasm of cementoblasts. The majority of these rare neoplasms occur in mandibular molars or premolars and are diagnosed before the age of 20. Very seldom a primary molar is affected. Radiographically they are seen as a densely mineralized mass attached at the apex of the affected tooth.

They can be confused with *hypercementosis*, (Fig. 7.25) which is not a neoplastic deposition of excessive cementum, as it is continuous with the normal radicular cementum around the root. The apices of the teeth appear a little more blunted on radiographs, as the cementum accumulates at the apical third of the root. The biggest differential with the cementoblastoma is that with hypercementosis the periodontal ligament space and the lamina dura remain intact and it occurs more in adulthood than in childhood.

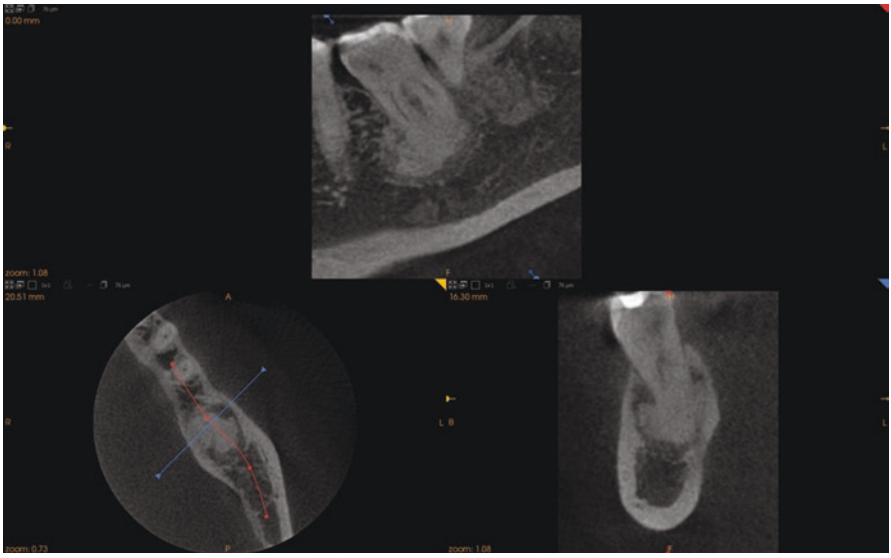

Fig. 7.24 This small-field-of-view cone beam computed tomography scan of the first left-hand-side mandibular permanent molar with a cementoblastoma shows a uniform radiopaque mass attached to the mesial root. The lamina dura and the periodontal ligament space have disappeared and the mass extends towards buccal and lingual cortical plates of the mandible

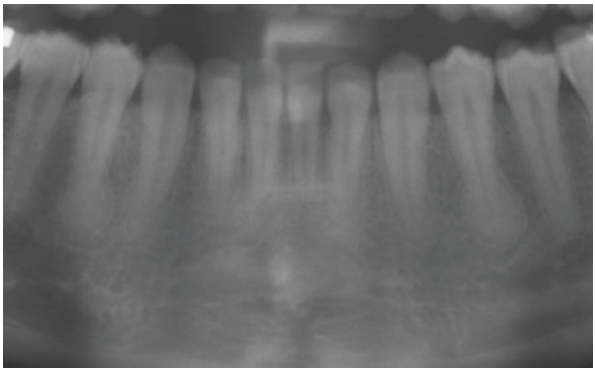

Fig. 7.25 This is a cropped panoramic radiograph which shows hypercementosis on the second right-hand-side mandibular premolar and the first left-hand-side mandibular premolar. One can appreciate the presence of a lamina dura and a periodontal ligament space around the hypercementosis area in the apical third of the respective root. This is a radiograph of a 25-year-old woman. Nevertheless the author considered it was useful to show an example, since hypercementosis is not common in children and one needs to be able to differentiate from cementoblastoma or true cementoma

7.9 Eruption Issues Requiring Imaging

There can be several reasons why teeth are delayed in eruption or are simply not erupting. The latter can involve anatomical restrictions (e.g., no space to erupt), pathology (e.g., dentigerous cyst), or trauma. Delayed eruption can be related to the patient's growth in general or due to therapy (e.g., chemotherapy), which in many cases also causes hypoplasia of teeth. Figures 7.26 and 7.27 are illustrations of common eruption issues with mandibular third molars. Both cases deal with the proximity and location of the inferior alveolar nerve which has to be identified prior to extraction of the respective tooth.

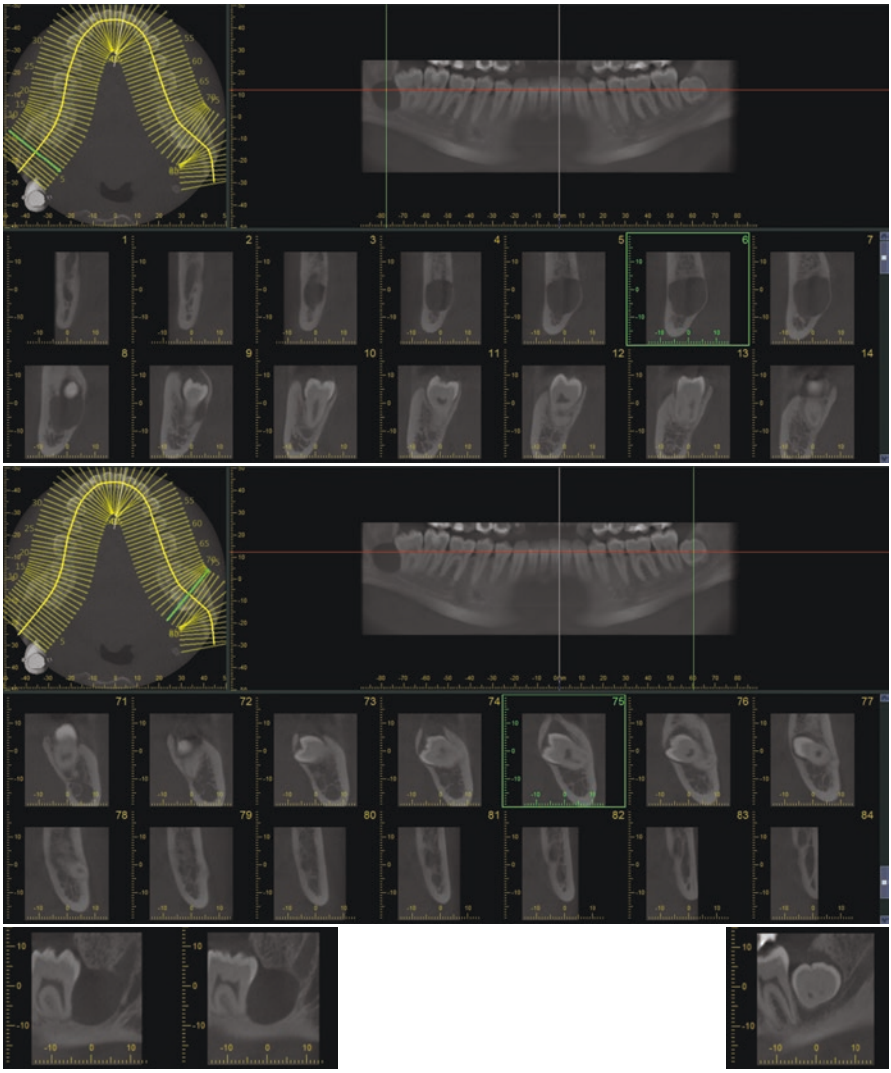

Fig. 7.26 This is a case of an 18-year-old male who required mandibular third molar extractions. In the fourth quadrant one can appreciate a round, uniform radiolucent, well-defined lesion, adjacent to the distal root of the third molar, which appears to have displaced the inferior alveolar nerve inferiorly and which also appears to be expanding the lingual cortical plate of the mandible and eroding the buccal plate of the mandible. Based on its radiographic appearance, this can be either a dentigerous cyst, an odontogenic keratocyst, or an ameloblastoma. Histopathology determined it as a dentigerous cyst. The third molar in the third quadrant appeared to be horizontal with its crown facing the lingual aspect of the mandible and its apices appeared to almost perforate the buccal cortical plate of the mandible. The inferior alveolar nerve can be identified as running against the inferior surface of the crown of the tooth. The latter information was important for the oral surgeon who performed the exodontia

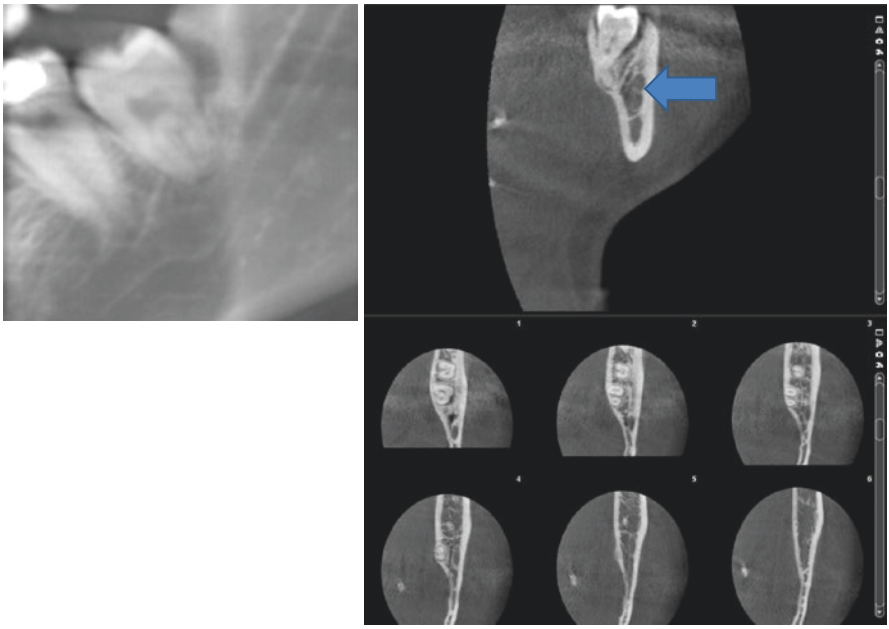

Fig. 7.27 This 18-year-old girl was planned for surgical exodontia of the third molar in the third quadrant. From the cropped panoramic radiograph, one can see that the apices of the third molar appear to deviate the inferior alveolar nerve. Therefore a cone beam computed tomography was ordered, which showed that the mandibular canal ran buccal to the apices of the tooth, instead of what is mentioned in anatomy books. This information was important to the oral surgeon who performed the extraction

Further Reading

Alhilou A, Beddis HP, Mighell AJ, Durey K. Dentin dysplasia: diagnostic challenges. BMJ Case Rep. 2018; https://doi.org/10.1136/bcr-2017-223942.

Al-Tuwirqi A, Lambie D, Seow WK. Regional odontodysplasia: literature review and report of unusual case located in the mandible. Ped Dent. 2014;36:62–7.

Andersson K, Malmgren B, Astrom E, Dahllof G. Dentinogenesis imperfecta type II in Swedish children and adolescents. Orphanet J Rare Dis. 2018;13(145) https://doi.org/10.1186/s13023-018-0887-2.

Bloch-Zupan A, Huckert M, Stoetzel C, Meyer J, Geoffrey V, Razafindrakoto RW, Dollfus H. Detection of a novel DSPP mutation by NGS in a population isolate in Madagascar. Front Physiol. 2017;7:70. https://doi.org/10.3389/fphys.2016.00070.

Cawson RA, Odell EW. Cawson's essentials of oral pathology and oral medicine. 8th ed. London: Churchill Livingstone Elsevier.

Chen D, Li X, Lu F, Wang Y, Xiong F, Li Q. Dentin dysplasia type I – a dental disease with genetic heterogeneity. Oral Dis. 2018;. 10.111/odi.12861

Daryani D, Nair G, Naidu G. Dentin dysplasia type II: an exclusive report of two cases in siblings. J Indian Ac Oral Med Rad. 2017:132.

De Rio EP, Sir-Mendoza FJ, Carbal-Gonzalez AC. Odontomas: report and clinical case series. School of Dentistry, University of Cartagena, 2010-2015. Revista Odontologica Mexicana. 2017;21:e208–11.

De Sa Cavalcante D, Fonteles CSR, Ribeiro TR, Kurita LM, de Pimenta AVM, Carvalho FSR, Costa FWG. Mandibular regional odontodysplasia in an 8 year old boy showing teeth disorders, gubernaculum tracts, and altered bone fractal pattern. Int J Clin Ped Dent. 2018;11(2):128–34.

Gasse B, Prasad M, Delgado S, Huckert M, Kawczynski M, Garret-Bernardin A, Lopez-Cazaux S, Bailleil-Forestier I, Maniere M-C, Stoetzel C, Bloch-Zupan A, Sire J-Y. Evolutionary analysis predicts sensitive positions of MMP20 and validates newly- and previously- identified MMP20 mutations causing amelogenesis imperfecta. Front Physiol. 2017;8:398. https://doi.org/10.3389/fphys.2017.00398.

Kammoun R, Behets C, Mansour L, Ghoul-Mazgar S. Mineral features of connective dental hard tissues in hypoplastic amelogenesis imperfecta. Oral Dis. 2018;24:384–92.

Kim YJ, Kang J, Seymen F, Koruyucu M, Gencay K, Shin TJ, Hyun H-K, Lee ZH, Hu JC-C, Simmer JP, Kim J-W. Analysis of MMP20 missesnse mutations in two families with hypomaturation amelogenesis imperfecta. Front Physiol. 2017;8:229. https://doi.org/10.3389/fphys.2017.00229.

Kim Y, Seymen F, Kang J, Koruyucu M, Tuloglu N, Bayrak S, Tuna EB, Lee ZH, Shin TJ, Hyun H-K, Lee S-H, Hu J, Simmer J, Kim J-W. Candidate gene sequencing reveals mutations causing hypoplastic amelogenesis imperfecta. Clin Oral Invest. 2018; https://doi.org/10.1007/s00784-018-2577-9.

Li F, Liu Y, Yang J, Zhang F, Oral FH. Phenotype and genotype analyses in seven families with dentinogenesis imperfecta or dentin dysplasia. Dis. 2017;23:360–6.

Neville D, Allen B. Oral and maxillofacial pathology. 2nd ed. Philadelphia: Saunders.

Rajasekharan S, Martens L, Vanhove C, Aps J. In vitro analysis of extracted dens invaginatus teeth using various radiographic imaging techniques. Eur J Paediatr Dent. 2014;15:265–70.

Smith MH, Cohen DM, Katz J, Bhattacharyya I, Islam NM. Segmental odontomaxillary dysplasia. An unrecognized entity. JADA. 2018;149(2):153–62.

Taleb K, Lauridsen E, Daugaard-Jensen J, Nieminen P, Kreiborg S. Dentinogenesis imperfecta type II-genotype and phenotype analysis in three Danish families. Mol Genet Genomic Med. 2018;6:339–49.

Umapathy T, Veena A, Nagarathna C, Rakesh CB. Non-syndromic form of bilateral bimaxillary bull teeth – a case report with challenges in pediatric dentistry. OHDM. 2015;14:405–8.

Wang X, Wang J, Liu Y, Yuan B, Ruest LB, Feng JQ, Qin C. The specific role of FAM20C in dentinogenesis. J Dent Res. 2014;94(7):330–6. https://doi.org/10.1177/0022034514563334.

Whitt J, Rokos JW, Dunlap CL, Barker BF. Segmental odontomaxillary dysplasia: report of a series of 5 cases with long-term follow-up. Oral Surg Oral Med Oral Pathol Oral Radiol Endod. 2011;112:e29–47.

Different Types of Dysplasia in Pediatric Dental Practice

8

This chapter contains examples of different types of dysplasias on radiographic images taken with different radiographic techniques and their radiographic differential diagnoses. The aim of this chapter is to familiarize the reader with the different results of the techniques explained in the previous chapters. This is a grasp of what general pediatric dental practice could provide so at least the reader will get a better feel about how the images turn out and what information can be retrieved from them.

Names of distinguished colleagues who supplied the images for this chapter are mentioned with the radiographs. If there is no name mentioned with the radiographs, the radiographs were taken by the author of this book or collected from the different university clinics he has worked in (Ghent University in Belgium, University of Washington in Seattle, USA, and University of Western Australia in Perth, Australia).

8.1 Cleidocranial Dysplasia

Dysostosis cleidocranialis, or cleidocranial dysplasia as it is called today, is a syndrome associated with hyperdontia and in some occasions also with cleft lip and/or palate. These supernumerary teeth cause serious issues, as many don't even erupt and teeth stay embedded in the jaws, giving rise to dentigerous cysts. This rare familial disorder is characterized by defective formation of the clavicles (patient can bring shoulders extremely forward and almost touching if the clavicles are missing), delayed closure of the fontanelles (causing bulging of frontal, parietal, and occipital bones), and sometimes retrusion of the maxilla (a hypoplastic midfacial development). Figures 8.1 through 8.3 are three examples of patients with cleidocranial dysplasia.

J. Aps, *Imaging in Pediatric Dental Practice*,
https://doi.org/10.1007/978-3-030-12354-3_8

Fig. 8.1 This panoramic radiograph of a 10-year-old patient with cleidocranial dysplasia shows the haphazard organization of the teeth and the supernumerary tooth germs in both jaws (courtesy of Dr. Thierry Boulanger, Belgium)

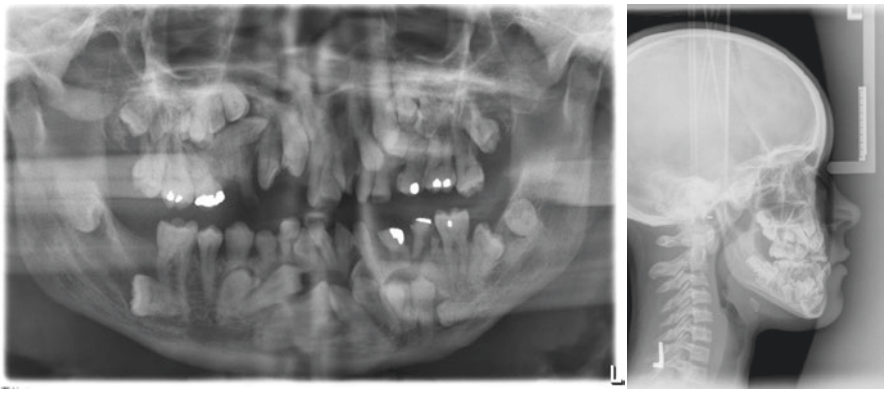

Fig. 8.2 This panoramic radiograph of a 15-year-old girl with cleidocranial dysplasia shows the impacted supernumerary teeth and also the superiorly displaced mandibular third molars. One can also appreciate the position of the supernumerary teeth in the maxilla obliterating the maxillary sinuses. The latter can also be seen on the cephalometric radiograph that was taken

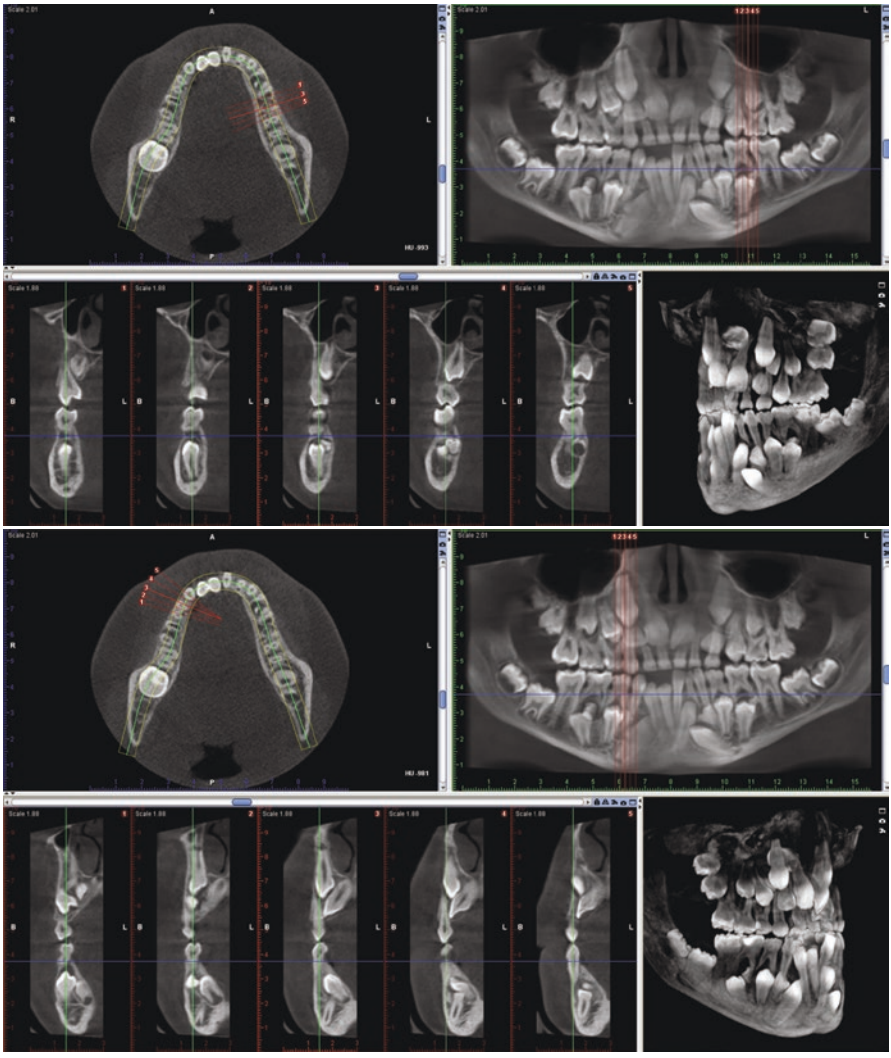

Fig. 8.3 This is a cone beam computed tomography of an 8-year-old girl with cleidocranial dysplasia, taken for surgical planning purposes to determine which supernumerary teeth were going to be sacrificed for extraction. The top image shows a couple of slices through the left-hand side of the patient's jaws, while the bottom images show the patient's right-hand side. Notice the supernumerary teeth on the lingual side in the mandible which can easily be missed on a traditional panoramic radiograph. The three-dimensional reconstructed radiographs can help the surgeon in this case to visualize the impacted supernumerary teeth better in relation to the erupted teeth

Cleidocranial dysplasia is a rare skeletal dysplasia with autosomal dominant inheritance (chromosome 6p21, OMIM 119600). A great number of different mutations are identified and studied, but what is interesting is the variable phenotype of the syndrome. Patients usually present with short stature, aplastic or hypoplastic clavicles, and delayed ossification of the calvaria, with accompanied delayed ossification of the sutures, leading to Wormian bones, wide forehead with broad midline furrow, midface hypoplasia, persistent mandibular symphysis, and several dental anomalies. The latter include lack of exfoliation of primary teeth, presence of multiple supernumerary teeth, abnormal anatomy especially of the roots of teeth, and not erupting permanent teeth.

8.2 Fibrous Dysplasia

Fibrous dysplasia (Figs. 8.4 through 8.7) is characterized by a localized change in the normal bone metabolism, resulting in replacement of cancellous bone with fibrous tissue. This translates in a typical radiographic appearance of fingerprint or orange peel appearance of the affected spongy bone. Expansion of the jaws is not uncommon and is usually the reason why radiographs are taken and how the pathology is found. There are mono- and poly-ostotic forms of fibrous dysplasia. The mono-ostotic form is more prevalent in the jaws; however the most common sites are ribs, femur, and tibia. The poly-ostotic form is usually found in children under the age of 10 years old.

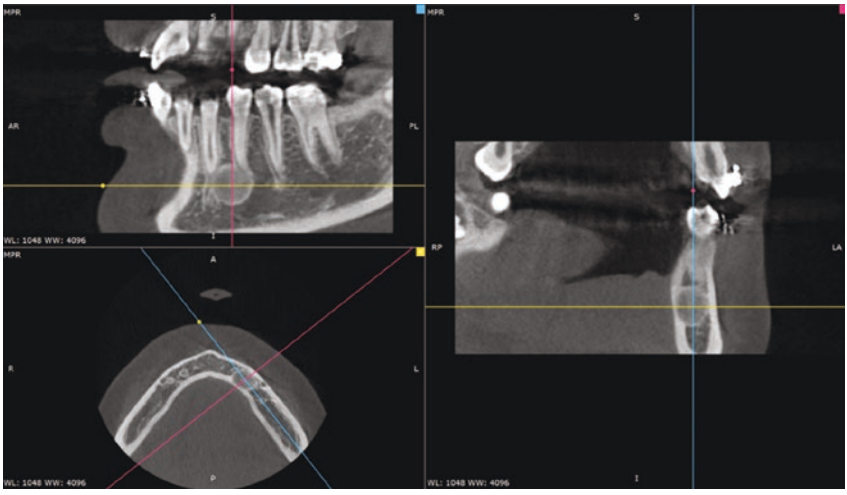

Fig. 8.4 This cone beam computed tomography shows a well-defined, corticated, uniform-appearing lesion, located between the apices of the left-hand-side mandibular canine and first premolar. The radiopaque border is typical for young lesions, whereas older lesions tend to have ill-defined borders. In this case the lingual cortical plate of the mandible is affected slightly and further expansion of the lesion can be expected. Since the lesion is not associated with the apex of a tooth, the differential diagnosis can exclude periapical cemento-osseous dysplasia, which by the way occurs in an older patient age group. The radiopaque border would be unusual for ossifying fibroma, which cannot be excluded from the differential diagnosis

Fig. 8.5 The panoramic radiograph of this 4-year-old boy shows massive changes in the circumference of the mandible, as well as in the radiographic appearance of the cancellous bone which is typical for fibrous dysplasia. As can be seen from the cropped clinical photograph, the disfigurement is substantial (courtesy of Dr. Nik Kantaputra, Thailand)

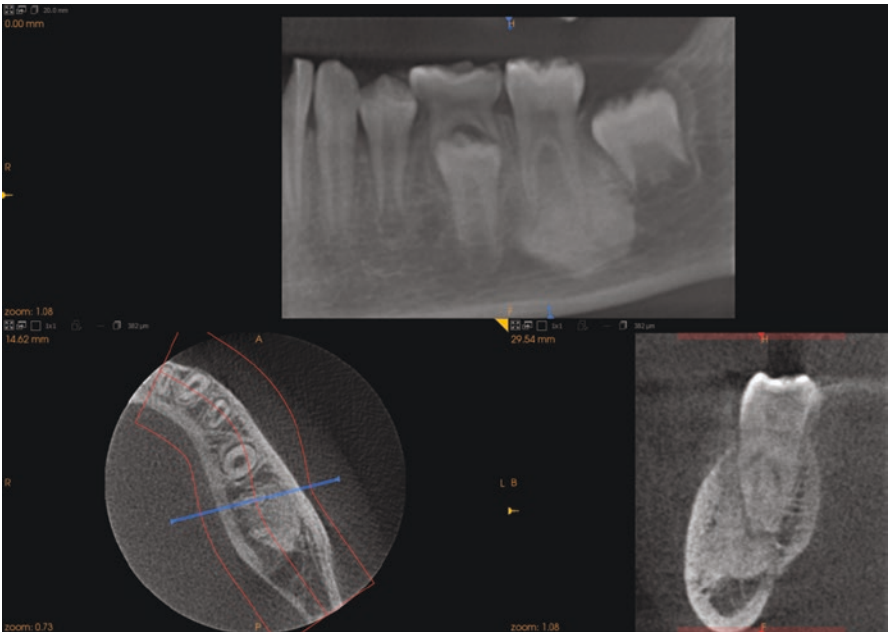

Fig. 8.6 This is a small-field-of-view cone beam computed tomography of a patient with fibrous dysplasia around the roots of the left-hand-side permanent first mandibular molar. In the coronal section one can appreciate the difference in radiopaque character between the lesion, the dentin of the tooth involved, and the cortical bone. One can also differentiate the periodontal ligament space between the tooth's root and the lesion, which helps identifying it from a dense bony island, hypercementosis, and cementoblastoma

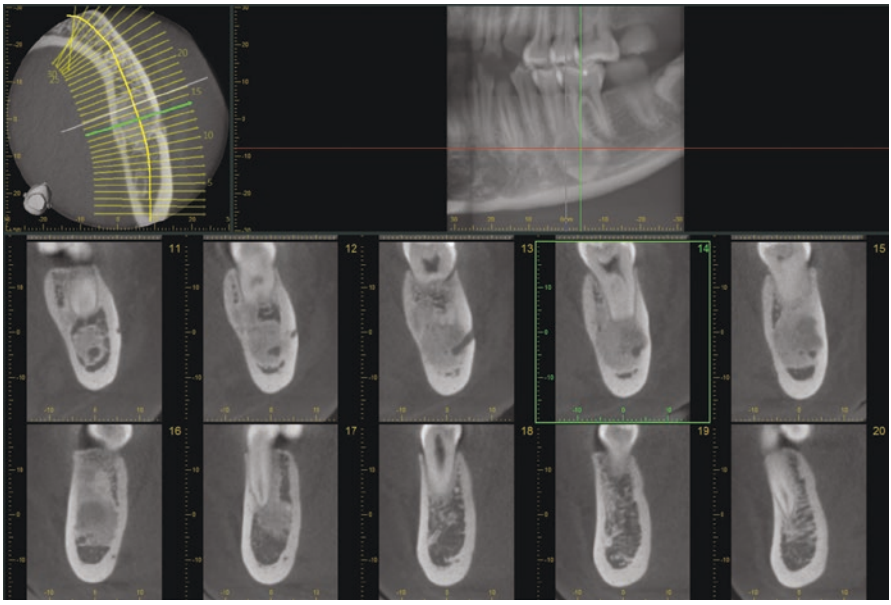

Fig. 8.7 This is another case of fibrous dysplasia which is located between the left-hand-side mandibular second premolar and first molar. One can appreciate the lesion forming around the inferior alveolar canal and expanding into the buccal and lingual cortical plates of the mandible. The integrity of the teeth is not affected, which differentiates this lesion from hypercementosis, cementoblastoma, and dense bony island

The pathogenesis of fibrous dysplasia is known to involve a postzygotic mutation of the GNAS1 gene. This results in an altered biochemical pathway, which leads to constitutive activation of G proteins and proliferation of undifferentiated mesenchymal cells. Mutations occur sporadically and postzygotically, which results in mosaicism and highly variable presentations. Abnormal bone matrix and growth of abnormal tissue are the consequences. It can occur at any age, both as monostotic and poly-ostotic or as part of McCune-Albright syndrome. The poly-ostotic variant affects the skull often, with 50–100% of cases having this involvement, with a preference for the frontal bone. The monostotic variant may arrest after puberty, whereas the poly-ostotic variant may continue through adulthood. Patient can have symptoms, like pain and mass effect on adjacent structures. This condition is benign, but in less than 1% can turn malignant. If asymptomatic, fibrous dysplasia does not require treatment.

8.3 Ectodermal Dysplasia

Ectodermal dysplasia is a large group of autosomal dominant, autosomal recessive, and X-linked inherited conditions in which two or more ectodermal derived tissues fail to develop properly, resulting in hypoplasia or aplasia of skin, hair, nails, teeth, salivary glands, or sweat glands. Teeth can be missing and/or shapes can be aberrant (usually conical) and both dentitions are involved. In general these patients will show hypodontia (Figs. 8.8 and 8.9) or even anodontia.

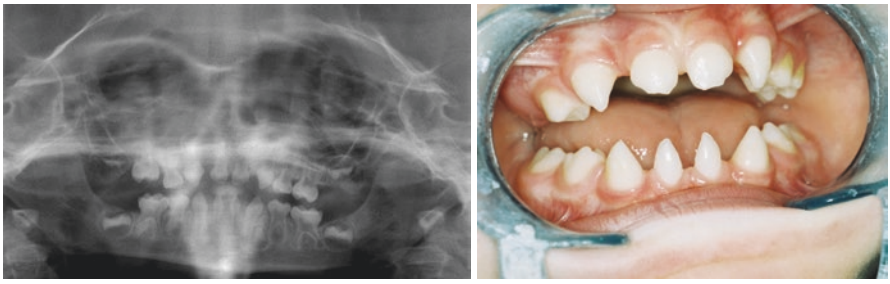

Fig. 8.8 This is a panoramic radiograph of a 4-year-old boy with hypohidrotic ectodermal dysplasia. Notice the conical shaped anterior teeth on both the panoramic radiographs as the clinical picture. Unfortunately there is no follow-up panoramic radiograph of the boy at an older age to verify hypodontia in the permanent dentition

Fig. 8.9 This is a panoramic radiograph of an adult patient with ectodermal dysplasia. Notice the severe hypodontia, and most of the permanent molars appear to have a normal anatomy, while the opposite can be observed for the incisors and canines, which appear rather conical and short in root length

Human WNT10A mutations are associated with developmental dental abnormalities and adolescent onset of a broad range of ectodermal defects. Hair follicles, sebaceous glands, taste buds, nails, and sweat ducts are also affected. The WNT10A gene is the most commonly mutated gene in human non-syndromic selected agenesis of permanent teeth and these mutations are also associated with ectodermal dysplasia syndromes odonto-onycho-dermal dysplasia and Schöpf-Schulz-Passarge syndrome. Patients with these mutations exhibit variable developmental dental defects, which include microdontia in the deciduous dentition, defective root and molar cusp formation, and even anodontia of the permanent dentition. Besides these dental associations, other tissues are affected as well, resulting in palmoplantar keratoderma, thinning of hair, sweating abnormalities, smooth tongue surface, and defective nail growth appearing in adolescence or even at later age.

8.4 Segmental Odontomaxillary Dysplasia

Hemimaxillofacial dysplasia (Fig. 8.10) is a synonym for this anomaly, which is developmental and of unknown etiology. The process affects the maxilla unilaterally and also affects the teeth and the attached gingiva in that section. The alveolar process is enlarged, with or without hypertrophy of the gingiva, and with dental anomalies. The latter involve missing teeth, hypoplastic teeth, and/or non-erupting teeth. In some cases, the following features have been observed as well: ipsilateral hypertrichosis, closely packed sebaceous glands in the upper lip, hyper- or hypopigmentation of the skin, Becker's nevus (pigmented hairy epidermal nevus), cleft lip, and/or palate. Depending on the hyperplasia of the alveolar crest, facial enlargement can occur, with facial asymmetry resulting. Radiographically the orientation of the trabeculae in the affected side of the maxilla is vertical. The roots and crowns of the affected primary teeth are larger than on the unaffected side. Absence of normal resorption of these teeth and a hypoplastic maxillary sinus are also common features. Permanent teeth eruption is delayed often. Differential diagnosis with fibrous dysplasia might be challenging.

Fig. 8.10 The clinical pictures of this 5-year-old girl with segmental odontomaxillary dysplasia show the changes in the position of the teeth on the affected side of the maxilla. This case did not have significant mucosal hypertrophy, though the position of the teeth worried the parents of the girl and the dentist. On the radiograph one can depict the double-rooted right-hand-side maxillary deciduous canine and the large crown of the second deciduous molar (courtesy of Dr. Anouk Eloot, Belgium)

Further Reading

Bohring A, Stamm T, Spaich C, Haase C, Spree K, Hehr U, Hoffmann M, Ledig S, Sel S, Wieacker P, Roepke A. WNT10A mutations are a frequent cause of a broad spectrum of ectodermal dysplasias with sex-biased manifestation pattern in heterozygotes. Am J Human Gen. 2009;85:97–105.

Cawson RA, Odell EW. Cawson's essentials of oral pathology and oral medicine. 8th ed. London: Churchill Livingstone Elsevier.

Koenig. Diagnostic imaging, oral and maxillofacial. Salt Lake City: Amirsys.

Koong B. Atlas of oral and maxillofacial radiology. Hoboken: Wiley Blackwell.

Kreiborg S, Jensen BL. Tooth formation and eruption – lessons learnt from cleidocranial dysplasia. Eur J Oral Sci. 2018;126(Suppl.1):72–80.

Larheim TA, Westesson P-LA. Maxillofacial imaging. 2nd ed. Berlin: Springer.

Neville D, Allen B. Oral and maxillofacial pathology. 2nd ed. Philadelphia: Saunders.

Penn DL, Tartarini RJ, Glass CH, De Girolami U, Zamani AA, Dunn IF. Natural history of cranial fibrous dysplasia revealed during long-term follow-up: case report and literature review. Surg Neurol Int. 2017;8:209.

Whaites E, Drage N. Essentials of dental radiography and radiology. 5th ed. London: Churchill Livingstone Elsevier.

White SC, Pharoah MJ. Oral radiology. In: Principles and interpretation. 7th ed. Amsterdam: Elsevier.

Wu H, Yang L, Li S, Xu J, Lu J, Zhang C, Teng L. Clinical characteristics of craniomaxillofacial fibrous dysplasia. J Cranio Maxillo Facial Surg. 2014;42(7):1450–5. https://doi.org/10.1016/j.jcms.2014.04.009.

Xu M, Horrell J, Snitow M, Cui J, Gochnauer H, Syrett CM, Millar SE. WNT10A mutation causes ectodermal dysplasia by impairing progenitor cell proliferation and KLF4-mediated differentiation. Nat Commun. 2017;8:15397. https://doi.org/10.1038/ncomms15397.

Examples of Common Cystic Lesions in Pediatric Dental Practice

9

This chapter contains some examples of common cystic lesion examples and their radiographic appearance and their radiographic differential diagnoses. Obviously not all types of pathology were captured in this textbook chapter, but at least the reader will get a better feel about how the images turn out and what information can be retrieved from them.

Names of distinguished colleagues who supplied the images for this chapter are mentioned with the radiographs. If there is no name mentioned with the radiographs, the radiographs were taken by the author of this book or collected from the different university clinics he has worked in (Ghent University in Belgium, University of Washington in Seattle, USA, and University of Western Australia in Perth, Australia).

9.1 Dentigerous Cyst and Ameloblastic-Fibroma and Ameloblastic Fibro-Odontoma

The radiographic appearance of a *dentigerous cyst* is one of a uniform radiolucent, unilocular, well-defined, and corticated lesion that surrounds the crown of an erupted tooth. This developmental cyst appears to be attached to the cementoenamel junction and prevents normal eruption of the affected tooth and may displace the tooth considerably. It is more common in males, but not very common in children or adolescents. One should also keep in mind that some ameloblastomas and keratocystic odontogenic tumors can mimic a dentigerous cyst.

Ameloblastic fibro-odontoma is a mixed tumor with the same constituents as an *ameloblastic fibroma*, with the difference being the latter lacking collections of enamel and dentin (Figs. 9.1 and 9.2). There might be a tooth missing or a tooth might not have erupted. Differential diagnosis must include the following: ameloblastic fibroma, odontoma, adenomatoid odontogenic tumor, calcifying cystic odontogenic tumor, and calcifying epithelial odontogenic tumor.

J. Aps, *Imaging in Pediatric Dental Practice*,
https://doi.org/10.1007/978-3-030-12354-3_9

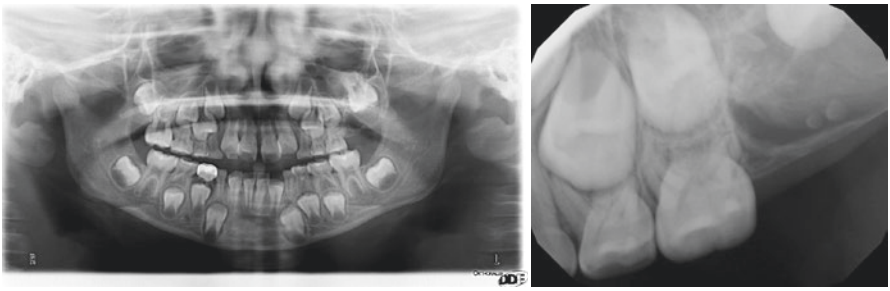

Fig. 9.1 The panoramic radiograph was taken because the maxillary left-hand-side first permanent molar had not yet erupted, while all other first permanent molars had and were in occlusion. The radiograph shows the presence of a well-defined, corticated, radiolucent lesion around the superiorly displaced left-hand-side maxillary first permanent molar and a congenitally missing second permanent molar. The periapical radiograph showed small round-shaped radiopaque entities within the radiolucent lesion

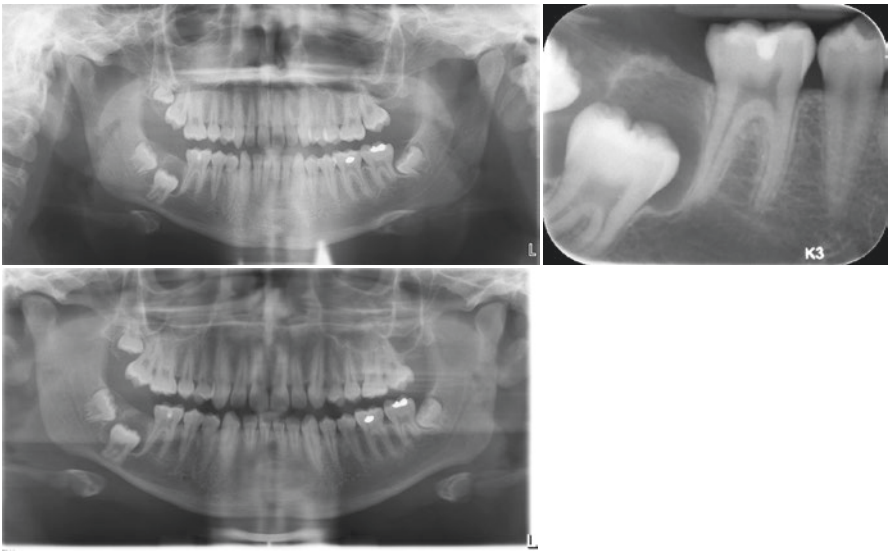

Fig. 9.2 The panoramic radiograph at the top was taken 1 year before the radiograph shown at the bottom. The periapical radiograph was taken when the second panoramic radiograph was taken. The reason for the right-hand-side second mandibular molar not erupting in this 14-year-old boy is because there is a dentigerous cyst, which has displaced the tooth inferiorly, with its roots impinging on the inferior cortical border of the mandible. Differential diagnosis should include ameloblastic fibroma and ameloblastoma. Unfortunately one was not able to follow up on this patient and hence the final diagnosis and treatment could not be included here

A dentigerous cyst is assumedly derived from cystic changes in the remains of the enamel organ after the enamel formation is completed. They seem to occur more in patients between 20 and 50 years of age. Progressive growth of the cyst leads to dilation of the dental follicle. They are most common around teeth which happen to have a great prevalence for failure to erupt: maxillary canines and mandibular third molars.

9.2 Cherubism

Cherubism is a giant cell lesion and is painless (Fig. 9.3). The typical radiographic appearance of cherubism is multilocular lesions (the result of fine bony septa extending between the soft-tissue masses) in the maxilla and mandible that start in childhood. They enlarge in the first place and then regress when the patient goes into adolescence. It is inherited as an autosomal dominant trait; however, there might be no previous report of cherubism in the family. It is also twice as common in males and the disorder seems to be rare in Japan. Teeth are frequently displaced and may be loosened and if the maxilla is affected the borders of the maxillary sinuses and even the orbits can be affected. Cervical lymphadenopathy can be present, despite the lack of inflammation, but due to reactive hyperplasia and fibrosis.

Cherubism is mapped to chromosome 4p16. The name refers to the children's facial appearance, which resembles that of plump-cheeked angels, angelic chubby cheeks of cherubs, which one can find in Catholic churches and in paintings from the Renaissance. Additionally, one can also recognize these patients, by their eyes being "upturned," due to a wide rim of exposed sclerae below the iris of the eye. The latter is caused by involvement of the inferior rim of the orbit and its floor, which pushed the eyeball upwards. Simultaneously the upper eyelids are pulled down, which accentuates the "eyes to heaven" appearance. Depending on the bony expansion and the areas involved, the patient's aesthetics will be impacted. Besides dental consequences such as unerupted and displaced teeth, and impaired mastication, also speech difficulties and loss of normal hearing and vision can be a problem. This adds all up to the psychological pressure in these patients. Erroneously, cherubism has also been called familial fibrous dysplasia, despite the condition not being related to fibrous dysplasia at all.

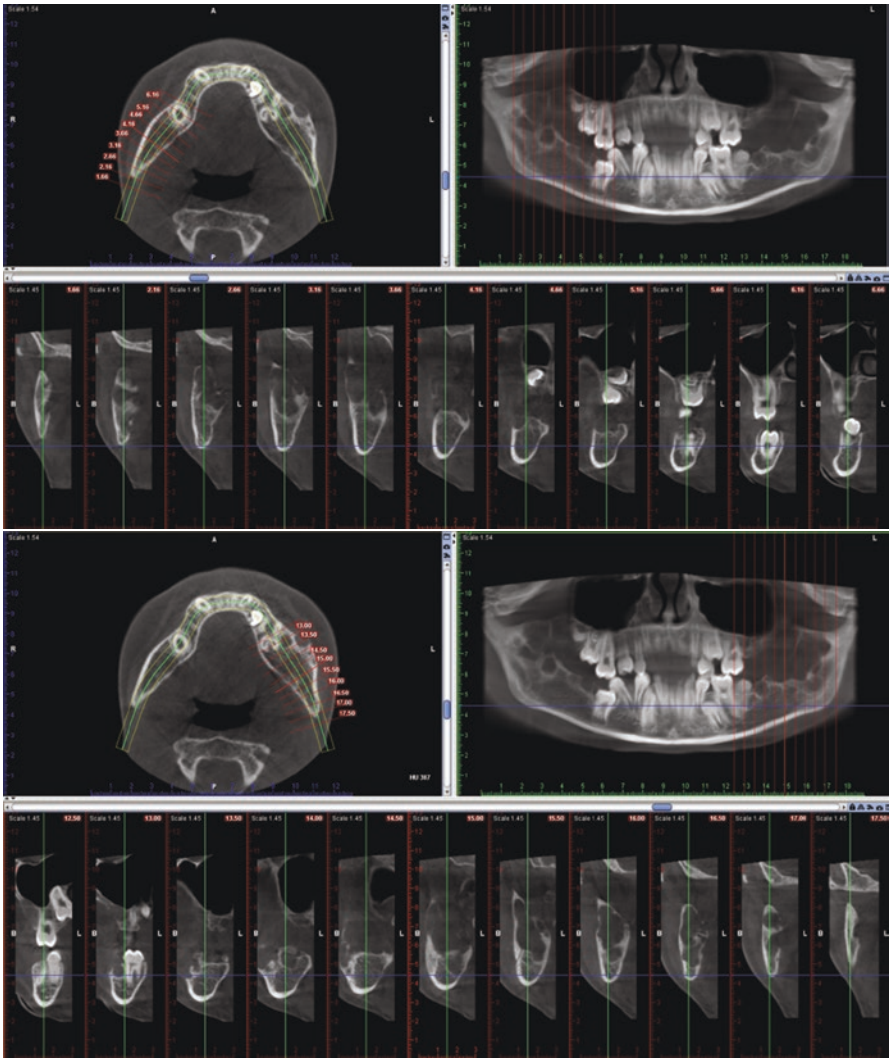

Fig. 9.3 This is a cone beam computed tomography of a boy with cherubism. The top image shows the slices through the right-hand side of the mandible and maxilla, while the bottom images are slices through the left-hand side of both jaws. One can appreciate the missing molars in both jaws, and the multilocular lesions in the mandible, which have caused substantial expansion of the buccal and lingual contours of the mandible, especially on the patient's left-hand side

9.3 Buccal Bifurcation Cyst

Synonyms for this cyst are *paradental cyst*, *infected buccal cyst*, and *inflammatory paradental cyst* (Figs. 9.4 and 9.5). The first permanent mandibular molar is affected most, compared to the second molar. A painless, hard buccal swelling is clinically

visible. It can occur bilaterally, but that is definitely not the rule of thumb. If secondary infection occurred, the patient can report pain. Radiographically a radiolucent area can be appreciated in the region of the furcation and distal to the root of the tooth. Buccal bifurcation cysts may be derived from epithelial cell rests of the periodontal membrane, located at the bifurcation of the molar tooth, and histologically they have the same characteristics of a radicular cyst. It is suggested that the paradental cyst on the third molar and the buccal bifurcation cyst, which is typically related to the first or second permanent mandibular molar, are the same cyst. However, this is food for discussion and falls outside of the scope of this book. Buccal bifurcation cysts cause delayed eruption of the affected tooth, which is in turn due to the position of the cyst, pushed with its roots against the lingual cortical plate of the mandible, causing the lingual cusps to be positioned higher than the buccal cusps. The tipping of the tooth is typical and distinguishes this lesion from any other lesion that can mimic this (e.g., periodontal cyst and Langerhans cell histiocytosis). In some cases the cyst involves an enamel spur or pearl. Not all buccal bifurcation cysts require surgical intervention.

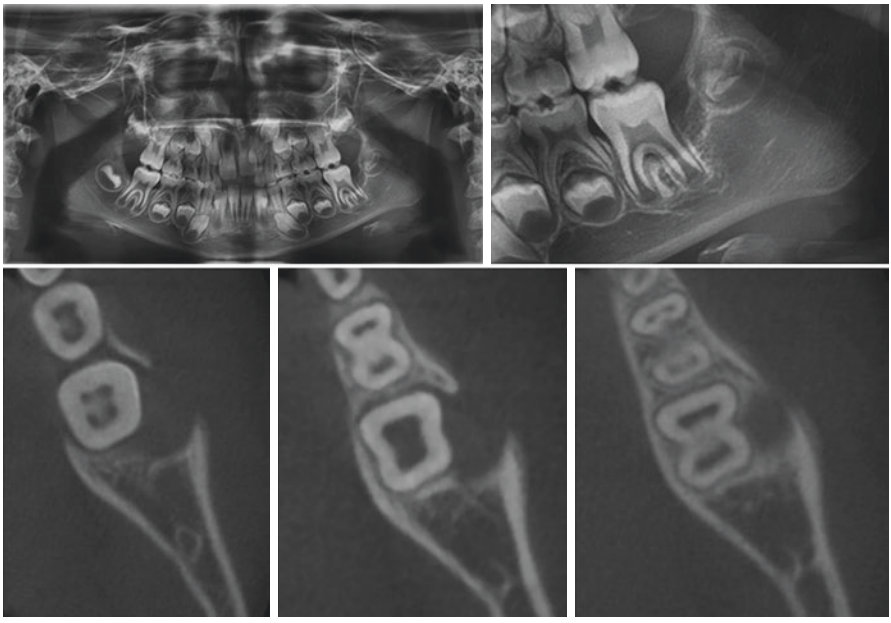

Fig. 9.4 The panoramic radiograph of this 6-year-old boy shows an unusual radiolucent area distal to the first left-hand-side mandibular molar. The cropped part of that radiograph shows a magnification of that area. The cropped cone beam computed tomography images below show the expansion and perforation of the buccal cortical plate of the mandible. This tooth did not have an enamel spur or pearl. The diagnosis was histologically supported as buccal bifurcation cyst. Noteworthy is to emphasize on the fact that the calcification of the second left-hand-side mandibular molar is delayed as well, compared to the other three second molars. The latter requires follow-up (courtesy of Dr. Annelore De Grauwe, Belgium)

Fig. 9.5 This panoramic radiograph clearly shows delayed eruption of the left-hand-side first permanent molar and the adjacent radiolucent area, indicating a buccal furcation cyst. A closer inspection (cropped panoramic image) reveals an enamel spur in the furcation and one can appreciate the extension of the radiolucent area distal of the involved tooth. The cropped cone beam computed tomography image shows the borders of the lesion clearly and the proximity to the second permanent mandibular molar (courtesy of Dr. Annelore De Grauwe, Belgium)

9.4 Solitary Bone Cyst

There are a plethora of synonyms for solitary bone cyst: *simple bone cyst, traumatic bone cyst, hemorrhagic bone cyst, extravasation cyst, progressive bone cavity, and unicameral bone cyst* (Figs. 9.6 and 9.7). It is actually a pseudocyst, devoid of epithelial lining, but with connective tissue lining the walls and depending on the sources empty or filled with a sanguineous or serous fluid. Its etiology is unknown and it is usually an incidental radiographic finding in adolescent patients. Boys seem to be affected twice as much as girls. The most common site in the jaws is the mandible and more specific anterior and premolar region. Typical radiographic feature of this uniform radiolucent lesion is that the superior borders of the lesion usually scallop between the roots of the teeth and that with or without a clear corticated border. Whereas the teeth are not displaced, the cortical borders of the mandible might be slightly. It needs to be emphasized that these bony cavities occur often inside lesions of cemento-osseous dysplasia and fibrous dysplasia. Obviously the latter do not occur in the age group described in this book.

Fig. 9.6 This panoramic radiograph taken in a 16-year-old boy showed, besides two supernumerary molars in the second and third quadrants, also a uniform radiolucent lesion at the apex of the left-hand-side mandibular canine. This solitary bone cyst is partially well corticated and scallops between the roots of the adjacent teeth

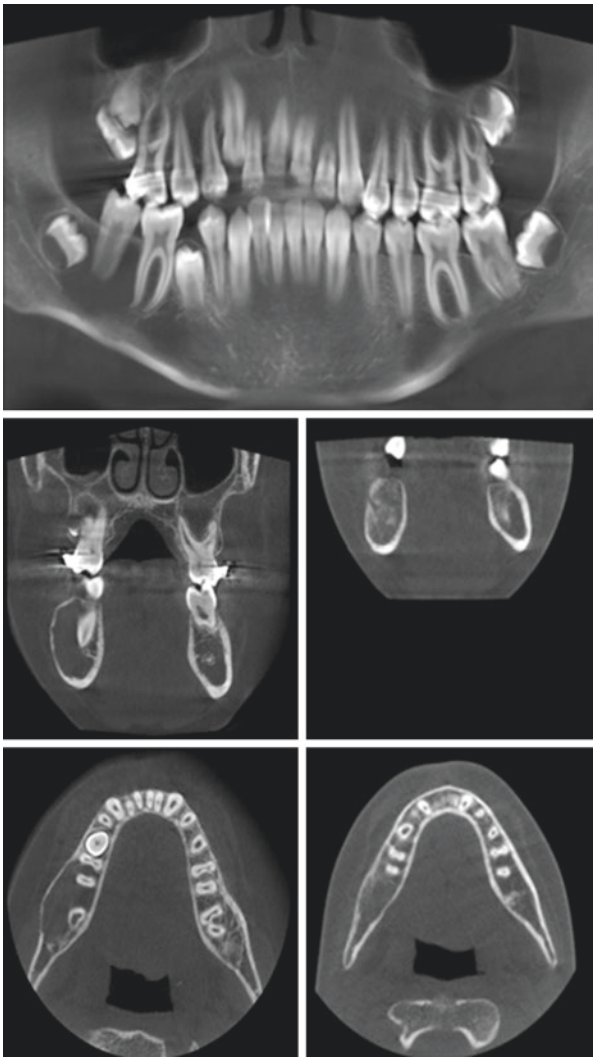

Fig. 9.7 This 14-year-old boy was followed up by a different orthodontist than the one who started the orthodontic treatment initially. Because the second orthodontist noticed a swelling in the right mandible, a panoramic radiograph was taken (not included here). The diagnosis was not conclusive, so the orthodontist ordered a cone beam computed tomography (top and bottom left-hand-side images). An ill-defined uniform radiolucent lesion, that scalloped between the roots of the right-hand-side mandibular molars, was observed. The teeth were not displaced but the buccal cortical wall of the mandible was clearly expanded. Surgery was performed and according to the oral surgeon's report the lesion was empty, which correlated with the diagnosis of solitary bone cyst. The image bottom right-hand side is the smaller field and lesser resolution cone beam computed tomography which was made 3 months post-surgery. It is clear from these coronal and axial slices that the lesion is healing and that the expansion of the mandible has decreased

9.5 Radicular or Periapical Cyst

Necrosis of the pulp can stimulate the apical epithelium to form a true epithelial lined cyst. The inflammatory response appears to trigger keratinocyte growth factor by periodontal stroma cells, which then subsequently start growing. The source of epithelium is usually cells rests of Malassez, but can also be from crevicular epithelium, sinus lining, or epithelial lining of fistulous tracts. Cysts will develop in 7–54% of necrotic teeth. The difference between a periapical granuloma and periapical cyst can only be made histologically. Radiographic appearance may be similar though. If exodontia is considered and the cyst is not enucleated, a residual cyst can develop. Some of the latter may heal spontaneously, but many may not. The radiographic appearance of a radicular cyst is usually a round lesion, centered around the root of the necrotic tooth. They can, however, expand and displace teeth and cause root resorption as well. Figure 9.8 is an illustration of a radicular cyst on a primary molar that mimicked a dentigerous cyst on the underlying premolar.

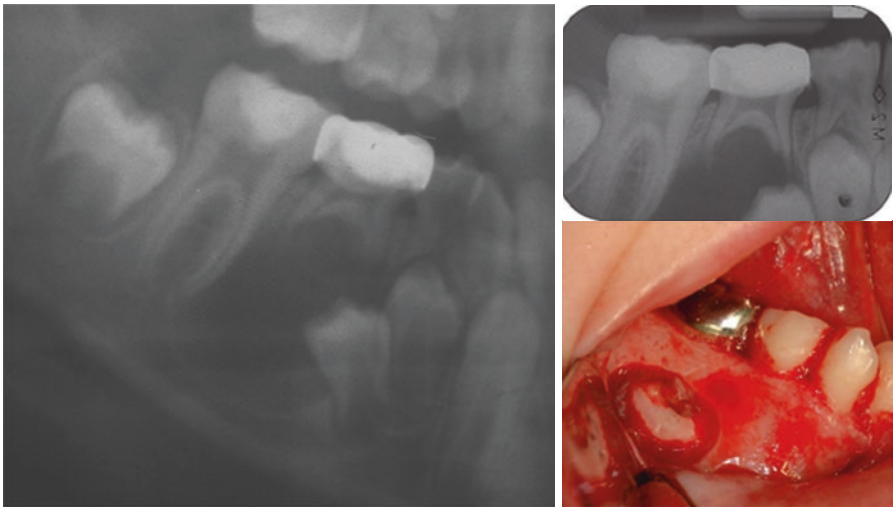

Fig. 9.8 This is a case of a 9-year-old patient who had a swelling buccal to the right-hand-side mandibular second primary molar. The cropped panoramic radiograph and the periapical radiograph at the top show a well-defined, uniform radiolucent, unilocular lesion apically to the deciduous molar. The permanent successor appears to be displaced inferiorly and the radiographs suggest a dentigerous cyst, as the cyst could be attached to the cementoenamel junction of the second premolar. When the surgeon explores the site, the lesion appears to be attached to the roots of the primary molar, which confirmed the diagnosis of radicular cyst. The primary tooth with the radicular cyst was removed and spontaneous eruption of the premolar followed soon (panoramic radiograph at the bottom of 9.5A)

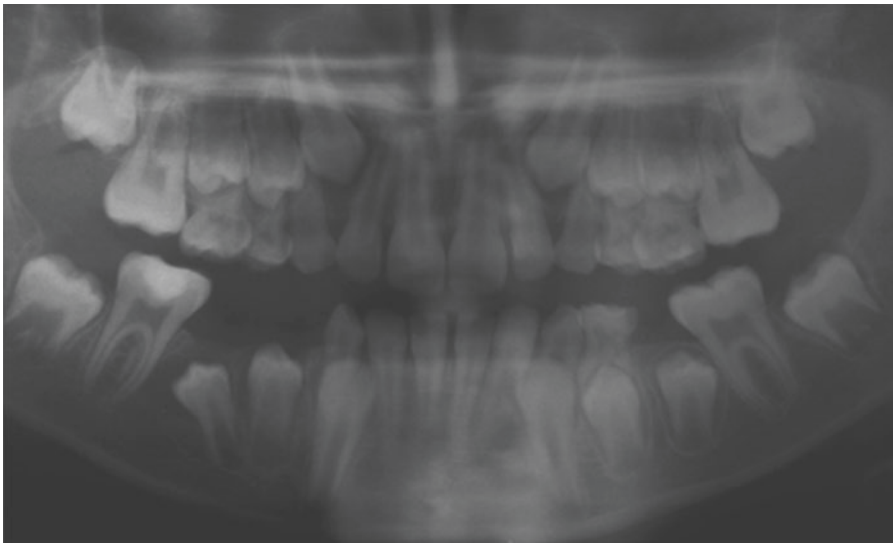

Fig. 9.8 (continued)

Further Reading

Battisti MPL, Soares MQS, Rubira CMF, Bullen IRFB, Lauris JRP, Damante JH. Assessment of spontaneous resolution of idiopathic bone cavity. J Appl Oral Sci. 2018;26:e20170288.

Cawson RA, Odell EW. Cawson's essentials of oral pathology and oral medicine. 8th ed. London: Churchill Livingstone Elsevier.

De Grauwe A, Mangione F, Mitsea A, Kalyvas D, Yfanti Z, Ahbab G, Salmon B, Jacobs R. Update on a rare mandibular osteolytic lesion in childhood: the buccal bifurcation cyst. BMJ Case Rep. 2018;4:20170109.

De Souza Tolentino E, Stuchi Centurion B, Cuhna Lima M, Freitas-Faria P, Consolaro A, Sant'ana E. Ameloblastic fibro-odontoma: a diagnostic challenge. Int Dent J. 2010; https://doi.org/10.1155/2010/104630.

Koenig. Diagnostic imaging, oral and maxillofacial. Salt Lake City: Amirsys.

Koong B. Atlas of oral and maxillofacial radiology. Hoboken: Wiley Blackwell.

Larheim A, Westesson P-LA. Maxillofacial imaging. T2nd ed. Berlin: Springer.

Machado RA, Pontes HAR, Pires FR, Silveira HM, Bufalino A, Carlos R, Tuji FM, Alves DBM, Santos-Silva AR, Lopes MA, Capistrano HM, Coletta RD, Fonseca FP. Clinical and genetic analysis of patients with cherubism. Oral Dis. 2017;23:1109–15.

Neville D, Allen B. Oral and Maxillofacial Pathology. 2nd ed. Philadelphia: Saunders.

Whaites E, Drage N. Essentials of dental radiography and radiology. 5th ed. London: Churchill Livingstone Elsevier.

White And SC, Pharoah MJ. Oral radiology. In: Principles and interpretation. 7th ed. Amsterdam: Elsevier.

Examples of Congenitally Acquired Pathology in Pediatric Dental Practice

10

This chapter contains examples of congenitally acquired pathology. Obviously not all types of pathology were captured in this textbook chapter, but at least the reader will get a better feel about how the images turn out and what information can be retrieved from them.

Names of distinguished colleagues who supplied the images for this chapter are mentioned with the radiographs. If there is no name mentioned with the radiographs, the radiographs were taken by the author of this book or collected from the different university clinics he has worked in (Ghent University in Belgium, University of Washington in Seattle, USA, and University of Western Australia in Perth, Australia).

10.1 Cleft Palate Patients

The etiology of cleft lip or palate has a genetic component in 40% of cases. If one or both parents are affected, the chance of having a child with a cleft lip and/or palate is higher than if none of the parents are affected. Cleft lip, with (58%) or without cleft palate (22%), is more seen in males, whereas a cleft palate alone (20%) is twice as often observed in girls. The prevalence of isolated cleft lip is 1 in every 1000 live births, and the prevalence of isolated cleft palate is 1 in every 2000 live births. It is obvious that in terms of radiation dose, cone beam computed tomography can be beneficial in planning and following up of the surgeries these children with palatal clefts require, compared to medical CT. Figures 10.1 and 10.2 illustrate the use and benefits (image quality and low dose compared to medical CT) of cone beam computed tomography in patients with cleft palate.

J. Aps, *Imaging in Pediatric Dental Practice*,
https://doi.org/10.1007/978-3-030-12354-3_10

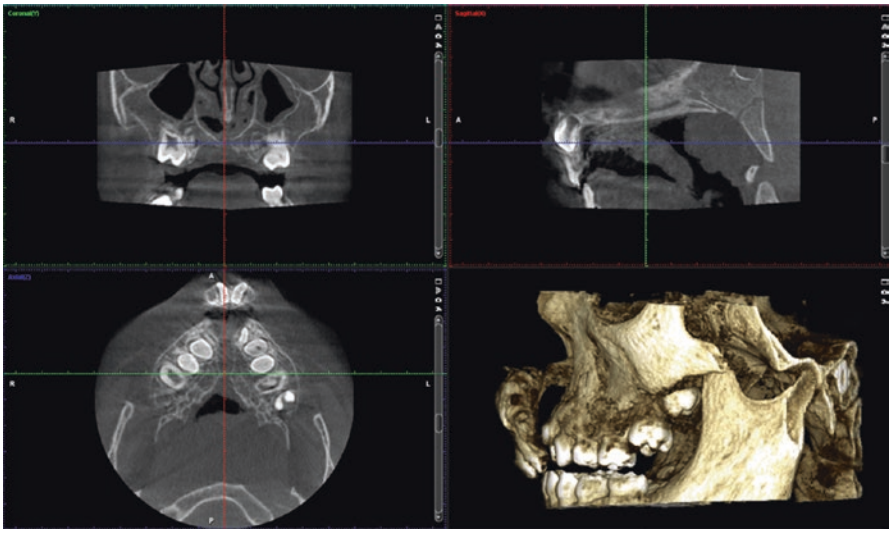

Fig. 10.1 This is a cone beam computed tomography of the maxilla of a 10-year-old patient with a cleft lip and palate. The defect in the bony palate can be clearly observed and assessed and the surgeon can plan their surgery to fix the premaxilla. Also notice the mucosal hypertrophy in the left-hand-side maxillary sinus and the spheno-occipital synchondrosis

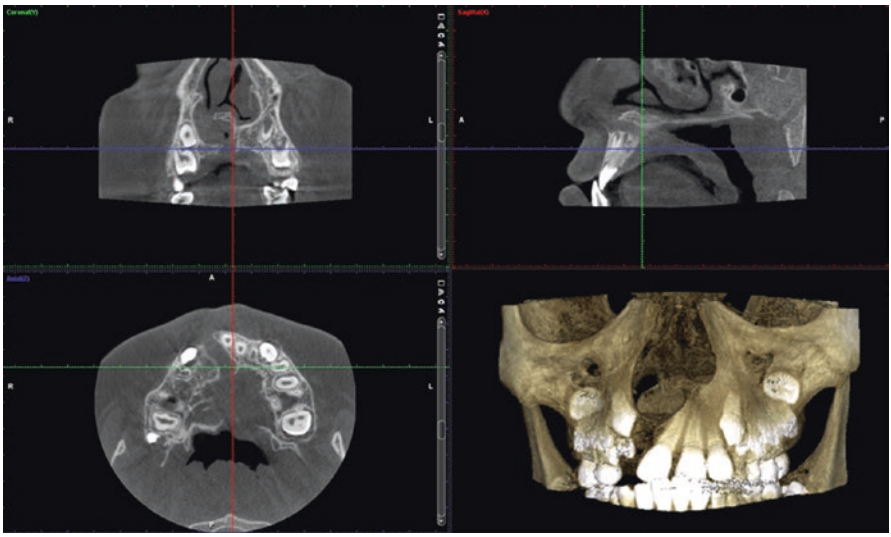

Fig. 10.2 This is a cone beam computed tomography taken in an 8-year-old boy with a unilateral cleft lip and palate on his right-hand side. Typical is the missing tooth (right-hand side maxillary lateral incisor) in the cleft and the deviation of the nasal septum as is clear from these images. Also notice the presence of the spheno-occipital synchondrosis and the rather large foramen of the sphenoid sinus into the nasal cavity (sagittal view)

A synchondrosis is a fusion between two bones to form one bone. The sphenooccipital synchondrosis consists of the basilar part of the occipital bone and the body of the sphenoid bone, hence the synonym called sphenobasilar synchondrosis. They both form the clivus, which is the slope from the posterior clinoid process towards the foramen magnum. The union between the two bones signifies adulthood and although there is not 100% consensus in the literature when the synchondrosis is ossified, the age span is between 18 and 25 years of age, with females being 2 years ahead of males, in general. Ossification starts from the clivus towards the base of the skull, so from intracranial to extracranial.

10.2 Hemifacial Microsomia

Hemifacial microsomia or *hemifacial hypoplasia, craniofacial microsomia,* and *lateral facial dysplasia* are all synonyms and syndromes associated with it are Goldenhar syndrome and oculo-auriculo-vertebral dysplasia. It is the second most common developmental craniofacial anomaly after cleft lip and palate. The patients show reduced growth, and development of the affected side of the face, rendering their appearance asymmetrical. This is due to the fact that the anomaly is related to the first and second branchial arches. If bilateral, it is called craniofacial microsomia.

If an entire side of the cranial anatomy is affected, the following structures will be involved and hypoplastic: mandible, maxilla, zygoma, external and middle ear, hyoid bone, parotid gland, vertebrae, cranial nerves V (trigeminal nerve) and VII (facial nerve), and all associated soft tissues (e.g., microtia, musculature). Hypodontia and/or failure of teeth to erupt on the affected side are common features, as is malocclusion obviously. There is a progressive form which is known under the name of Parry-Romberg syndrome. The latter patients do not have any features at birth and their ears are normal. Figures 10.3 and 10.4 illustrate a case of hemifacial microsomia where cone beam computed tomography was used. It is obvious that collaboration with a dentomaxillofacial or medical radiologist is essential as this large field of view CBCT scan goes beyond the field of expertise of a paediatric dentist and additional information from either radiology specialist may affect the comprehensive treatment plan of the patient.

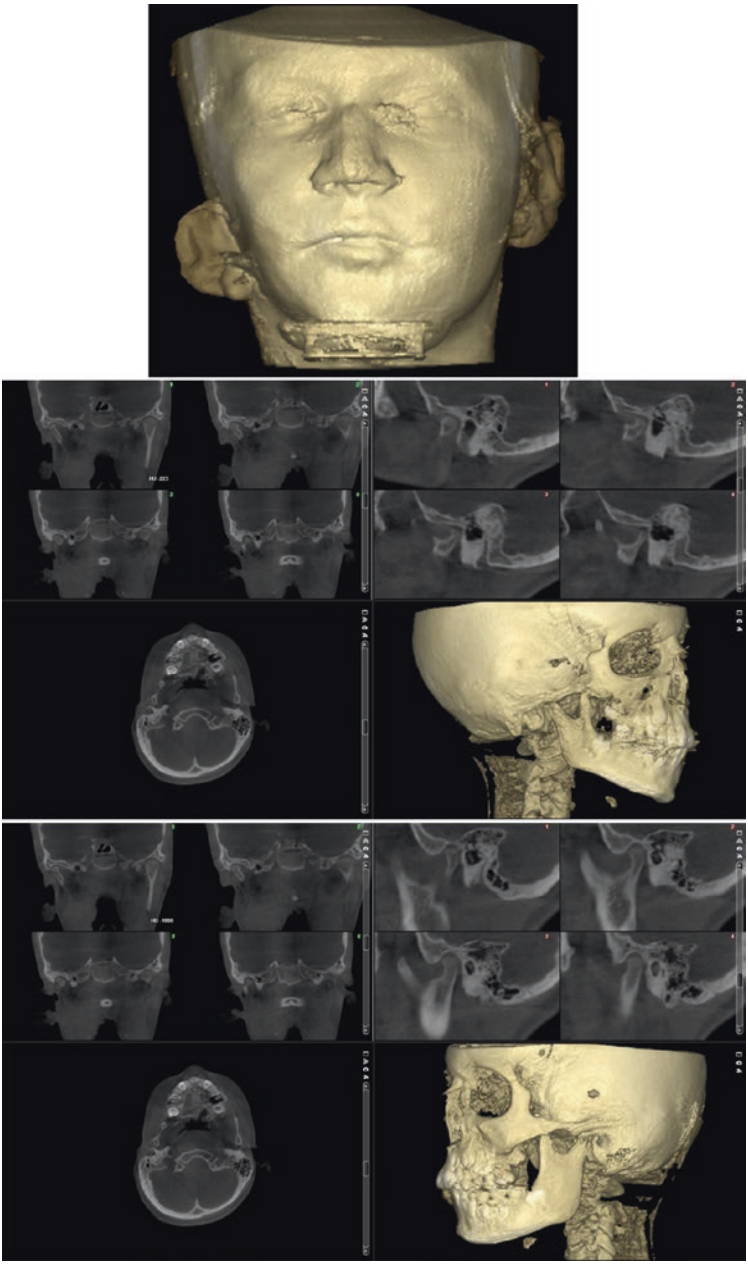

Fig. 10.3 This is a large-field-of-view cone beam computed tomography of a girl with hemifacial microsomia on the right-hand side of her face. At the top the three-dimensional reconstructed image of the soft tissues is shown to illustrate the shape of the right-hand-side auricle, which is obviously hypoplastic and more inferior than the auricle on the patient's left-hand side. The other images illustrate the difference in the mandibular condyles (seen in both lateral and anterior views—top image being the patient's right-hand side), rami, and mandibular notches

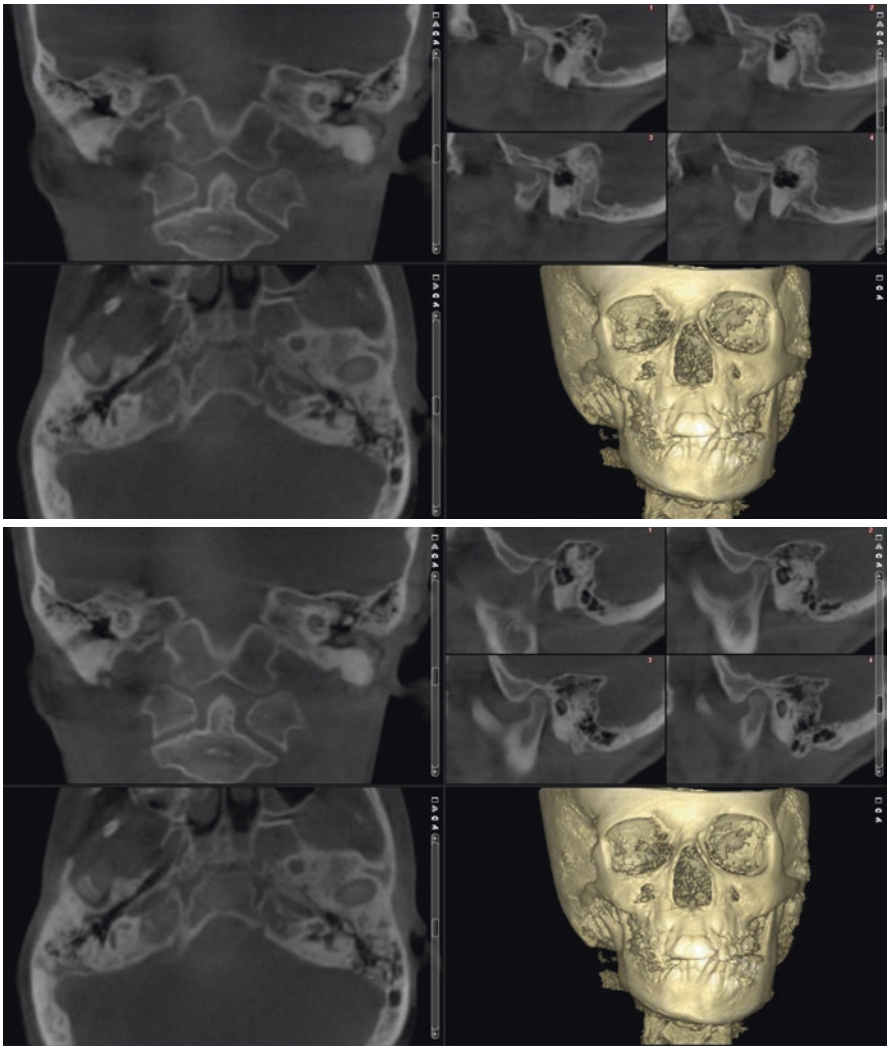

Fig. 10.4 This is the same patient as in Fig. 10.3. These images illustrate the differences in the ossicles between the right-hand side (top) and left-hand side (bottom). The aberrant anatomy of the inner right ear explains why the patient is deaf on that side. From the three-dimensional reconstructed images one can appreciate the malocclusion in this young girl's dentition due to her hemifacial microsomia

Fig. 10.5 This is a panoramic radiograph of a patient with Treacher Collins syndrome who had orthognathic surgery done. Despite the surgical paraphernalia in place to reconstruct the craniofacial skeleton, one can distinguish the following features: hypoplasia of the zygomatic arches, steep mandibular angles with distinct antegonial notches, auricular implants placed to establish a better aesthetical appearance, and a genioplasty to reconstruct the anterior mandible and to create a more prominent chin

10.3 Treacher Collins Syndrome

Treacher Collins syndrome and *mandibulofacial dysostosis* are synonyms and it is the most common type of mandibulofacial dysostosis. These patients can have a wide range of anomalies, but the most prominent one is the absence or hypoplasia of the zygomatic bones, hypoplasia of the mandible with a steep angle, (Fig. 10.5) and malformation of the auricles and often also the ossicles, all which give these patients their typical facial appearance: small narrow face with a high palate, downward inclination of the palpebral fissures, downturned wide mouth, and sometimes complete absence of auricles and external acoustic meatus. Occasionally patients also have cleft lip and/or palate. If the ossicles are affected, deafness is also a feature.

10.4 Mucopolysaccharidosis

Mucopolysaccharidosis (MPS) is caused by deficiency of iduronate-2-sulfatase which is characterized by excretion of dermatan sulfate and heparin sulfate in urine. Hurler-Hunter syndrome (Fig. 10.6) is another terminology often used; however, Hurler and Hunter are two separate entities or syndrome types of MPS, the former being autosomal recessive inherited and the gravest and the latter being X-linked recessive. Typical orofacial features of MPS include heavy brow ridges, stiff temporomandibular joints, cloudy degeneration of the corneas, macroglossia, gingival hyperplasia, thin enamel, pointed cusps sometimes (Morquio-B type), and impacted teeth.

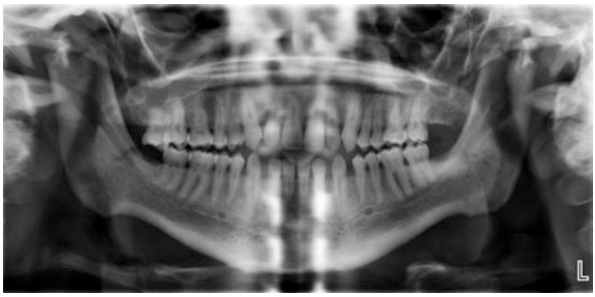

Fig. 10.6 This patient, with Hunter-Hurler syndrome diagnosis, was seen for a dental checkup. From this panoramic radiograph one can appreciate the unusual spacing in the anterior mandible, due to gingival hyperplasia. The canines show rather conically shaped crowns, but what is most prominent is the aberrant anatomy of the mandibular rami and their condyles, with posterior concavities and absence of mandibular notches and prominent coronoid processes. The latter can explain the restricted mouth opening and jaw movements. Distinct antegonial notches are also present, which can be related to the forces applied to the masseteric muscles

Fig. 10.7 This 11-year-old patient had an alveolar rhabdomyosarcoma of the hard palate, diagnosed at age 3. The panoramic radiograph shows generalized short roots. The latter is caused by chemotherapy and probably partially by the radiation therapy the patient received earlier. One can appreciate the longer root lengths on the mandibular incisors, compared to the maxillary, which can be linked to the therapy and the period in the patient's life the therapy was delivered (courtesy of Dr. Maite Demeester, Belgium)

10.5 Alveolar Rhabdomyosarcoma of the Palate

Rhabdomyosarcoma is a malignant neoplasm of skeletal muscle origin and it is the most common soft-tissue sarcoma in children. Approximately 40% occur in the head and neck region and the genitourinary tract is the second most common location. In the head and neck region, the orbit is most often affected, followed by nasal cavity and nasopharynx. The palate is the most common site if this neoplasm occurs intraorally (Fig. 10.7). In the latter case, they usually have a polypoid clinical appearance, sometimes resembling a cluster of grapes (botryoid). Treatment consists of surgical removal, chemotherapy, and radiation therapy. If no metastasis is present, 5-year survival rates are around 60–70%.

Further Reading

Cawson RA, Odell EW. Cawson's essentials of Oral pathology and Oral medicine. 8th ed. London: Churchill Livingstone Elsevier.

Koehne T, Koehn A, Friedrich RE, Kordes U, Schinke T, Muschol N, Kahl-Nieke B. Differences in maxillomandibular morphology among patients with mucopolysaccharidoses I, II, III, IV and VI; a retrospective MRI study. Clin Oral Invest. 2018;22:1541–9.

Koenig. Diagnostic imaging, oral and maxillofacial. Salt Lake City: Amirsys.

Koong B. Atlas of oral and maxillofacial radiology: Wiley Blackwell.

Larheim TA, Westesson P-LA. Maxillofacial imaging. 2nd ed. Berlin: Springer.

Neville D, Allen B. Oral and maxillofacial pathology. 2nd ed. Philadelphia: Saunders.

Peters SM, Kunkle T, Perrino MA, Philipone EM, Yoon AJ. Mandibular embryonal rhabdomyosarcoma with cartilaginous metaplasia: report of a case and review of literature. Oral Surg Oral Med Oral Pathol Oral Radiol. 2017;124:e288–93.

Scheuer L, Black S. The juvenile skeleton. Amsterdam: Elsevier; 2004.

Whaites E, Drage N. Essentials of dental radiography and radiology. 5th ed. London: Churchill Livingstone Elsevier.

White SC, Pharoah MJ. Oral radiology. In: Principles and interpretation. 7th ed. Amsterdam: Elsevier.

Examples of Dentoalveolar Traumatology in Pediatric Dental Practice

11

This chapter contains examples of dentoalveolar trauma cases.

Names of distinguished colleagues who supplied the images for this chapter are mentioned with the radiographs. If there is no name mentioned with the radiographs, the radiographs were taken by the author of this book or collected from the different university clinics he has worked in (Ghent University in Belgium, University of Washington in Seattle, USA, and University of Western Australia in Perth, Australia).

11.1 Bony Fractures

Dentoalveolar trauma is a common fact in pediatric dentistry. Children fall all the time and often nothing bad results; however in some cases, even in the very young age dental radiographs are indicated to verify intrusion or avulsion of primary teeth. The techniques described in Chap. 3 can be used to obtain adequate and diagnostic radiographic material. In older children these techniques can also be used of course, especially if positioning the image detector is painful or difficult. In this section a myriad of examples are given and commented. Figures 11.1 and 11.2 are illustrations of cone beam computed tomography scans taken for jaw traumas. The first is a very young child, whereas the second one is an 18 year old young man who presented with several fractures after being kicked in the face.

J. Aps, *Imaging in Pediatric Dental Practice*,
https://doi.org/10.1007/978-3-030-12354-3_11

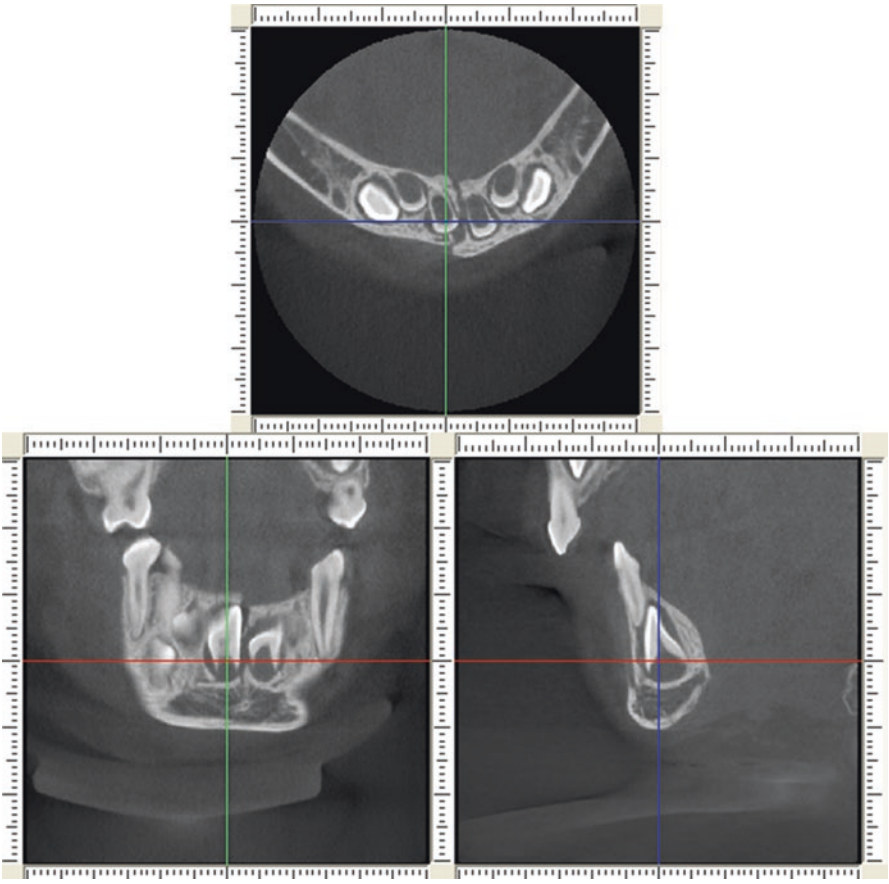

Fig. 11.1 This is a small-field-of-view cone beam computed tomography of a 4-year-old child with a mandibular symphysis fracture. The axial slice shows nicely how the fracture line meanders between the tooth germs of the permanent central incisors. In the coronal view one can appreciate the step in the alveolar crest, with the patient's mandibular body on the left-hand side being a little more inferior than that on the right-hand side. One can debate if this was an accident or child abuse (courtesy of Prof. Dr. Edgar Hirsch, Germany)

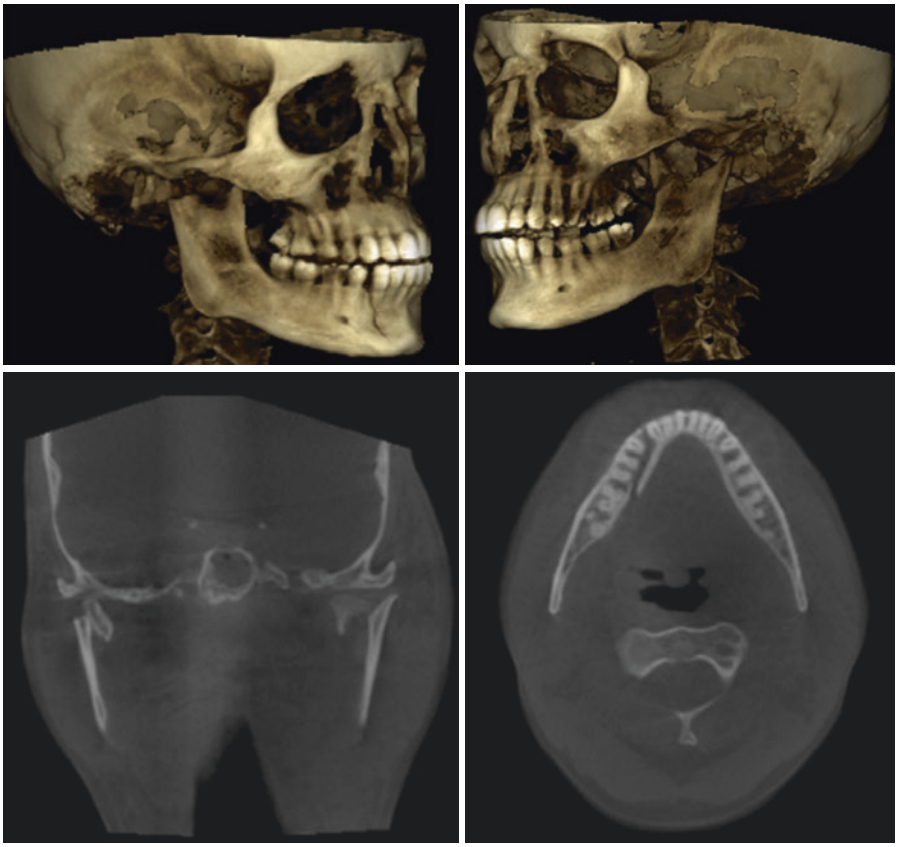

Fig. 11.2 This large field of cone beam computed tomography was taken on an 18-year-old man, who celebrated his day after his 18th birthday in hospital after being kicked in the face at a party. He suffered multiple jaw fractures: bilateral condylar neck fractures (especially well visible on the coronal view), right body of mandible fracture (especially well visible on the axial view), and a left-hand-side coronoid process fracture (upper right-hand-side image)

11.2 Dental Trauma

Figures 11.3 through 11.11 are all examples of dento-alveolar trauma cases. Some of them were diagnosed with only two-dimensional image techniques and others were assisted with cone beam computed tomography scans.

Fig. 11.3 This is an occlusal radiograph (for technique see Chap. 3) of a 3-year-old boy that was taken after dentoalveolar trauma on the maxillary primary central incisors. Both central incisors have a fractured root and their coronal parts are displaced lingually. The coronal parts were removed and the root fragments were given a chance to resorb. Radiographic follow-up was indicated for this case

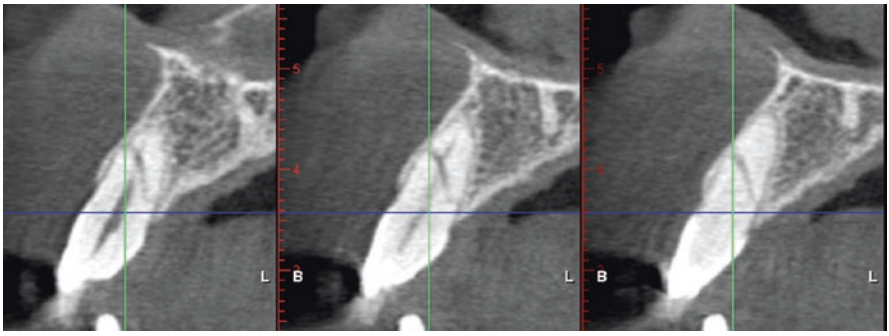

Fig. 11.4 This is a cropped image of a small-field-of-view cone beam computed tomography of the right-hand-side maxillary permanent central incisor, which had been hurt in a bicycle accident 2 months prior to this exposure. Since the tooth was slightly mobile and the periapical radiograph (not included) was inconclusive the CBCT was taken and revealed an oblique fracture line from cervico-palatal to apico-buccal. Since there were no complaints from the patient it was decided to leave the tooth as it was

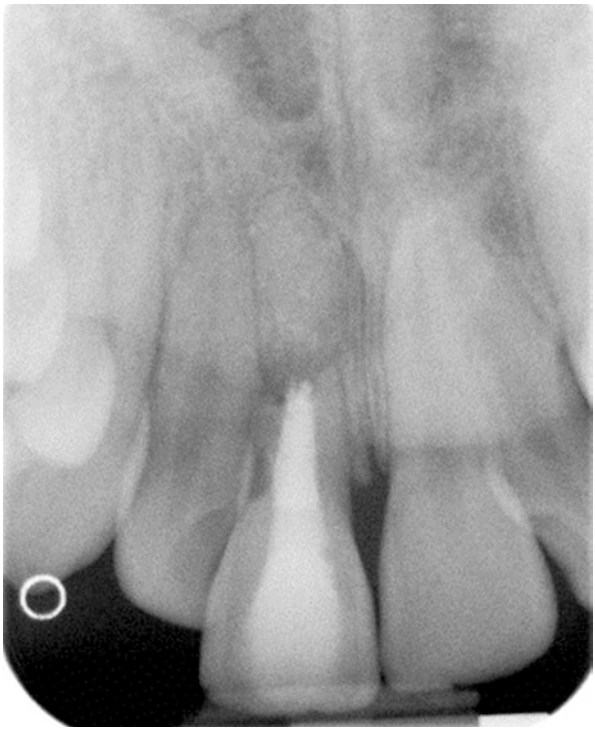

Fig. 11.5 This periapical shows the right-hand-side maxillary permanent incisor with a finished root canal treatment and a fractured apical third that appears to have an obliterated pulp canal. At the distal cervical margin one can also appreciate a saucer-shaped resorption. This tooth was avulsed 6 years prior to the date of this radiograph. The tooth was avulsed during a skateboard accident. The patient immediately picked up the tooth and ran to a dental office nearby. The dentist unfortunately cleaned and dried the tooth very thoroughly, destroying the root sheath and the cementum. Replantation and splinting were performed and subsequently the patient was referred to a pediatric dentist, who then executed pulpotomy with calcium hydroxide paste. After 12 months, the apical third of the root appeared to have separated from the rest of the tooth, due to resorption. It was assumed that cellulose of the paper napkin the dentist used to dry the tooth had caused the apical third to resorb partially. The coronal section of the root was then filled with Ketac-Molar® at the time to preserve the rigidity of the root. An implant was placed successful 7 years after the initial trauma. Keeping the tooth as long as possible facilitated the preservation of the alveolar ridge

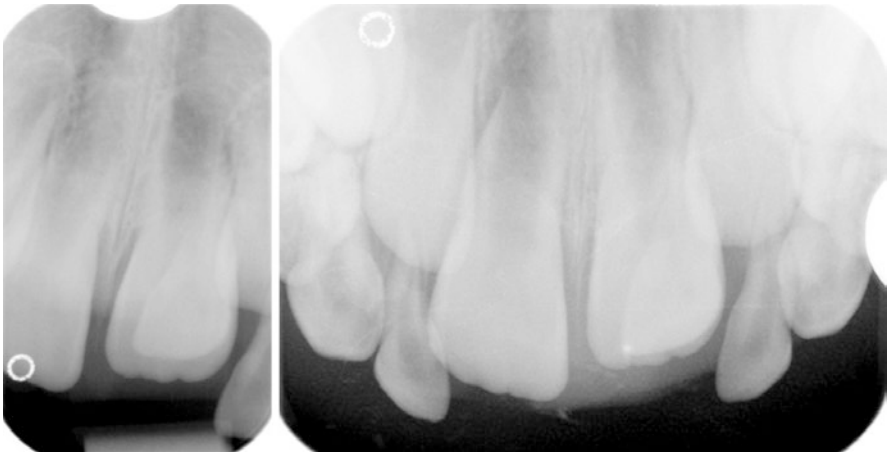

Fig. 11.6 This is a case of intrusion of the left-hand-side maxillary primary central incisor. Both radiographs were taken using the occlusal technique at a 65^0 angle of the X-ray beam to the occlusal plane, while the photostimulable phosphor plate was on the occlusal surface. The child was sitting on the mother's lap, who was wearing a lead-equivalent apron. The mother was also holding a thyroid shield under the child's chin to protect the thyroid gland from being irradiated by the primary radiation beam. The intruded primary incisor was removed under local anesthesia, as the eruption of the permanent teeth was eminent

Fig. 11.7 The periapical radiograph was taken to identify the reason for the ectopic eruption of the permanent left-hand-side maxillary central incisor, as the primary predecessor was very mobile and ready to exfoliate clinically. The radiograph shows that the root of the primary predecessor was fractured off and mesio-apically displaced and caused a physical obstruction for the permanent successor to erupt in its correct place. The dentist then made an attempt to take a lateral radiograph to determine the position of the root fragment; however he did not manage to visualize the fragment as it was much more superior. Nevertheless, this was a good attempt, which also shows the buccal cortical plate of the maxilla (courtesy of Dr. Pieter Van Ingelgem, Belgium)

Fig. 11.8 These two periapical radiographs were taken after the patient was seen at an emergency dental clinic 2 days before. A skateboard accident was the cause of the complicated fracture of the left-hand-side maxillary permanent central incisor. A clear vertical fracture line is visible and close examination shows a horizontal root fracture as well in the middle third of the root. The radiopaque shadow of the nose makes the horizontal fracture a little bit more difficult to depict. One can also see that the image on the left side is taken with a solid-state sensor and the image on the right is taken with a phosphor storage plate and that both images were taken from different angles

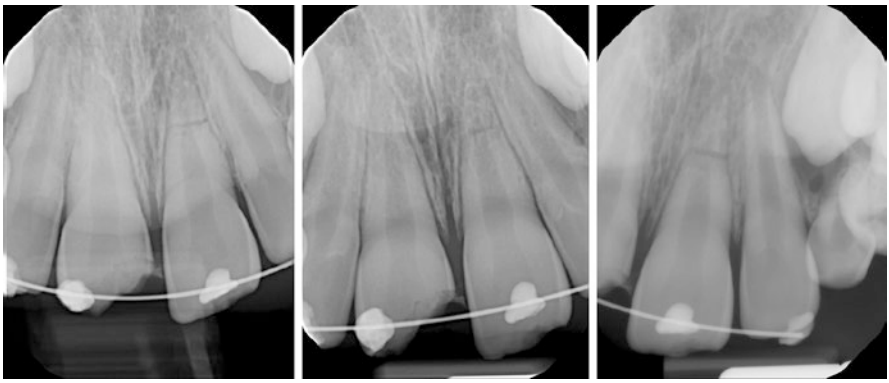

Fig. 11.9 This is another case of a dental trauma to the permanent central maxillary incisors. The 10-year-old boy had been in a bicycle accident a few days before and a splint was placed at the emergency appointment. The right-hand-side central incisor suffered a complicated enamel-dentine fracture and the left-hand-side central incisor a horizontal root fracture in the apical third. Taking radiographs from different angles can be extremely useful in trauma cases to assess and identify root fractures

Fig. 11.10 This periapical radiograph was taken with a solid-state sensor to verify the primary maxillary central incisors after a trauma that occurred 3 weeks before. The right-hand-side primary central incisor was clinically gray. The radiograph shows a widened pulpal system in that tooth, indicating that the tooth had suffered at least one other trauma sometime before the last one 3 weeks ago. A slightly widened periodontal ligament space was observed on both primary central incisors. Careful examination and interpretation of the radiograph are necessary to put the radiographic findings of the pulp canals and the clinical appearance into perspective

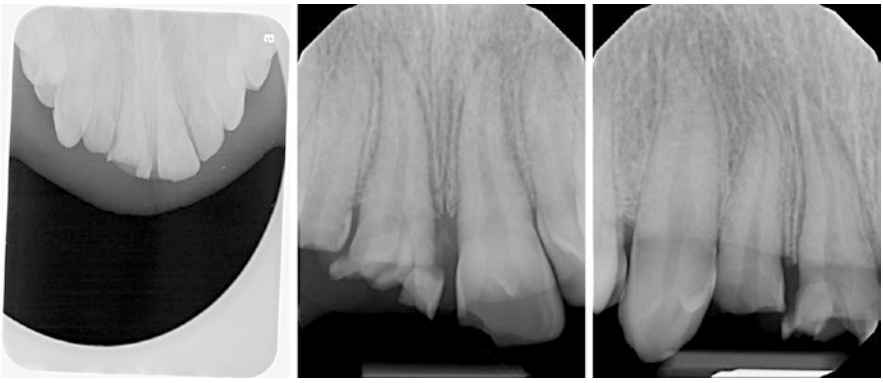

Fig. 11.11 These radiographs were taken immediately after this teenager suffered a dental trauma, injuring his right-hand-side permanent maxillary lateral incisor and both his central incisors. An attempt was made to take a true maxillary occlusal, but a lot of useless radiation was aimed at his chest. More accurate periapical radiographs were subsequently obtained using a solid-state sensor. One can appreciate the widened periodontal ligament space around the right-hand-side central incisor, indicating that the impact on that tooth must have been tremendous. The shattered tooth crown is evidence of that. The occlusal radiograph should have been taken more carefully though (see Chap. 3)

Dental traumatic injuries are diagnostic challenges as these injuries have a huge array of presentations. Correct identification of the traumatic injury will have a huge impact on the treatment and hence the success of the treatment and the outcome for the patient. Correct and appropriate choice of imaging is essential and will benefit the patient. Justification is required to use three-dimensional imaging. If fracture lines are running mesiodistal, they cannot be depicted with periapical or occlusal radiographs and cone beam computed tomography is crucial in identifying the issue. It is essential to keep an open scope when assessing dental trauma and not to focus on the teeth only. The mouth opening should always be checked even if the chin was supposedly not involved in the impact. Temporomandibular joints, range of motion of the mandible, and displacement of articular discs should be assessed and based on the findings appropriate imaging should be performed. Three-dimensional imaging can also be beneficial in cases of luxation of teeth, as it will visualize the buccal cortical plate of the jaw better and provide information about its position and status.

11.3 Follow-Up and Assessment After Trauma

Radiographic follow-up after trauma treatment or as a follow-up when no treatment was carried out is important. One can take two-dimensional as well as three-dimensional images, which may prove to be beneficial after all. For instance the true extent of a nonhealing periapical lesion can be visualized with CBCT. The same holds for destruction of bony barriers when inflammation spreads after a traumatic impact with necrosis of the pulp of the affected tooth. Figures 11.12 through 11.15 are examples of follow-up of dento-alveolar trauma with the use of two dimensional imaging and cone beam computed tomography.

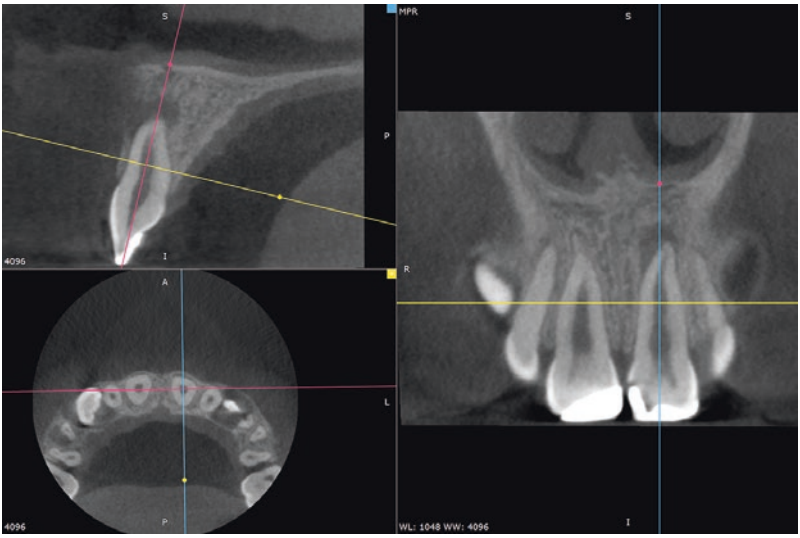

Fig. 11.12 This is a case of trauma to both permanent central maxillary incisors. They were restored previously but clinically the left-hand-side central incisor showed a buccal fistula at the level of its apex. A periapical radiograph cannot show the true extent of the inflammatory lesion and as such a small-field-of-view cone beam CT was made, which showed clearly the three-dimensional characteristics of this lesion. Destruction of the buccal cortical plate is evident. Note that the slices shown in this image are carefully chosen and follow the long axis of the tooth. This is necessary to avoid misinterpretation of the length of the tooth (courtesy of Dr. Stephane Diaz, France)

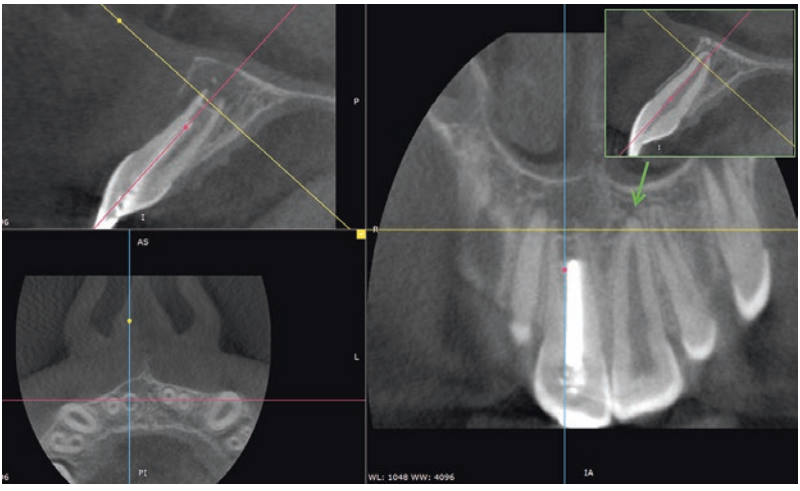

Fig. 11.13 This is a case of trauma in the permanent dentition with open apices. The right-hand-side maxillary central incisor was not healing according to plan and a large inflammatory lesion developed at its apex, destroying almost the entire buccal cortical wall anterior to that tooth's root. A conventional two-dimensional radiograph would never be able to show the extent of the bone destruction. As such this CBCT is definitely beneficial as proper assessment of the situation can take place and an appropriate treatment can be executed. In the upper right corner of the image, the left-hand-side central incisor is shown and one can appreciate the nice image of the thin layer of buccal cortical bone over the root of that tooth (courtesy of Dr. Stephane Diaz, France)

Fig. 11.14 This is a periapical radiograph, taken with a solid-state sensor of an 8-year-old child who suffered a dental traumatic injury earlier. One can appreciate the external resorption that has started on the distal aspect of the root of the right-hand-side permanent maxillary central incisor (courtesy of Dr. Stephane Diaz, France)

Fig. 11.15 Traumatic injury to the left-hand-side permanent maxillary incisor with open apex. Pulp capping and reattachment of the fractured crown fragment performed (second from the left) and followed up after 3 months (middle), 9 months (second from the right), and 18 months (right). One can appreciate that the apex is further developing and the dentinal walls of the pulp canal are increasing in thickness (courtesy of Dr. Stephane Diaz, France)

Further Reading

Cawson RA, Odell EW. Cawson's essentials of oral pathology and oral medicine. 8th ed. London: Churchill Livingstone Elsevier.
Choenca N, Silberman A. Contemporary imaging for the diagnosis and treatment of traumatic dental injuries. A review. Dent Traumatol. 2017;33:321–8.
Koenig. Diagnostic imaging, oral and maxillofacial. Salt Lake City: Amirsys.
Koong B. Atlas of oral and maxillofacial radiology. Hoboken: Wiley Blackwell.
Larheim TA, Westesson P-LA. Maxillofacial imaging. 2nd ed. Berlin: Springer.
Neville D, Allen B. Oral and maxillofacial pathology. 2nd ed. Philadelphia: Saunders.
Whaites E, Drage N. Essentials of dental radiography and radiology. 5th ed. London: Churchill Livingstone Elsevier.
White SC, Pharoah MJ. Oral radiology. In: Principles and interpretation. 7th ed. Amsterdam: Elsevier.